Lipid Requirements for Adenovirus Infection

Dissertation

zur

Erlangung der naturwissenschaftlichen Doktorwürde (Dr. sc. nat.)

vorgelegt der

Mathematisch-naturwissenschaftlichen Fakultät

der

Universität Zürich

von

Stefania Luisoni

von

Stabio TI

Promotionskomitee

Prof. Dr. Urs F. Greber, (Vorsitz, Leitung der Dissertation)

Prof. Dr. Ari Helenius

Prof. Dr. Howard Riezman

Zürich, 2015

Table of contents

SUMMARY

Early events in virus infections critically depend on host membrane dynamics involving both proteins and lipids. How lipids tune the viral life cycle has remained largely elusive, however. Here, we used adenovirus as a model to study the role of lipid metabolism in viral invasion. Adenovirus is a non-enveloped virus that relies on its capsid proteins to hijack host machineries and overcome the cellular membrane barrier. Incoming adenoviruses engage with the receptor CAR and the co-receptors $\alpha_v\beta_{3/5}$ integrins to elicit their internalization. Concomitantly with binding and endocytosis, the viral capsid undergoes a stepwise uncoating program. These early events are crucial for infection and lead to the exposure of membrane active internal viral capsid proteins, such as protein VI. Protein VI is the membrane lytic factor that mediates the escape of the virus from endosomes to the cytosol. Yet, how the 90 nm capsid penetrates the endosomal membrane remains poorly understood.

Lipid profiling of infected cells revealed a rapid and selective enrichment of ceramides during adenovirus entry. This change in the lipid composition was required for infection and was mediated by the enzyme acid sphingomyelinase (ASMase). ASMase constitutively generates ceramide from sphingomyelin in lysosomes. Interestingly, inhibition of ASMase activity affected multiple steps of viral invasion. Adenovirus endocytosis was delayed, association of protein VI with the cell membrane was impaired, and the escape of viruses to the cytosol was reduced. Remarkably, *in vitro* experiments with liposomes showed that protein VI preferentially associated with and ruptured membranes containing ceramides. To address how a lysosomal enzyme could regulate events at the plasma membrane, we tracked the sub-cellular localization of ASMase. We found that ASMase was released from lysosomes to the extracellular space within the first minutes after virus binding in a process that has been previously described as lysosomal exocytosis. This is a cellular response regulated by calcium (Ca^{2+}) to repair small lesions of the plasma membrane. Consistently, we observed a transient influx of extracellular Ca^{2+} into the cytosol. Moreover, we observed a simultaneous influx of membrane-impermeable propidium iodide across the plasma membrane, suggesting that the plasma membrane of virus infected cells contained small, temporary lesions within the first few minutes of infection. Further experiments involving fluorescence microscopy and mutant viruses indicated that protein VI was partially released already at the cell surface and mediated plasma membrane permeabilization.

We propose a model where virus uncoating at the cell surface leads to a partial release of protein VI from the inside of the virus. This leads to the formation of transient, and rapidly resolved membrane lesions. These lesions serve as a portal for the influx of extracellular calcium, which triggers lysosomal exocytosis and delivers ASMase to the plasma membrane. ASMase increases surface ceramide to enhance virus endocytosis and VI exposure. In endosomes, VI interacts with ceramide-enriched membranes to enhance endosomal lysis and virus escape into the cytosol. Together, this study shows how an incoming, non-enveloped virus modulates lipid metabolism for efficient invasion and productive infection.

ZUSAMMENFASSUNG

Die ersten Schritte einer Virusinfektion hängen von der Dynamik der Zellmembran ab. Wie Lipide den viralen Lebenszyklus beeinflussen ist weitgehend ungeklärt. In dieser Studie benutzten wir Adenovirus als Modell um die Rolle des Lipid Metabolismus in der viralen Invasion zu studieren. Adenoviren sind nicht-behüllte Viren, das heisst sie sind nicht von einer Membran umschlossen, und sind deshalb auf ihr virales Kapsid angewiesen um zelluläre Maschinerien zu beschlagnahmen und die Zellmembran zu überwinden. Eintretende Adenoviren binden an den Rezeptor CAR und an den Co-Rezeptor $\alpha_v\beta_{3/5}$ Integrin um ihre Aufnahme in die Zelle zu initiieren. Gleichzeitig mit der Bindung an einen Rezeptor und der Aufnahme in die Zelle begeht das Virus ein Enthüllungsprogramm. Dies führt dazu dass das Kapsid-interne virale Proteine, wie z.B. Protein VI exponiert werden. Protein VI ist ein Membran-lytischer Faktor, welcher das Austreten der Viren aus einem Endosom ins Zytoplasma vermittelt. Die Frage wie das Kapsid mit einem Durchmesser von 90 nm die endosomale Membran durchbricht bleibt weitgehend offen.

Durch eine Profilierung der Lipide in infizierten Zellen fanden wir heraus, dass sich während der Infektion Ceramide schnell anreichern. Diese Änderung in der Lipid komposition war notwendig für eine Infektion und wurde durch das Enzym Acid Sphingomyelinase (ASMase) vermittelt. ASMase generiert Ceramide aus Sphingomyelin konstitutiv in Endosomen. Interessanterweise beeinflusste eine Inhibition von ASMase verschiedene Schritte der viralen Invasion. Die Endozytose der Adenoviren war verlangsamt, die Assoziation von dem Protein VI mit der Zellmembran war beeinträchtigt und das Austreten des Virus ins Zytosol war vermindert. Bemerkenswerterweise zeigten *in vitro* Experimente dass Protein VI bevorzugt Membrane bricht die Ceramide enthalten. Um herauszufinden wie ein lysosomales Enzym die viralen Ereignisse an der Plasmamembran regulieren kann, haben wie die sub-zelluläre Lokalisation von ASMase verfolgt.

Wir fanden dass die ASMase innerhalb von wenigen Minuten nach der Bindung des Virus von Lysosomen in den extrazellulären Raum geschleust wurde. Dieser Prozess wurde als lysosomale Exozytose beschrieben, als eine Kalzium (Ca^{2+}) abhängige zelluläre Antwort um kleine Läsionen in der Plasmamembran zu reparieren. Konsistenterweise beobachteten wir dass extrazelluläres Ca^{2+} in das Zytosol aufgenommen wurde und gleichzeitig auch grössere Moleküle wie Propidium Iodid was darauf hindeutete, dass das Virus in den ersten Minuten nach der Bindung an den Rezeptor kleine, temporäre Läsionen in der Plasmamembran induzierte. Nachfolgende Experimente mittels Fluoreszenzmikroskopie und Virusmutanten zeigten dass das Protein VI schon teilweise an der Zelloberfläche vom Viruskapsid entlassen wurde was zu einer Permeabilisierung der Plasmamembran führte.

Wir schlagen ein Modell vor wo die Virusenthüllung an der Zelloberfläche zu einer partiellen Entlassung von Protein VI aus dem Viruskapsid führt. Dies führt zu transienten und schnell resolvierten Membranläsionen welche als Portal für das Eintreten von extrazellulärem Kalzium dienen. Dies löst eine lysosomale Exozytose aus wodurch ASMase an die Plasmamembran gelangt. ASMase erhöht die Konzentration von Ceramid an

der Zelloberfläche und beschleunigt die Endozytose des Virus. Protein VI interagiert in Endosomen mit Ceramid-angereicherten Membranen was deren Lyse und das Austreten des Virus ins Zytosol beschleunigt. Zusammengefasst zeigt diese Studie dass eintretende, nicht-behüllte Viren den Metabolismus von Lipiden modulieren um die Zelle zu infizieren.

INTRODUCTION

1. EARLY EVENTS OF VIRUS INFECTION

Viral diseases have dramatic repercussions on humanitarian, economic and political aspects of our society. Advances on vaccines and antiviral research greatly contributed to the control, prevention, or even eradication of viral disease. Nonetheless, there is a need to further improve our knowledge on virus infections as viral diseases continue to threat global health. Since viruses require their host cells for infection and disease development, a better understanding of the biology of virus-host interactions may offer new perspectives for the treatment of viral disease.

The first point of contact between a virus and the host cell is the plasma membrane (PM). The PM constitutes a physical barrier against viral invasions, but is also a platform for complex and dynamic interactions. Incoming viruses engage with surface cellular receptors and signaling factors. They trigger a cascade of events that prime both cell metabolism and virus structures for infection.

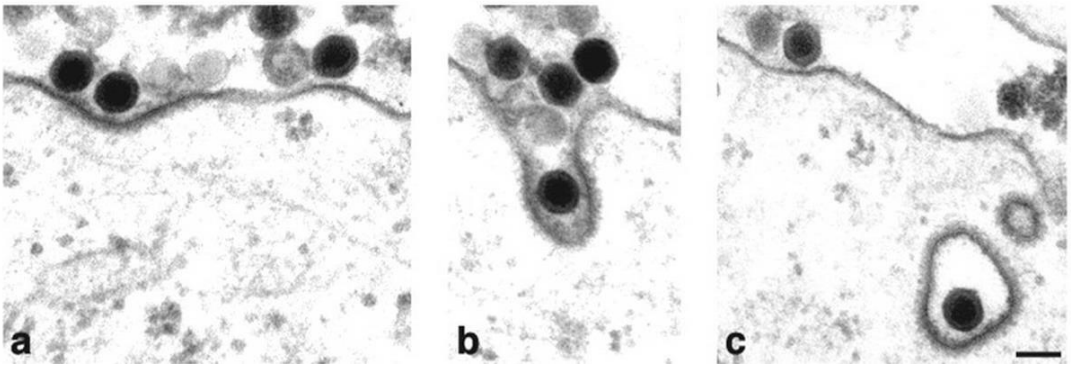

Fig. 1: EM micrographs of early steps of adenovirus entry. Binding (a), invagination (b) and endosomal localization of HAdV-C2 in HeLa cells. Scale bar: 100 nm (Meier et al., 2002).

It is becoming increasingly clear that early infection events determine whether the virus will successfully spread or be neutralized. Recent studies highlight the importance of lipid metabolism and membrane dynamics during viral infections. This work focuses on the interplay between viruses and host cell lipids during virus entry.

1.1 MEMBRANE PENETRATION OF NON ENVELOPED VIRUSES

A major challenge for viruses is to transiently destabilize and cross the host membranes without compromising cell viability. For example, lysis of the PM would be detrimental to the cell and eventually lead to cell death before the invading viruses would have replicated. To avoid PM lysis, most viruses induce their own internalization by receptor-mediated endocytosis and accomplish the actual step of penetration from intracellular compartments. This strategy limits cellular damage to specific intracellular compartments

and ensures clearance of viral components from the cell surface where they are exposed to the immune system. While it is well established that enveloped viruses carry fusion machineries to merge their own envelope with cellular membranes, it remains poorly understood how non-enveloped viruses cross the host lipid bilayer.

Capsids of non-enveloped viruses are highly ordered and tightly packed protein structures that enclose and protect the viral genome. A key feature that determines virus infectivity is the capsid meta-stability. On the one hand, capsids must stay intact and protect the viral genome from environmental and physiological insults, and on the other hand they need to disassemble in the host cell to activate their dormant genome. Throughout the binding and entry process, capsids undergo finely controlled structural rearrangements dictated by sequential interactions with cellular cues (Suomalainen and Greber, 2013). Conformational changes that prime the capsid for uncoating can occur at the early stage of receptor binding. Additional mechanical or chemical cues drive a spatiotemporally coordinated exposure of membrane interacting domains (Bilkova et al., 2014; Suomalainen and Greber, 2013). In general, membrane-interacting domains are either hydrophobic or amphipathic and sometimes require proteolytic processing to become membrane-active. They induce membrane leakage or rupture, locally modify the lipid composition, or interact with cellular factors that mediate membrane translocation (Moyer and Nemerow, 2011).

While virus entry and replication strongly depend on host factors, the actual membrane penetration step is thought to predominantly rely on viral factors. A role of the host lipids in these processes is poorly understood.

1.1.2 Non receptor-mediated membrane permeabilization

Particular proteins capable of perturbing membrane integrity have evolved across kingdoms. An example are bacterial pore-forming toxins that perform a selective, receptor-mediated membrane perforation. Generally these toxins bind to a cellular target, a specific lipid, a sugar moiety or a surface protein, and oligomerize into a pore-structure that inserts into membranes. These pores allow translocation of bacterial components into the target cell or mediate efflux of cytosolic components, thereby compromising the cell integrity (Bischofberger et al., 2012; Los et al., 2013).

Other peptides are capable of non-receptor mediated membrane perforation and are therefore bioactive against a wide range of targets. Among these, antimicrobial peptides (AMPs) and components of the complement system participate in host defense against a broad spectrum of pathogens (Andersson et al., 2004; Brogden, 2005). Also, cell penetrating peptides (CPPs) can translocate across several biological membranes (Vivès et al., 2008). Finally, amyloid peptides promote the pathogenesis of several diseases, including Alzheimer disease, by permeabilizing cellular membranes (Hebda et al., 2009) without receptor recognition.

Lessons from the widely studied pore forming process by AMPs might help to understand how non-enveloped viruses penetrate membranes.

Common structural features of several AMPs, amyloid peptides, CPPs as well as some viral lytic factors are their amphipathic nature and the short size, usually less than 50 amino acids (Last et al., 2013; Moyer and Nemerow, 2011). These proteins are soluble in water and generally have a disordered structure (Marion et al., 1988; Williamson et al., 2009) until they reach proximity of the lipophilic environment of cell membranes. This promotes their folding into a secondary structure with amphipathic properties (Shai, 1999). Amphipathic structures increase their energetic stability in a way that the polar side chain remains exposed to the solvent, while the non-polar region partitions between the lipid head groups into the membrane acyl core (Huang, 2006; Marion et al., 1988). The initial association of amphipathic helices with membranes is thought to occur laterally, with the helix oriented in a parallel fashion to the lipid bilayer. This was shown for the AMP cecropin A (Marassi et al., 1999) and the amyloid peptide α-synuclein (Apostolidou et al., 2008; Marion et al., 1988). Afterwards peptides can also insert into the membrane and form a transmembrane domain (Ding and Chen, 2012). Generally, accumulation of these peptides leads to thinning of the bilayer in a dose-dependent manner (Chen et al., 2003). When a critical peptide/membrane ratio is reached, peptides finally insert into the bilayer and trigger a localized collapse of the membrane (Chen et al., 2002; Shai, 1999). Various modalities of permeabilization have been proposed and mostly depend on local protein concentration, membrane affinity and protein-protein affinity. Mechanisms include formation of a lipid-peptide toroidal pore, a peptide-peptide barrel-stave inserted into the bilayer, or interference with the bilayer integrity similar to detergents. In the following section, well-characterized models of membrane poration are discussed.

The carpet model

The carpet model incorporates both short-lived poration and membrane solubilization events. This model was first described as mode of action for the porcine intestinal AMP cecropin P1 (Gazit et al., 1995). Cecropins are 31-39 aa peptides that fold into an amphipathic alpha-helix in presence of lipid bilayers (Hultmark et al., 1980). It contains several cationic amino acids that bind with high affinity to the head groups of phospholipids in bacterial membranes, which are negatively charged. Cecropin A binds to membranes in a parallel fashion (Marassi et al., 1999). Such binding expands the surface area of the outer leaflet, promotes the thinning of the bilayer (Chen et al., 2003; He et al., 1996; Heller et al., 1997; Lee et al., 2004; Mecke et al., 2005) and induces a positive membrane curvature (Hallock et al., 2003; Matsuzaki et al., 1998a). While the outer leaflet of the membrane is strongly modified, the lipid packaging of the inner leaflet remains intact. This mismatch likely favors peptide insertion or aggregation (Hallock et al., 2003).

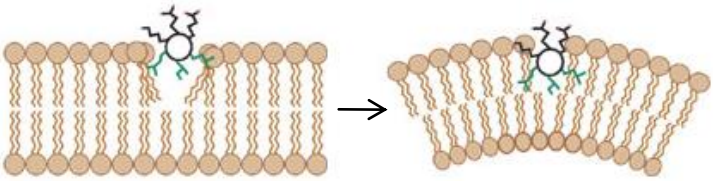

Fig. 2: Schematic representation of the insertion of an amphipathic alpha-helical peptide into a lipid bilayer and the subsequent induction of positive membrane curvature. (McMahon and Gallop, 2005)

Depending on the protein to lipid ratio, two different scenarios are possible: the sinking raft model or the detergent model. In the sinking raft model, single peptides or small aggregates intercalate between lipids and translocate across the bilayer. The translocation process disturbs membrane integrity and permits leakage events. Immediately following translocation the bilayer barrier is resealed, giving rise to short lived membrane openings (Pokorny and Almeida, 2004). When a critical peptide concentration is reached, peptides can act like detergents and partially solubilize membranes (Hristova et al., 1997).

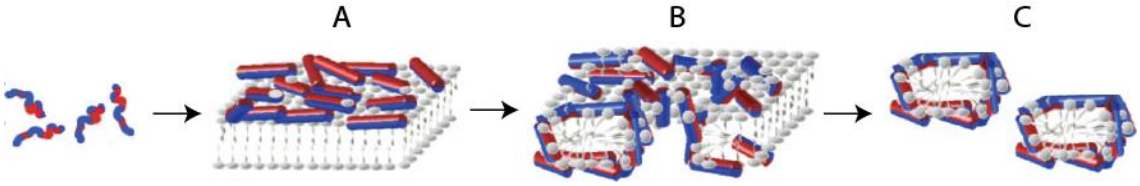

Fig. 3: Schematic representation of the carpet model. (A) The hydrophobic side of peptides (red) associates in parallel to membranes. After a critical concentration is reached, the membrane is transiently permeabilized (B) or disrupted (C). (Shai, 2002)

The toroidal and barrel-stave pore models

The toroidal and barrel-stave models explain the formation of long-lived pores. In the toroidal-pore model, the association of AMPs with the membrane induces a back-bending of lipids until the outer and inner leaflet are connected and the peptides perpendicularly intercalate between phospholipids (Hallock et al., 2003; Huang, 2000; Ludtke et al., 1996; Matsuzaki et al., 1996; Yang et al., 2001). Thereby, lipids facilitate the poration process as they cooperate with peptides that are too short to span the lipid bilayer.

In the barrel-stave pore model peptides are required to associate into a channel-like structure and to be sufficiently long to traverse the lipid bilayer (Christensen et al., 1988; Juvvadi et al., 1996; Kagan et al., 1990; Porcelli et al., 2004; Westerhoff et al., 1989). A well-characterized example is alamethicin, a 20 amino acids hydrophobic peptide from the fungus *Trichodermaveridae*. Monomers of alamethicin aggregate into the membrane and form voltage-gated channels (Barranger-Mathys and Cafiso, 1994; Cafiso, 1994; Huang, 2000; Mueller and Rudin, 1968). Alamethicin pores consist of 8 or 9 α-helices per channel and have a

diameter from 18 to 26 Å depending on the lipid composition of the surrounding membrane and the hydration degree (Heller et al., 1997; Rizzo et al., 1987).

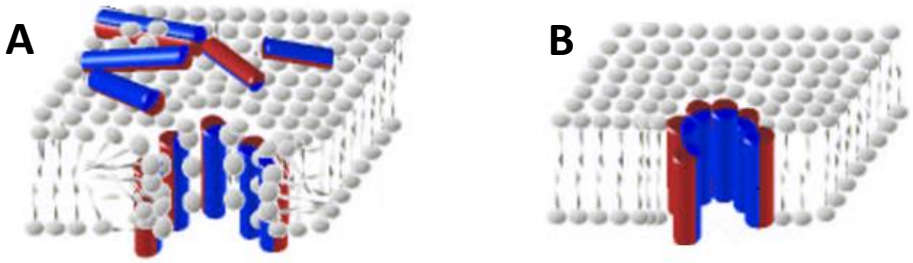

Fig. 4: Schematic representation of a toroidal pore (A) and a barrel-stave pore (B). In both cases, the lipophilic side of the lipids faces the hydrophobic core of the bilayer. In (A) peptides and lipids cooperate to form a pore, whereas in (B) peptides assemble into a channel structure. (Shai, 2002)

These models are supported by a large number of studies and are widely accepted. However, several studies on AMPs suggest a more complex landscape of permeabilization modalities. For example, the component of bee venom melittin preferentially forms pores in vesicles composed of neutral lipids (Lee et al., 2008) but acts via detergent-like mechanism in presence of anionic lipids (Ladokhin and White, 2001). Similarly, magainin 2 switches between two modes of action depending on the protein/lipid ratio: at low concentration it provokes toroidal pores (Ludtke et al., 1996), while at high concentrations it generates chaotic pores (Gregory et al., 2009). Also, the cholesterol content of membranes influences insertion and bioactivity of several AMPs (Mason et al., 2007; Nicol et al., 1996; Won et al., 2012). These findings underline that the modality of membrane perforation does not exclusively depend on the intrinsic properties of the peptides but also on the biophysical properties of the target membrane. This topic is further considered in the discussion.

1.1.3 Membrane-active viral factors

Membrane active factors of non-enveloped viruses generally contain either amphipathic alpha-helical domains or hydrophobic residues, are myristoylated or even encode a lipid modifying function (Moyer and Nemerow, 2011). The following section describes mechanisms of penetration by selected non-enveloped viruses with a focus on the membrane rupture step and the role of cellular lipids.

An amphipathic α-helical lytic factor sensitive to lipids: gamma of flock house virus

Flock house virus (FHV) is a positive-sense RNA virus of about 30 nm capable to infect plants, insects, yeast and mammalian cells. To date, surface receptors and the uptake mechanism of this virus are not known. The formation of the viral capsid begins with the self association of a single structural protein, protein alpha, followed by enclosure of the RNA genome. Capsid maturation proceeds with autoproteolytic cleavage of protein alpha into the structural protein beta and the membrane-active peptide gamma. In

intact viruses peptide gamma is located whithin the capsid, and is only occasionally exposed to the surface during capsid breathing (Bothner et al., 1998). During endocytosis FHV interacts with surface receptors (Walukiewicz et al., 2006) and is exposed to a low pH in endosomes (Banerjee and Johnson, 2008). The combination of these events elicits conformational changes leading to the externalization of peptide gamma.

Gamma is composed of 44 aa, of which the first 21 residues form an amphipathic alpha helical domain, gamma-1 (Schneemann et al., 1992; Zlotnick et al., 1994). Theoretically, the length of gamma-1 is sufficient to span the endosomal membrane. (The thickness of a lipid bilayer is 6 nm, where 3 nm are hydrophobic core and 2x1.5 nm hydrophilic head. A typical alpha-helix has 3.6 residues per turn, and 0.54 nm is the vertical distance between consecutive helical turns. The length of a 21 aa alpha-helix is 3.15 nm.)

Structural studies with intact viruses showed that gamma peptides assemble into pentameric bundles of amphipathic alpha-helices and form a channel-like structure (Cheng et al., 1994). This suggested that FHV can form pores in the endosomal membrane, through which the RNA genome might pass into the cytosol. However, studies with a synthetic peptide encompassing the first 21 aa of gamma showed that these alpha-helical peptides associate with membranes in a parallel fashion (Janshoff et al., 1999). Also, viral infectivity is not affected by the deletion of one or two turns of the helix (Banerjee and Johnson, 2008). Together, these data exclude the hypothesis of pore production but rather support the concept that gamma destabilizes membranes by modifying their lipid packaging. The lipid composition of the membrane is in turn proposed to modulate membrane lysis. Maia and collaborators performed liposome leakage assays with synthetic gamma-1 (Maia et al., 2006). They observed that increasing the cholesterol content of a model lipid bilayer from 0.2 mol% (PC:PE:SM:Cho 1:1:1:0.2) to 1.5 mol% (PC:PE:SM:Cho 1:1:1:1.5) strongly reduced the capacity of gamma-1 to permeabilize membranes (Fig. 6; Maia et al., 2006). How cholesterol metabolism affects FHV *in vivo* remains obscure, however these results highlight the importance of membrane lipid composition for efficient membrane penetration.

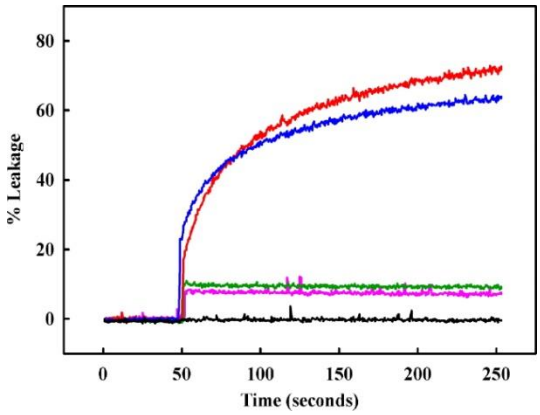

Fig. 6: Liposome leakage mediated by the gamma peptide. Gamma was exposed to vesicles containing PC/PE/SPM/Cho (1:1:1:1.5) at pH 6.5 (green line) and pH 4.0 (purple line) or to

vesicles composed of PC/PE/SPM/Cho (1:1:1:0.2) at pH 6.5 (red line) and pH 4.0 (blue line). (Maia et al., 2006)

Membrane tension as a trigger for endosomal rupture? The example of Rotavirus

Rotavirus is a major cause of dehydrating childhood diarrhea and accounts for over 400'000 deaths annually (Parashar et al., 2003). Rotaviruses consist of three layers of proteins that form an icosahedral shell and enclose the double-stranded RNA genome (Fig. 7; Li et al., 2009; Prasad et al., 1988; Settembre et al., 2011; Yeager et al., 1990). Most Rotaviruses bind to surface glycans (Haselhorst et al., 2009; Hu et al., 2012) via the outer shell proteins VP7 and VP4. Cell attachment depends on the presence of extracellular Ca^{2+} (Dormitzer et al., 2000). VP4 dictates which endocytic route will be taken (Díaz-Salinas et al., 2014). Strikingly, VP4 cleavage by trypsin in the gut is essential for infection (Estes et al., 1981). The result of VP4 cleavage is the generation of the two fragments VP8* and VP5*. VP5* first mediates the interaction with entry cofactors and in a second step the lysis of endosomal membranes (Lopez and Arias, 2006).

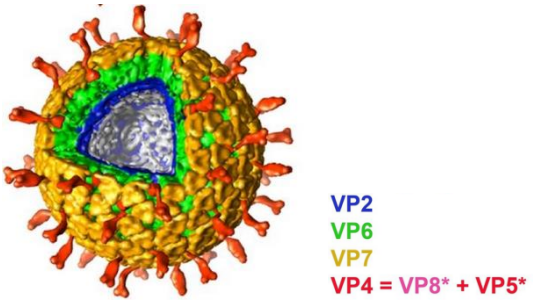

Fig. 7: Multilayered structure of a rotavirus particle, based on cryo-EM three-dimensional image reconstructions (Chen et al., 2009; Li et al., 2009). Color coding for the structural proteins is indicated by labels. (Trask et al., 2010)

Endocytosis occurs very rapidly and virions reside in internalized vesicles no longer than 1-3 min. Notably, the vesicles from which virions escape are very small. They have a minimal diameter required to enclose viruses (Abdelhakim et al., 2014). Loss of calcium in these vesicles triggers the dissociation of VP7 (Settembre et al., 2011). As a consequence, VP5*-VP8* is de-capped and VP5* undergoes conformational changes that expose three hydrophobic domains at the terminal tip of a beta barrel (Denisova et al., 1999; Graham and Estes, 1980). The extended hydrophobic apex is proposed to bind to the endosomal membrane before folding-back into a more stable conformation (Fig. 8, Dormitzer et al., 2004). The "back-folding" likely provides the free energy required for membrane rupture.

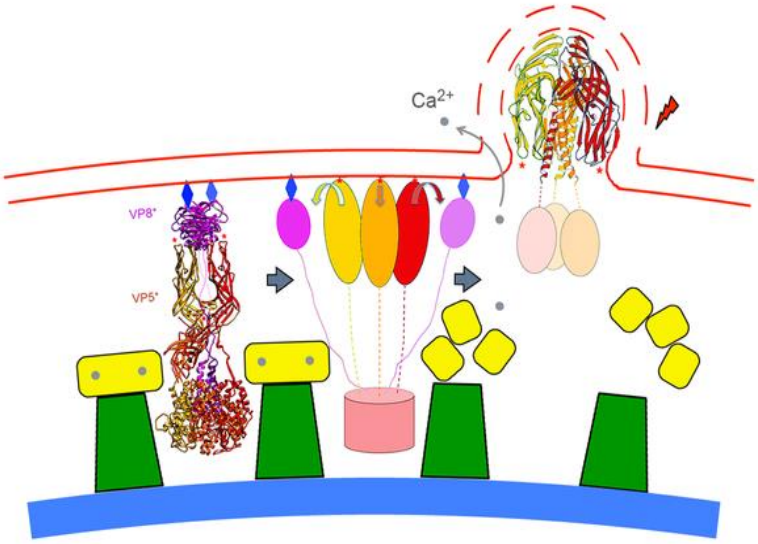

Fig. 8: Schematic representation of the VP5* intermediate interacting with the limiting membrane, its "back-folding" into a stable structure and the resulting membrane extension. (Abdelhakim et al., 2014)

How does the rupture occur? Cells respond to local stretching of the PM by either increasing pulling tensions through the cytoskeleton, by providing further membrane reservoirs through exocytosis, or by regulating ion channels (Groulx et al., 2006). However, these compensatory mechanisms hardly apply to endocytic vesicles, rendering their membrane more prone to stretching-mediated rupture. In fact, a 3% increase in surface area is the lowest threshold for stretching-mediated membrane rupture (Abdelhakim et al., 2014). Binding of a single VP5* already increases the surface of the limiting vesicle by 0.5%. As such, even an incomplete processing of the 60 copies of VP5* would be sufficient for membrane rupture. Of note, viruses found in bigger vesicles, such as Rab5-positive endosomes of about 200 nm diameter, are non-infectious (Abdelhakim et al., 2014).

Entry from endosomes or PM? The case of Reovirus

Reoviruses infect most mammalian species, albeit with low pathogenicity in humans (Ouattara et al., 2011). The primary site of infection is the gastrointestinal tract, where reovirus uses JAM-A and sialic acid as receptors (Barton et al., 2001a; Barton et al., 2001b; Forrest et al., 2003; Reiss et al., 2012). In rare cases, the primary infection is followed by viremia and results in infections of the central nervous system. The neurotropism of reoviruses relies in the engagement with Nogo receptor 1 (Konopka-Anstadt et al., 2014).
Reoviruses have a double-stranded RNA genome enclosed in two concentric capsid layers, with the outer layer being constituted by σ3 (Nibert, 1998). Virions are internalized by clathrin mediated endocytosis and delivered to late endosomes (Maginnis et al., 2006; Mainou and Dermody, 2012; Mainou et al., 2013). There, virions are subjected to a stepwise, acid-dependent proteolytic processing by cathepsins B and L.

These disassembly steps produce intermediate subviral particles, named ISVPs. ISVPs are characterized by the loss of the outer σ3 shell, the autocatalytic cleavage of μ1 and the extrusion of μ1N (Ebert et al., 2002).

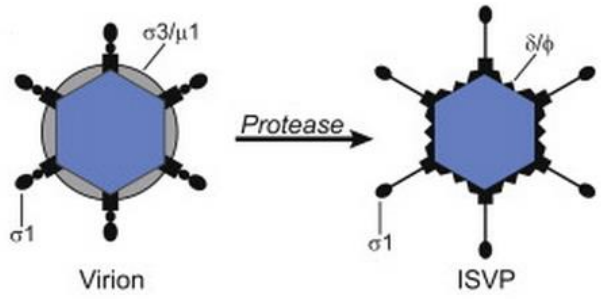

Fig. 9: Representation of a reovirus mature particle and an ISVP. (Konopka-Anstadt et al., 2014)

μ1N is myristoylated and contains a region of alternating hydrophobic residues, features that are essential for virus escape (Agosto et al., 2007; Drayna and Fields, 1982; Hooper and Fields, 1996; Zhang et al., 2009). Myristoylated μ1N generates pores of about 5 nm diameter in erythrocytes and liposomes (Agosto et al., 2006; Ivanovic et al., 2008; Zhang et al., 2009). Yet, such openings are not sufficient for capsid translocation considering that the core of reoviruses which ultimately reaches the cytosol has a diameter of about 75 nm (Agosto et al., 2006). Instead, small pores might be the initial trigger of osmotic swelling or engagement with cellular factors or other events required for efficient membrane penetration in a second moment (Ivanovic et al., 2007). Another possibility proposed by Zhang and collaborators is that a 70 nm pore is generated per endosome. The full release of μ1N would provide 600 copies contained in one endosome of about 250 nm in diameter, for a final peptide concentration of approximately 0.1 mM. This potentially favors the assembly of 250 μ1N hairpins, which would be sufficient to generate a β-barrel pore of 70 nm in diameter (Zhang 2009).

Interestingly, both mature reovirus particles and ISVPs are infectious (Chandran and Nibert, 1998; Chandran et al., 1999). An intriguing question is whether ISVPs, which have the appropriate conformation required for membrane permeation, enter cells via receptor mediated endocytosis or penetrate directly from the PM. Like intact virions, ISVPs bind to JAM-A, but instead of depending on endocytosis they are thought to enter from the PM (Barton et al., 2001b; Borsa et al., 1979; Boulant et al., 2013). Indeed, ISVPs can directly damage membranes (Chandran et al., 2002; Coffey et al., 1998). Studies by Schulz and colleagues addressed this topic and proposed that ISVPs enter cells via a caveolar pathway. Yet, they did not formally exclude the possibility of direct membrane penetration. All in all, these reports suggest that although ISVPs have the potential to directly lyse the PM, the preferred entry pathway seems to be receptor-mediated endocytosis (Schulz et al., 2012). Besides the reasons discussed in the previous section, one possibility is that ISVPs are endocytosed before the critical μ1N/lipid ratio for lysis is reached. Another reason might be that additional intracellular factors required for efficient escape are exclusively recruited from endosomes.

Escape without membrane insertion of viral factors: the unique (?) case of parvoviruses

Parvoviruses are among the smallest viruses with a capsid diameter ranging from 18 to 26 nm, enclosing a single stranded DNA genome. Parvoviruses infect vertebrates as well as insects using a variety of receptors to induce their uptake, mostly by clathrin-mediated endocytosis (Bilkova et al., 2014; Mani et al., 2006; Ros et al., 2006).

Parvovirus capsids are sensitive to pH changes (Bartlett et al., 2000; Parker and Parrish, 2000; Sonntag et al., 2006; Suikkanen et al., 2003), endosomal proteases (Farr et al., 2006; Mani et al., 2006) and lipid composition of the surrounding membrane (Karttunen et al., 2008). Interestingly, Karttunen and colleagues described that the presence of either sphingomyelin or phosphatidylserine in membranes was sufficient to induce capsid rearrangements. A crucial event during rearrangement of the capsid is the exposure of the parvovirus escape factor, VP1. The N-terminus of the minor coat protein VP1 has a conserved domain with Ca^{2+}-dependent phospholipase A2 activity (PLA2) (Dorsch et al., 2002; Filippone et al., 2008; Girod et al., 2002; Vihinen-Ranta et al., 1997).

Mutations that abrogate the enzymatic activity of the PLA2 domain lead to a strong decrease in infection of minute virus of mice (MVM), adeno-associated virus 2, and parvovirus B19 (Farr et al., 2005; Filippone et al., 2008; Stahnke et al., 2011; Zádori et al., 2001). Interestingly, such mutations do not affect capsid assembly, binding and entry, but impair the delivery of the viral genome to the nucleus.

For MVM, defects in PLA2 are rescued by inducing endosomal lysis with either polyethylenimine treatment or co-infection with adenovirus (Farr et al., 2005; Filippone et al., 2008; Stahnke et al., 2011; Zádori et al., 2001), suggesting a specific role for PLA2 in membrane permeabilization. PLA2 catalyses the cleavage of phospholipids into lyso-phospholipids and arachidonic acid. Transformation of phosphatidylcholine, a cylindrical lipid into lyso-phosphatidic acid, an inverted cone-shaped lipid, implies a local modification of membrane curvature. Topologically, this change induces the budding of the limiting membrane towards the endosomal lumen (Shin et al., 2012). Endosomal escape of parvoviruses does not support the co-delivery to the cytosol of other molecules of varying size like FITC-dextran (10 kDa) or sarcin (Parker and Parrish, 2000; Suikkanen et al., 2003). Assuming that uptake markers and viruses are contained in the same endosomal vesicles, these observations indicate that membrane destabilization by PLA2 is small, temporary and rapidly reverted. Of note, Karttunen and collaborators showed that neither SM nor PS affected the enzymatic activity of PLA2 (Karttunen et al., 2008). Together, these observations propose multiple roles for lipids in parvovirus penetration. Firstly, lipids induce rearrangements in the viral capsid, and secondly they support the escape of the virus into the cytosol. Notably, local rearrangements of lipids in terms of membrane shaping are sufficient to destabilize endosomes. Thus, the insertion of viral components into confining membranes is not a pre-requisite for viral penetration, but might rather be part of a more general endosomal destabilization strategy.

2. MEMBRANE DYNAMICS AND SPHINGOLIPID METABOLISM

2.1 Ceramide

Structure, metabolism and compartmentalization

Ceramide was discovered as a structural component of cellular membranes and later emerged as a bioactive lipid. Ceramide is involved in the regulation of cellular processes, such as stress response, apoptosis, cell senescence and growth arrest (Błachnio-Zabielska et al., 2008; Dickson, 2008; Dobrzyń and Górski, 2002; Goldkorn and Filosto, 2010; Guillas et al., 2003; Hannun, 1996; Nikolova-Karakashian and Rozenova, 2010; Pattingre et al., 2009; Stiban et al., 2010).

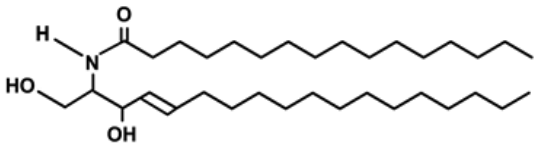

Fig. 10: ceramide C16 (natural).

Ceramide is composed of a sphingoid base connected to a fatty acyl via an amide bond and has an hydroxyl-group exposed on the head. While the sphingoid base is mostly sphingosine, the fatty acyl chains vary in length, saturation and hydroxylation. Ceramide metabolism comprises at least 28 enzymes that generate over 200 structurally distinct ceramides in a combinatorial fashion (Hannun and Obeid, 2011). Most mammalian ceramides have long (C16-20) or very long acyl chains (C22-24), with a few exceptions such as C26-36, which is selectively found in keratinocytes and male germ cells (Sandhoff, 2010). The biological implications of the high variety in ceramide species remain poorly understood (Castro et al., 2014). It is notable, however, that the ceramide metabolism is highly compartmentalized (Ohanian and Ohanian, 2001). Natural ceramides are highly hydrophobic and insoluble in water. They preferentially reside in the membrane where they have been generated. The sub-cellular location of the ceramide generating enzymes therefore is an important factor for the bioactive function of ceramides, for example as cells respond to specific stimuli (Hannun and Obeid, 2011).

Ceramide *de novo* synthesis occurs in the ER (Fig. 11). The first, rate limiting step is the condensation of serine and palmitoylCoA by serine-palmitoyltransferase (Bartke and Hannun, 2009; Carpinteiro et al., 2008). The acyl group is added by ceramide synthase, that combines the metabolite sphinganine with fatty-acylCoA. Mammals have 6 isoforms of ceramide synthase and each displays selectivity for acylCoA of different lengths (Mullen et al., 2012). Thus, ceramide synthases dictate the synthesis of ceramides with different chain lengths. From the ER, ceramide is transported to the Golgi either via ceramide transfer proteins (CERT) or vesicular trafficking. In the Golgi, where ceramide is a building block for the synthesis of either sphingomyelin or glycosphigolipids (Fig. 12 a).

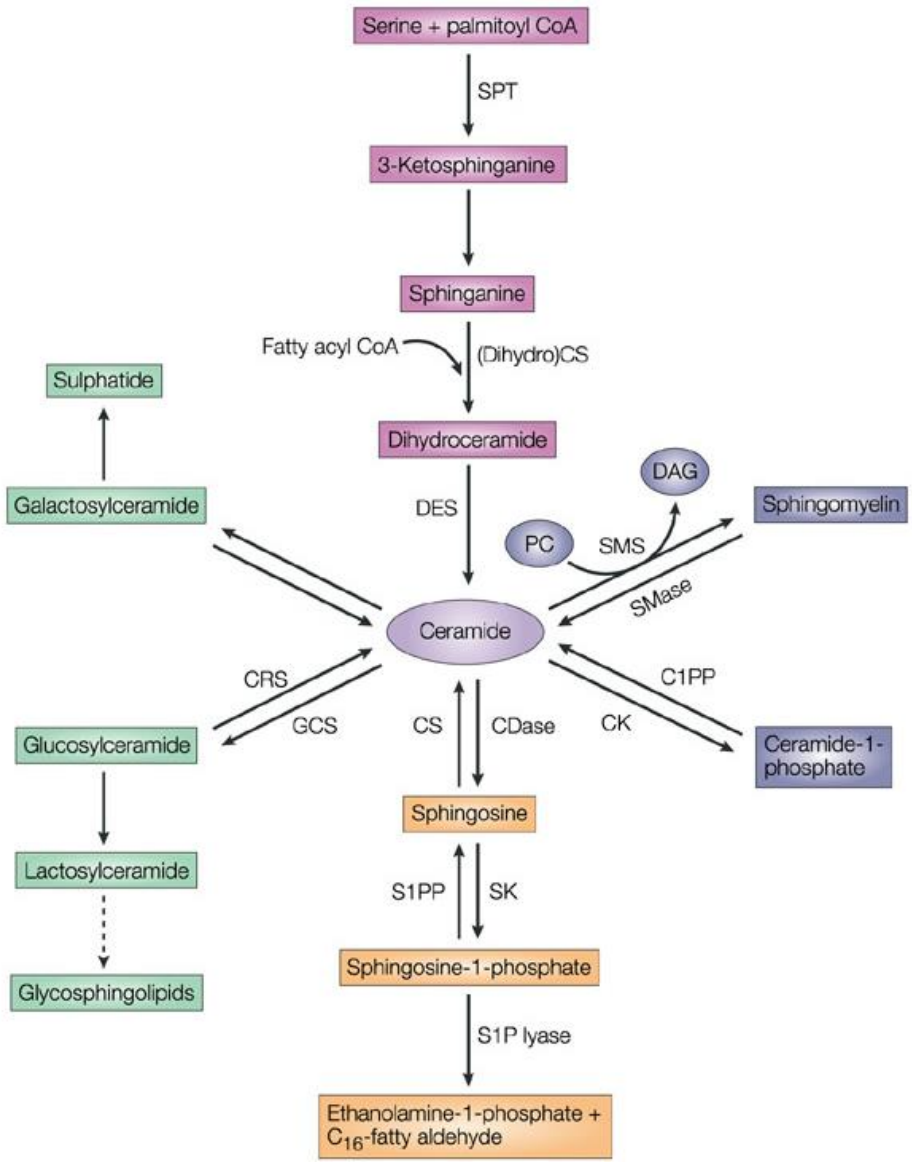

Fig. 11: schematic representation of the ceramide metabolic network. Ceramide is produced *de novo* (violet), or from hydrolysis of sphingomyelin (blue) or cerebrosides (green). Ceramide itself is a substrate for the synthesis of sphingomyelin and glycolipids or the phosphorilation by ceramide kinase (CK) (Sugiura et al., 2002). Ceramides are metabolized by ceramidases (CDase) (el Bawab et al., 2002; Mao et al., 2001; Strelow et al., 2000) to produce sphingosine. Sphingosine is the precursor sphingosine-1-phosphate (S1P), a the last metabolite before final breakdown of sphingolipids into ethanolamine-1-phosphate and C_{16}-fatty-aldehyde by S1P lyase. C1PP, ceramide-1-phosphate phosphatase; CRS, cerebrosidase; CK, ceramide kinase; CS, ceramide synthase; DAG, diacylglycerol; DES, dihydroceramidedesaturase; GCS, glucosylceramide synthase; PC, phosphatidylcholine; S1PP, S1P phosphatase, SMS, sphingomyelin synthase; SMase, sphingomyelinase; SPT, serine-palmitoyltransferase. (Ogretmen and Hannun, 2004)

Besides *de novo* synthesis, ceramide can be generated via the degradation of complex sphingolipids in an ensemble of reactions named salvage pathway. The salvage pathway involves sphingomyelin hydrolysis and breakdown of sphingosine and gluco- or galactosylceramide. Among these, the most frequent and best characterized step is sphingomyelin hydrolysis by acid and neutral sphingomyelinases. Thereby, ceramides are selectively generated at the plasma membrane (Fig. 12 e), in mitochondrial membranes (Fig. 12 b) or in membranes of the endolysosomal system (Fig. 12 d). Further details are described in the section 'Acid sphingomyelinase'.

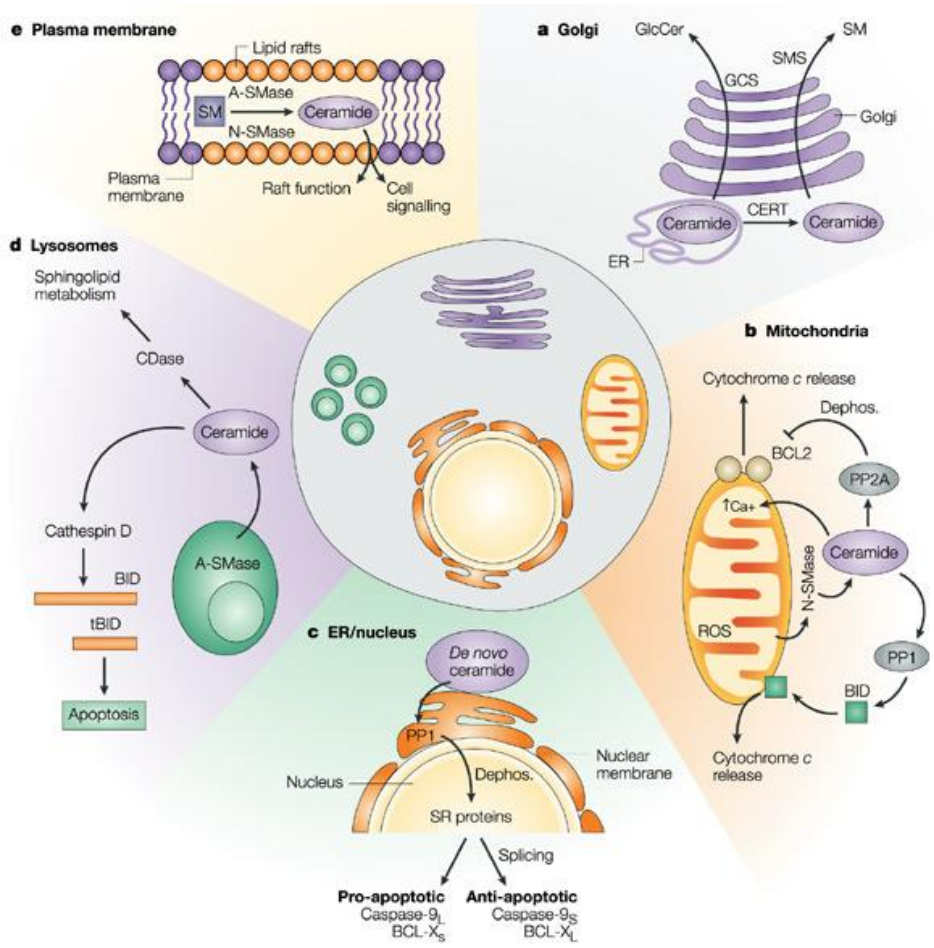

Fig. 12: Selected biological functions of compartmentalized ceramides. Ceramide is generated *de novo* in the endoplasmic reticulum (ER) and transported by CERT to Golgi, where SM is synthesized (Hanada et al., 2003). Glucosylceramides (GlcCer) are produced by glucosylceramide synthase (GCS) in a CERT-independent manner (a). In mitochondria, reactive oxygen species (ROS) activate neutral sphingomyelinase (NSMase) and in turn ceramide production. Mitochondrial ceramide can activate protein phosphatases PP1 and PP2A. These are involved in inactivation of anti-apoptotic factors such as BCL2 (Ruvolo et al., 1999) and Akt or activation of pro-apoptotic factors such an BID (b). *De novo* generated ceramide in the ER and nucleus activates PP1, which dephospohorylates SR proteins (Chalfant et al., 2001). SR proteins in turn regulate the

production of pro/apoptotic factors by alternatively splicing (c). In lysosomes, ASMase generates ceramide from SM and thereby can activate cathepsin D. Cathepsin-D activation triggers a signaling cascade leading to apoptosis (Heinrich et al., 2004). Lysosomal ceramide can be converted to sphingosine by acid ceramidase. Sphingosine is used as a substrate to generate other sphingolipids in different cellular compartments (d). Ceramide can be generated by secreted ASMase on the outer leaflet of the PM, where it might coalesce in lipid rafts (e). Ceramide enriched domains might affect signaling pathways (Henry et al., 2013). CDase, ceramidase; SMS, sphingomyelin synthase. (Ogretmen and Hannun, 2004)

Within the complex network of ceramide metabolism there is one catabolite that stands out for its biologically well known signaling function, sphingosine-1-phosphate and its subsequent breakdown by S1P lyase. S1P binds to a family of five G-protein-coupled receptors and is implicated in angiogenesis, vascular maturation, cardiac development and immunity, as well as cell migration (Rosen et al., 2014). Recently, a role for S1P in endocytosis has been suggested (see discussion; Shen et al., 2014).

The study of ceramides: technical issues

The biological role of ceramides in membranes has been particularly difficult to study, due to technical limitations. Natural ceramides are highly hydrophobic and insoluble in water, therefore it is particularly difficult to tune their content in cells by add-back experiments (Kitatani and Luberto, 2010). This issue was often circumvented by employing synthetic short-chain ceramides such as C2 or C6. C2 and C6 are water-soluble and represent valuable tools for add-back experiments. Studies with C2 and C6 strongly contributed to the advances in the field of sphingolipid research. However, short ceramide species do not occur in cell membranes and have different biophysical properties compared to natural ceramides. Therefore a careful interpretation of the results is needed. Other studies employed synthetic ceramides coupled to fluorophores, to enable their visualization in cells. Yet, the conjugation with these fluorophores alters the natural behavior of ceramides in membranes (Wang and Silvius, 2000). Again, this renders it difficult to interpret data from such add-back experiments.

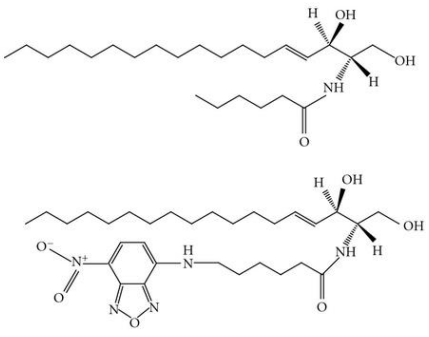

Fig. 13: C6-ceramide (above) and NBD-C6-ceramide (below).

The determination of the sub-cellular localization of ceramides remains a major challenge in the field. For some sphingolipids, an indirect visualization is possible by fluorescently tagging their ligand. Examples are cholera toxin for the detection of GM1 and lysenin to detect sphingomyelin (Sezgin et al., 2012; Yachi et al., 2012). Theoretically, lysenin allows to visualize the conversion of SM to ceramide by live imaging, in the form of the disappearance of the lysenin signal. For this, experimental conditions must be tightly controlled and accurately designed. Antibodies against ceramide would represent a great tool to follow sub-cellular localization of ceramides. Although it is easy to recognize planar ceramides spotted onto membranes, e.g. in lipid overlay assays, it is more challenging to selectively recognize ceramides inserted into bio-membranes, as they only expose a hydroxyl-group on the aqueous face of the membrane (Cowart et al., 2002). Another challenge is to fix lipids and permeabilize cells without compromising the actual lipid architecture of membranes. 'Clickable ceramides' might be valid tools to study ceramide localization. Ceramide analogues coupled to an azide group either in the head or the tail can react *in situ* via 'click chemistry' and be fluorescently tagged (Garrido et al., 2012). Furthermore, lipid probes with photoactivatable and clickable groups offer an opportunity to address protein-lipid interactions in the cellular context (Peng et al., 2014). Whether experimental conditions preserve the natural lipid-protein landscape remains to be determined, however.

Regarding ceramide quantification, the most commonly used biochemical methods are enzymatic diacylglycerol (DAG) kinase assay (Preiss et al., 1987), thin-layer chromatography (TLC; Górska et al., 2002) and high performance liquid chromatography (HPLC; Dobrzyń and Górski, 2002; Yano et al., 1998). Currently, the most valuable method for high-resolution ceramide profiling involves mass spectrometry (Bielawski et al., 2006; Merrill et al., 2005; Shaner et al., 2009; Sullards et al., 2007).

2.2 Acid sphingomyelinase

Sphingomyelinases (SMases) are important players in the sphingolipid metabolism. SMase are specialized phospholipases that catalyse the hydrolysis of sphingomyelin (SM) into ceramide (cer) and phosphorilcholine.

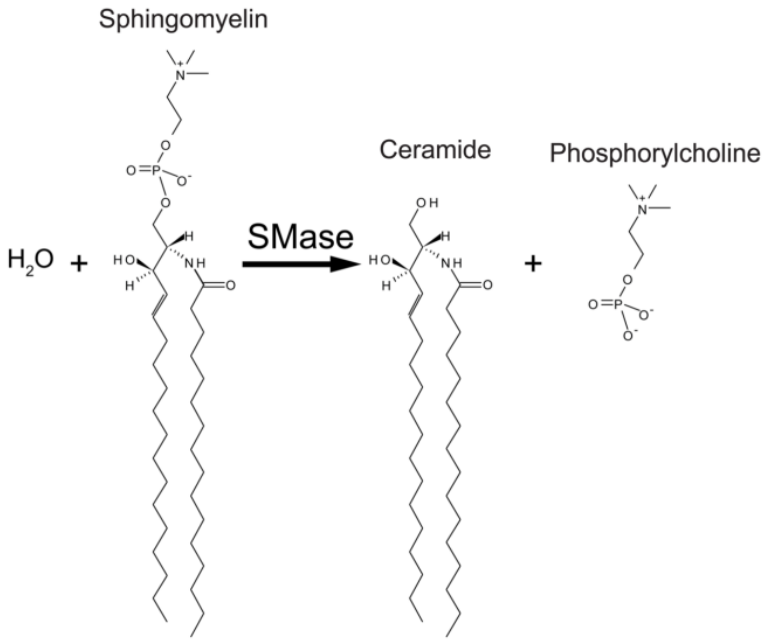

Fig. 14: Schematic representation of sphingomyelin hydrolysis to ceramide and phosphorylcholine by ASMase. (Jenkins et al., 2009)

SMases are categorized into three groups: acid-, neutral- or alkaline-SMase depending on the pH for optimal activity. Of particular interest for this research project is acid sphingomyelinase.

Human acid sphingomyelinase (ASMase) is ubiquitously expressed and enriched in the endothelium of blood vessels, Kupffer cells, spleen, bone marrow, lungs, and macrophages (Otterbach and Stoffel, 1995). ASMase is located in the lumen of acidic intracellular organelles, in particular lysosomes. ASMase shows an optimal enzymatic activity at pH of 4.5-5 (Callahan et al., 1983), but can hydrolyse sphingomyelin also at neutral pH, albeit with lower efficiency (Schissel et al., 1998). Lysosomal ASMase is protected from degradation in the acidic environment of lysosomes by glycosylation. Besides the lysosomal isoform, a second isoform of mature, functional ASMase is found in the secretory network and can be released from the cells (Schissel et al., 1996). The secreted isoform shows a different N-terminal processing and glycosylation profile and uses Zn^{2+} as a cofactor to hydrolyze SM at neutral pH (Callahan et al., 1983). Both isoforms derive from a common primary translation precursor, a pre-proform of 75 kDa. The pre-proform is subjected to removal of the signal peptide and converted into a 72 kDa proform in the ER/Golgi where it undergoes additional cleavages. This results in different forms of the peptide, such as Gly_{66} isolated from lysosomes, the secretory form His_{60} and a lysosomal Gly_{83} isolated from human placenta (Lansmann et al., 1996; Schissel et al., 1996). All forms have Zn^{2+} binding motifs and can be activated by Zn^{2+}, but only the lysosomal form encounters this ion during maturation and trafficking. For *in vitro* studies the activity of lysosomal ASMase is therefore independent of Zn^{2+}, while secretory ASMase requires Zn^{2+} supplementation (Schissel et al., 1996).

ASMase constitutively catalyses the turnover of endocytosed sphingomyelin to ceramide in lysosomes and has a fundamental role in membrane homeostasis. Genetic mutations in ASMase lead to a lysosomal storage disorder named Niemann-Pick disease type A and B (NPD), with an incidence of 1 in 250'000 (http://ghr.nlm.nih.gov/condition/niemann-pick-disease). NPD type A is caused by a severe deficiency in ASMase activity. The symptoms include neurodegeneration, which is manifested early after birth and leads to death within a few years. NPD type B retains some ASMase activity, sufficient to support the development of the neural system, but leads to later onset of pathology, underlined by abnormal accumulation of lipids in spleen, liver, lungs, bone marrow or brain (McGovern et al., 2013). Accumulation of sphingomyelin is often accompanied by disorders in cholesterol metabolism and causes the dysfunction of lysosomes (McGovern et al., 2004). Symptoms and severity of NPD type B depend on the residual ASMase activity. Generally NPD type B patients survive into adulthood without neurodegeneration (Schuchman, 2001).

Besides a constitutive function, ASMase can be activated in response to cellular stress. This increases the ceramide levels at the plasma membrane. This aspect has been extensively studied and a wide variety of stimuli have been identified, including cytokines, differentiation agents, anti-cancer drugs and ligation of death receptor-ligands and TNF receptor family members. In addition, physical stress, such as UV-light and ionizing radiation or chemical stress from ROS were reported to activate ASMase. The resulting cellular response is in most cases either apoptosis, arrest of cell growth or the stimulation of innate immunity (Henry et al., 2013; Stancevic and Kolesnick, 2010). A common feature of ASMase activation is the generation of ceramide enriched domains, which reorganizes PM sub-domains and thereby modulates signal transduction (Stancevic and Kolesnick, 2010). Notably, underlining mechanisms of ASMase translocation to the PM following stress signaling remain elusive.

2.3 Plasma membrane repair and acid sphingomyelinase

Biological, chemical and mechanical stress can trigger membrane perforation. Cell survival to wounding entirely depends on the efficiency of limiting the efflux of cytosolic components. Independent of the nature of the lesion, strategies to sense wounding and to repair the plasma membrane have to be readily available for cell survival. Indeed PM resealing occurs rapidly, within a few seconds. This involves processes dependent on extracellular calcium (Andrews et al., 2014). Extracellular calcium concentrations are approximately 1 mM, while cytosolic calcium concentrations are actively kept very low, around 100 nm (Syntichaki and Tavernarakis, 2003). Calcium normally does not freely diffuse through intact membranes but is transported through selective channels. However, when the PM is injured, calcium flows through the lesion and leads to a sudden increase its cytosolic concentration (Draeger et al., 2011). The small size of this

ion and the considerable difference between extracellular and intracellular levels ensures an increase in cytosolic calcium even after minor wounding events. Calcium is a key factor in signaling wounding and triggering the cellular responses for repair (Draeger et al., 2014).

Lysosomal excocytosis, acid sphingomyelinase and endocytosis of the lesions

Intracellular calcium increase triggers the exocytosis of lysosomes, mostly the membrane-proximal subset of lysosomes (Jaiswal et al., 2002; Rodríguez et al., 1997). Lysosomal exocytosis was first observed in cells containing specialized secretory organelles, such as melanocytes, cytotoxic lymphocytes and alveolar cells (Griffiths, 1996). It later emerged that Ca^{2+}-triggered exocytosis extends to a multitude of cells types, including for example muscle fibers (Andrews, 2000; Bergsbaken et al., 2011; Griffiths, 1996; Keefe et al., 2005). Exocytosis is modulated by the lysosomal proteins synaptotagmin VII (syt VII) and mucolipin-1. While syt VII senses calcium and promotes fusion of lysosomes with the PM (Pang and Südhof, 2010), mucolipin-1 is a non-selective cation channel through which cytosolic calcium concentration can be modulated (Medina et al., 2011).

The mechanisms of how lysosomal exocytosis contributes to membrane repair are currently debated (Andrews et al., 2014; Draeger et al., 2014). Exocytosis provides additional membranes that either facilitate spontaneous resealing by decreasing the overall membrane surface tension (Togo et al., 2000). Alternatively, they might directly ‚patch' the lesions (McNeil et al., 2000). Studies with pore-forming proteins such as bacterial streptolysin-O (SLO) and perforins released by cytotoxic lymphocytes revealed that injured cells undergo extensive endocytosis. Pores localize into numerous endocytic vesicles seconds after wounding and are found in larger vesicles after few minutes (Idone et al., 2008; Keefe et al., 2005). Remarkably, PM resealing by endocytosis is a common mechanism also found in non-mammals, such as crayfish neurons (Eddleman et al., 1998), or intestinal cells of *C. elegans* (Los et al., 2011).

Lysosomal exocytosis implies the release of lumenal hydrolases to the outer leaflet of the PM. Among these enzymes, ASMase emerged as a key regulator of endocytosis. Cells with reduced ASMase activity by either drug treatment, siRNA mediated knock down, or genetic mutation are competent for lysosomal exocytosis, but fail to produce surface ceramide (Babiychuk et al., 2008) and endocytosis mediated PM sealing (Tam et al., 2010). Importantly, the add-back of exogenous bSMase fully restores PM repair (Tam et al., 2010) even in absence of extracellular calcium (Tam et al., 2013a). This suggests that ASMase is the primary mediator of endocytosis and membrane sealing. Which cellular machinery is involved in ASMase-mediated endocytosis is still under characterization. ASMase-mediated PM repair involved dynamin-independent endocytosis (Corrotte et al., 2013; Idone et al., 2008; Tam et al., 2010).

Besides ceramide, cholesterol is required for endocytosis after PM injury (Idone et al., 2008; Lariccia et al., 2011). Cholesterol is known to associate with lipid rafts with SM and these rafts participate to caveolin-mediated endocytosis (Simons and Sampaio, 2011). Remarkably, siRNA mediated knock-down of caveolin inhibited the repair of cells wounded with SLO, and SLO pores were found to internalize in caveolin positive compartments (Corrotte et al., 2013). Other stress conditions, such as osmotic shock (Parton et al., 1994) and detachment from the substrate (del Pozo et al., 2005) triggered caveolar mediated endocytosis. In line with these findings, several cell types exposed to mechanical stress such as endothelial cells, adipocytes and muscle fibers show an enrichment in caveolar structures proximal to the PM (Parton and Simons, 2007). Accordingly, a role for caveolar endocytosis is proposed in maintaining sarcolemmal integrity of the sarcolemma in muscle cells (Bonilla et al., 1981; Gazzerro et al., 2010; Rajab et al., 2010; Repetto et al., 1999; Zhu et al., 2011). However, if lipid rafts/caveolin is the only endocytic pathway capable of endocytosis for PM repair remains an open question (Andrews et al., 2014).

PM blebbing, isolation of lesion in membranes and microvesicle shedding

PM permeabilization with SLO or employing UV laser revealed a cellular response involving the formation of PM blebs towards the extracellular space (Idone et al., 2008; Jimenez et al., 2014). Such blebs have been associated to transient remodeling of the actin cytoskeleton triggered by cytosolic calcium (Charras et al., 2006). These blebs might be either retracted or shed. Both possibilities are plausible and the outcome might depend on the amplitude of the calcium transients and the efficiency of membrane resealing (Idone et al., 2008). The shedding of microvesicles has been shown to remove pores induced by the complement (Morgan, 1989) as well as pores formed by bacterial toxins (Babiychuk et al., 2009; Keyel et al., 2011; Potez et al., 2011). The release of microvesicles is regulated by proteins of the annexin family (Atanassoff et al., 2014; Babiychuk et al., 2009; Potez et al., 2011). Annexins are ubiquitously expressed calcium sensitive proteins, that re-localize from the cytosol to the plasma membrane following intracellular calcium increase (Monastyrskaya et al., 2007). Annexins are capable of binding to negatively-charged phospholipids and fusing membranes (Babiychuk et al., 2009; Creutz et al., 1978; Potez et al., 2011). By these properties, annexins are proposed to be rapidly recruited to the site of wounding and fuse the tips of the membrane bleb enclosing the lesion (Atanassoff et al., 2014; Babiychuk et al., 2009; Bouter et al., 2011; McNeil et al., 2006; Potez et al., 2011).

Membrane blebbing also involves components of the ESCRT machinery (Jimenez et al., 2014). CHMP4B, CHMP2aA and Vps4 are recruited to the wounded sites and contribute to the repair of small openings (size < 100 nm), but not large lesions (Jimenez et al., 2014). The vesicles generated by ESCRT are generally about 50 nm in diameter (Cashikar et al., 2014; Murk et al., 2003) but membrane protrusions following PM injury range between 200 to 500 nm in size (Jimenez et al., 2014). Besides the discrepancy in the dimensions,

there is an additional issue with the timing: the recruitment of the ESCRT machinery to the wounded sites occurs in an energy independent manner, but too slowly to mediate resealing within a few seconds (Corrotte et al., 2013; Jimenez et al., 2014; McNeil and Kirchhausen, 2005; McNeil et al., 2000). Further investigations are required to understand the precise involvement of the ESCRT components in PM repair.

Using shedding or endocytosis, cells have evolved mechanisms to promptly isolate and remove lesions from the plasma membrane. Which repair strategy will be chosen depends on the cell type and morphology, the size and localization of the lesion and the extent of calcium influx. All in all, these processes collaborate to avoid catastrophic events of cell 'explosion' and ensure either full recovery of the compromised cells, or controlled cell death by apoptosis (Andrews et al., 2014; Draeger et al., 2014).

3. ADENOVIRIDAE

Adenoviruses are non-enveloped, double-stranded DNA viruses of about 90 nm (van Oostrum and Burnett, 1985). The family of Adenoviridae comprises 5 genera, infecting a broad variety of vertebrates. Human adenoviruses (HAdV) are the largest genus, and encompasses more than 60 characterized species. HAdV are associated to diseases of the upper and lower respiratory tract, gastroenteritis and conjunctivitis depending on the serotype (Table 1; Zhang and Bergelson, 2005). Infection symptoms are generally mild in adult immunocompetent individuals, but can be severe and life-threatening in children and immunocompromised people.

Species	Serotype	Tropism/ Diseases
A	12, 18, 31	Intestinal / Cryptic enteric infections
B1	3, 7, 16, 21, 50	Respiratory / Upper-airway infections
B2	11, 14, 34, 35	Renal/ Kidney and urinary tract infections
C	1, 2, 5, 6	Respiratory / Upper-airway infections, liver infections
D	8, 9, 10, 13, 15, 17, 19, 20, 22-30, 32, 33, 36-39, 42-47, 48, 49, 51	Ocular and other infections/ Epidemic keratoconjunctivitis
E	4	Respiratory/ Pneumonia
F	40, 41	Intestinal/ Gastroenteritis
G	52	Intestinal / Gastroenteritis

Table 1: Classification and diseases of human adenoviruses. (modified from Zhang and Bergelson, 2005)

Since their discovery by Rowe et al. in the fifties (Rowe et al., 1953) HAdV served as a tool to enlighten cell biology processes and host-pathogen interactions. HAdV are currently widely employed as oncolytic and gene therapy vectors (Wold and Toth, 2013).

HAdV has an icosahedral shell composed of three major proteins associated into 240 trimeric hexons, 12 pentameric penton base proteins at each vertex and 12 trimeric fiber proteins. Fibers are anchored to the penton base, protrude from the capsid and mediate attachment to host receptors via the globular knob domain. The capsid is additionally stabilized by complex networks involving the four minor proteins IIIa, VI, VIII and IX (Burnett, 1985; Stewart et al., 1993). Despite the recently accomplished great advances in solving adenoviral structures by crystallography and cryo-EM (Liu et al., 2010; Reddy et al., 2010; Reddy and Nemerow, 2014), the exhaustive 3D map of the minor proteins remains a matter of debate.

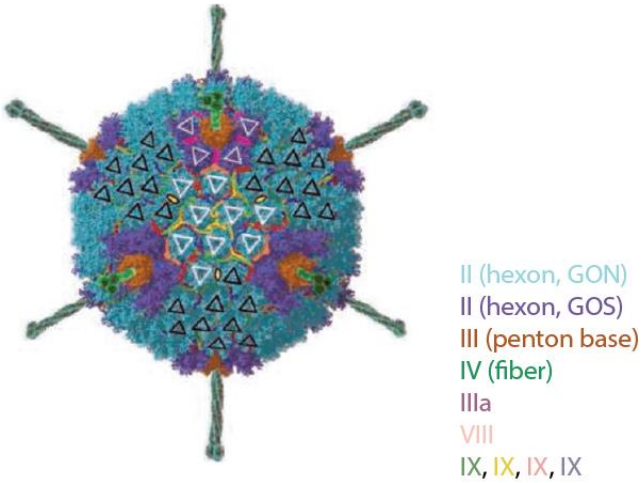

Fig. 15: Representation of an adenovirus with structural components highlighted. GON: 'groups of nine' are the hexon trimers that form a planar sheet-like structure within each face. GOS: 'group of six', assembly of 'peripentonal hexons' and pentons. (Harrison, 2010)

The importance of the minor proteins for virus infectivity emerged by studying the HAdV-C2 temperature sensitive mutant Ts1. Ts1 is successfully internalized by host cells but fails capsid maturation, uncoating and endosomal escape (Hannan et al., 1983). This phenotype is attributed to a point mutation in the viral cysteine protease L3/p23 (Imelli et al., 2009). The viral cysteine protease L3/p23 is located in the interior of the immature virion, is fully activated by binding to DNA and VI (Graziano et al., 2013; Mangel et al., 1993; Webster et al., 1993) and processes IIIa, VI, and VIII as well as the core components VII, X and the terminal protein (TP) (Hassell and Weber, 1978; Rancourt et al., 1995; Russell, 2009).

Protein VI is a 23 kDa polypeptide, present in about 360 copies per virion (Benevento et al., 2014; Lehmberg et al., 1999; van Oostrum and Burnett, 1985), with multiple functions during the whole viral life cycle. During entry and replication mature VI is indispensable for endosomal escape (Wiethoff et al., 2005) and prevents suppression of viral gene expression by innate immune components such as *Daxx* (Schreiner

et al., 2012). During viral assembly and maturation, immature VI shuttles the hexon trimers into the nucleus and triggers viral maturation (McGrath et al., 2003). In the intact virus, VI is likely located underneath the hexon trimers (Liu et al., 2010), with one VI tightly associated to each peripentonal hexon (Reddy and Nemerow, 2014) and interacts with the core protein V (Matthews and Russell, 1998). Yet, it remains difficult to understand the full picture of VI positioning: 360 copies of VI are too much for being associated one per hexon trimer (copy number 240) but too low to bind one per hexon (copy number 720) (San Martín, 2012).

During endocytosis and capsid uncoating, VI is exposed to the viral surface and its N-term domain folds into an amphipathic alpha-helix (Burckhardt et al., 2011; Reddy and Nemerow, 2014; Wiethoff et al., 2005). The role of VI in endosomal escape is further discussed in the section Adenovirus entry and penetration.

Protein IX is present in 240 copies per capsid (van Oostrum and Burnett, 1985), and is the only minor protein exposed to the surface of the intact virion (San Martín, 2012). IX is not essential for virus assembly but strongly contributes to the virion stability (Colby end Shenk, 1981). According to Liu et al., trimers of protein IX form a stable network on the capsid shell, where both C- and N-termini are exposed on the surface of the virion (Liu et al., 2010). Trimers of IX are interconnected by four helix bundles involving three C-term and one N-term and a trimeric joint of N-term domains with an hydrophobic core.

Protein IIIa is proposed to assemble under each vertex in a ring of 5 monomers, for a total copy number of 60. Several residues of IIIa (300 to 585) could not be traced by cryo-EM (Liu et al., 2010), suggesting that these residues interact with the core of the capsid which is non-icosahedral (San Martín, 2012). IIIa is proposed on the one hand to stabilize assembling and intact capsids and on the other hand to promote the release of vertices and genome during uncoating (D'Halluin et al., 1978; San Martín, 2012; San Martín et al., 2008).

The 120 copies of protein VIII are in the inner capsid, underneath the boundaries of penton bases and hexons (Liu et al., 2010).

3.1 Adenovirus entry and penetration

The overall process of adenovirus entry involves attachment to the host, internalization, endosomal escape, uncoating and delivery of the viral genome to the nucleus. Best studied is the entry pathway of the closely related serotypes HAdV-C2 and HAdV-C5. The specificity of HAdV-C2/5 for the host is mediated by the high affinity binding (Kd=15 nM) of the distal knob domain of the viral fiber to the coxsackievirus B and adenovirus receptor (CAR) (Bergelson et al., 1997; Howitt et al., 2003; Kirby et al., 2000). CAR is a type 1 transmembrane protein of the immunoglobulin superfamily, expressed in several human tissues including lung, liver, heart and brain and involved in cell-cell contacts and adherent-junctions (Howitt et al., 2003). Viruses bound to CAR undergo drifts on the plasma membrane, and confined motions that depend on

actomyosin-2, until they engage with immobile αvβ3 or αvβ5 integrins via the RGD domain on penton base (Burckhardt et al., 2011; Chiu et al., 1999; Wickham et al., 1993). Viruses anchored to integrins and simultaneously drifting on CAR are subjected to mechanical forces that trigger the release of the fibers, thereby initiating the stepwise uncoating program of the viral capsid (Burckhardt et al., 2011; Greber et al., 1993; Nakano et al., 2000). The integrin/penton base interaction induces the clockwise untwisting of the pentamere and further loosens the viral capsid (Lindert et al., 2009). Fiber loss is essential for infection (Nakano et al., 2000) and surface signaling events involving integrin stimulated clathrin- and dynamin mediated endocytosis of the viruses (Shayakhmetov et al., 2005). Internalization might be facilitated by the recruitment of the adaptor complex AP-2 by the NPXY (asparagine-proline-any amino acid-tyrosine) motif in β3 or β5 (Gastaldelli et al., 2008; Meier et al., 2002; Wang et al., 2000; Wolfrum and Greber, 2013).

In coordination with endocytosis, capsids undergo a stepwise dismantling program and start to release the major coat proteins penton and hexon, as well as the stabilizing proteins IX and VI (Greber et al., 1993; Martin-Fernandez et al., 2004). A crucial event for endosomal escape is the externalization of the inner capsid protein VI. VI has an N-terminal amphipathic α-helix (residues 34 to 54) with proposed membrane lytic activity (Wiethoff et al., 2005). This function was first suggested by *in vitro* experiments, in particular it was observed that heat-uncoated viruses lose the ability to lyse liposomes if VI is immunodepleted (Wiethoff et al., 2005). Of note, infectivity of HAdV-C5 and co-delivery to the cytosol of the toxin saporin were reduced in cells pre-incubated with anti-VI antibodies used for immunodepletion (Maier et al., 2010). Additional studies with recombinant versions of VI identified the residues 34 to 54 as being responsible for membrane disruption in a pH independent manner (Maier et al., 2010; Wiethoff et al., 2005). Importantly, the mutant VI-L40Q shows reduced membrane lytic capacities *in vitro* and HAdV-C5-VI-L40Q is less infectious compared to HAdV-C5 (Moyer et al., 2011). Another mutation in the alpha-helical domain of VI, G48C, also lowered *in vitro* membrane disruption capacities (Moyer and Nemerow, 2012). In addition, the insertion of cystein led to the formation of aberrant disulfide bonds between VI within the capsid.

As a consequence, VI release on the plasma membrane or endosomes was impaired (Moyer and Nemerow, 2012). Attempts to elucidate the mechanisms of lysis indicated that recombinant VI binds to model membranes in a parallel orientation and induces positive membrane curvature, thereby likely triggering membrane fragmentation (Maier et al., 2010). In contrast, VI-L40Q displays a different pattern of membrane interaction. Still, the precise mechanism of how the amphipathic alpha helical domain of VI lyses membranes remains poorly understood (Moyer and Nemerow, 2011). Part of the 360 copies of VI is proposed to be released from the capsid and associate to endosomal membranes (Maier et al., 2012). The rest of VI gets degraded presumably by virtue of the viral L3/p23 protease (Greber 1993, 1996).

By engaging with dynein intermediate chain and exploiting dynactin dependent transport (Kelkar et al., 2004; Suomalainen et al., 1999) capsids reach the nucleus. There, they dock on Nup214/Nup88 at the nuclear pore complex (NPC) (Trotman et al., 2001). The docking is mediated by the nucleoporin Nup214, and uncoating is facilitated by Nup358 which activates the heavy chain Kif5c of kinesin-1 (Strunze et al., 2011). Kinesin motions provide the pulling force to complete capsid uncoating, and partially compromise the integrity of the NPC. The viral genome is finally imported into the nucleus with the contribution of additional factors, including the histone H1, importin β1, β2 and β7 (Hindley et al., 2007; Saphire et al., 2000; Trotman et al., 2001; Wodrich et al., 2006).

During the early phase of infection regulatory proteins are synthesized to promote cell replication (Frisch and Mymryk, 2002), to suppress the detection of viral components by the immune system (Lichtenstein et al., 2004) and to block the cellular DNA damage response machinery (Bischoff et al., 1996). Meanwhile, the replication of the viral DNA is initiated. In the late phase structural components of the virus are produced and the new virions are assembled. The viral life cycle culminates with the release of the mature progeny viruses by cell lysis (Tollefson et al., 1996).

AIM OF THE THESIS

How HAdVs interact with lipids to cross host membranes remains poorly understood. The aim of this thesis is to identify and study specific lipid requirements during entry of HAdV-C2/C5. A particular focus is given to the differences between WT and the escape mutant Ts1, with the intention to reveal lipid rearrangements that specifically support viral escape from endosomes. Moreover, the molecular mechanisms underlining the regulation of lipids by incoming HAdV will be addressed.

RESULTS

Using mass spectrometry, we followed 159 lipid species during early steps of adenovirus infection. Only two ceramide species were significantly up-regulated at 30 minutes after infection with HAdV-C2 (Log2 fold change > 0.4, P-value < 0.05). Ceramide remodeling was induced by WT adenovirus but not by TS1 (Fig. 1a), a mutant that successfully engages with the primary receptor CAR and the co-receptor integrins but fails to uncoat and cross the endosomal membrane (Burckhardt et al., 2011; Gastaldelli et al., 2008; Greber et al., 1996; Nakano et al., 2000; Pérez-Berná et al., 2009). Ceramides are essential structural components of membranes and potent signalling factors involved in membrane microdomain function, such as formation of vesicles, cell signalling, or cell death (Bartke and Hannun, 2009; Goñi and Alonso, 2009). To identify which ceramide biosynthesis pathway was activated by incoming HAdV, we used a set of inhibitors targeting ceramide *de novo* synthesis (He et al., 2004), salvage pathway (Wang et al., 1991), and neutral (Luberto et al., 2002) and acid sphingomyelin hydrolysis (Kornhuber et al., 2008) (Fig. 1b). Solely inhibition or silencing of acid sphingomyelinase (ASMase) reduced adenovirus infection (Fig. 1 c,d, and S1a, d-f). On-target action of amitriptyline and siRNA against ASMase was confirmed by measuring the enzymatic hydrolysis of 6-Hexadecanoylamino-4-methylumbelliferylphosphorylcholine (HMU-PC), a fluorogenic, specific ASMase substrate (van Diggelen et al., 2005) (Fig. 1e). To further validate the requirement of ASMase for infection, we performed gain-of-function experiments in untransformed fibroblasts (GM00112) that exhibit no detectable ASMase activity (Levran et al., 1992). When the inoculum was supplemented with purified bacterial sphingomyelinase (bSMase), the infection level was strikingly increased (Fig. 1f). ASMase is a fundamental regulator of membrane homeostasis and constitutively hydrolyses sphingomyelin (SM) into Cer and phosphorilcholine in late endosomes and lysosomes (Ferlinz et al., 1994). SM plays an essential role in formation of lipid rafts (McIntosh et al., 1992), is enriched in the outer leaflet of the plasma membrane and traffics through the endolysosomal network (Koivusalo et al., 2007). To unravel the function of ceramide early in infection, we inhibited lysosomal ASMase by amitriptyline and dissected specific virus entry steps. Virus attachment and the initial step of uncoating, CAR mediated fiber shedding, were unaffected (Fig. S2a,b). However, we found that ASMase inhibition delayed the kinetics of adenovirus endocytosis (Fig. S2 c,d). BSMase addition to the inoculum rapidly increased ceramides (Fig. 2i), readily rescued the uptake of HAdV-C2 and accelerated internalization of TS1 (Fig. S2 d,e). Competitive inhibition of bSMase by HMU-PC, which is a soluble bSMase substrate, blocked the rescue (Fig. S2d,e). This underlines the specific requirement of the sphingomyelinase activity for HAdV infection. The results revealed that a spatiotemporal increase in ceramide abundance enhances virus internalization. Rapid internalization is critical for productive infection, as in the natural site of infection viral particles exposed extracellularly are vulnerable to neutralization by immune system mediators (Hendrickx et al., 2014; Smith and Nemerow, 2008).

Endocytosed virions traffic to early endosomal compartments, where the stepwise uncoating process culminates in the externalization of the membrane lytic factor protein VI (Burckhardt et al., 2011; Wiethoff et al., 2005). Protein VI interacts with lipid bilayers *in vitro* (Wiethoff et al., 2005) and mediates endosomal escape of the virus *in vivo* (Maier et al., 2010; Moyer and Nemerow, 2012; Moyer et al., 2011). Yet, how the lipid landscape influences this process is not known. To examine the involvement of ceramide in endosomal penetration, we analyzed the exposure and retention of VI on internalized viruses. While inhibition of ASMase reduced the exposure of VI, simultaneous addition of exogenous bSMase fully reverted this effect (Fig. 2a). We next determined the penetration efficiency by measuring cytosolic viruses using the SLO immunofluorescence assay and also EM analyses (Suomalainen et al., 2013). To exclude effects reminiscent of the kinetic delay in endocytosis, we evaluated endosomal escape when most viral particles were already internalized (Fig. S2f,g). Notably, limited VI exposure directly correlated with reduced endosomal escape (Fig. 2b, S2f). Interestingly, the addition of bSMase rescued the escape efficiency of WT virus, while TS1, which fails to expose VI, remained trapped in the endolysosomal network (Fig. 2b). These findings indicate that ceramide production at the plasma membrane before or during viral endocytosis enhances viral uptake and escape from endosomes. We next assessed if VI specifically interacted with ceramide-rich membranes. Partially uncoated viral particles (Fig. 2d) were exposed to liposomes composed of either POPC, POPC:SM 99:1 or POPC:CER 99:1. Liposomes bound to viral proteins were separated from empty liposomes and unbound viral components by floatation. The isolated fractions were and analyzed by immunogold EM with an antibody against VI (Fig. 2c,e). While VI floating with POPC vesicles was nearly undetectable, VI strikingly associated with sphingolipids containing membranes, with a strong preference for ceramide over SM (Fig. 2e,f). To analyze how these interactions influence the integrity of liposomes, we performed liposomes leakage assays (Fig. 2g). Liposomes were produced using total lipid extracts from HeLa cells (Wu et al., 1980), and enriched in ceramide by bSMase treatment (Fig. 2g). Uncoated HAdV-C5 triggered lysis of liposomes, a phenomenon that was remarkably enhanced by ceramide (Fig. 2h). To address the role of VI in this process, we tested the HAdV-C5 mutant VI-L40Q. L40Q harbors a point mutation in the N-terminal amphipathic α-helix of VI and exhibits attenuated membrane lysis activity (Moyer et al., 2011). VI-L40Q led to limited leakage of high-ceramide liposomes at equal doses as WT virus. This confirmed that VI is the primary mediator of leakage (Fig. 2h). Together, the results support a model where a lipid microenvironment enriched in ceramide favors endocytosis and endosomal escape.

How do incoming viruses ensure lipid remodeling at the right time and at the right place? We wondered if the lysosomal ASMase is subjected to re-localization during infection. To test this, we collected the supernatant of infected cells and measured the enzymatic activity of ASMase and another lysosomal enzyme, β-hexosaminidase (Rodríguez et al., 1997; van Diggelen et al., 2005). We found that the activity of both enzymes was increased at the exoplasmic leaflet of the PM immediately following virus binding (Fig. 3a,b, S3a,b). This event was ligand-specific, as TS1, cholera toxin B or competitive inhibition of virus binding

by soluble CAR (CARexFC) (Ebbinghaus et al., 2001) did not lead to release of ASMase or β-hexosaminidase into the supernatant (Fig. 3a). Importantly, β-hexosaminidase translocation was independent of ASMase activity, as HAdV inoculated cells treated with amitriptyline also released β-hexosaminidase (Fig. 3a). Neither control nor infected cells released the cytosolic enzyme lactate dehydrogenase, a tetramer with a molecular weight of about 140 kDa (Evans et al., 1985), indicating that the plasma membrane was not severely damaged by the virus (Fig. S3a,b). Lysosomal exocytosis is involved in the repair of small wounds in the plasma membrane (Idone et al., 2008; Tam et al., 2010) and is triggered by the influx of extracellular Ca^{2+} through the lesions. In accordance, lysosomal exocytosis was completely abrogated without extracellular Ca^{2+} but occurred normally without extracellular magnesium (Fig. 3c).

To visualize the dynamics of Ca^{2+} fluxes, cells expressing the Ca^{2+} sensor GCamP5G (Akerboom et al., 2012) were imaged during infection. While resting cells rarely showed spontaneous Ca^{2+} spikes, infected cells showed frequent, multiple and rapid increases in cytosolic Ca^{2+} coinciding with virus binding and endocytosis (Fig. 3e). This phenomenon was not observed with TS1 infection or in absence of extracellular Ca^{2+} (Fig. S4a,b). Of note, abrogation of extracellular Ca^{2+} after virus binding delayed endocytosis of WT but not Ts1 and reduced infection, consistent with being a trigger for lysosomal exocytosis (Fig. S3d-f). Lysosomal exocytosis was linked to viral escape, as both events were inhibited by nocodazole treatment (Fig. 3c,d, and S3g). Notably, the absence of lysosomal exocytosis could be bypassed by the addition of bSMase in the inoculum, indicating that surface ASMase was a critical factor to enhance virus escape from endosomes (Fig. 3d).

To identify how extracellular Ca^{2+} accessed the cytosol, we analyzed integrity of the plasma membrane by time-lapse imaging of propidium iodide (PI), a membrane impermeant nucleic acid dye (Jimenez et al., 2014). Incoming HAdV-C5 provoked the influx of PI from the extracellular medium, visible as discrete spots at the cell periphery (Fig. 3f). The influx of PI was quickly resolved and always correlated to cytosolic Ca^{2+} spikes (Fig. 3f,g), suggesting the existence of transient and rapidly resealing membrane lesions. In rare cases, cells exhibited a non-resolvable PI staining (Fig. 3g, S4d), likely indicating a failure of lesion repair. This was supported by the notion that these cells showed extensive plasma membrane blebbing, which can be a predictor for apoptosis (Fig. S4d) and (Jimenez et al., 2014).

We next tested the hypothesis that the transient membrane lesions were caused by a release of viral factors from the incoming virus. We monitored PI fluxes in cells expressing Dyn2K44A-GFP, conditions that block viral endocytosis but not the release of the fibers (Meier et al., 2002; Nakano et al., 2000). The results show that influx of PI occurs in presence of Dyn2K44A-GFP, indicating that the plasma membrane is permeabilized by incoming virus (Fig. S4f). We next tested if VI was involved in membrane permeabilization. The permeabilization of cells exposed to either VI-L40Q or uncoated HAdV-C5 incubated with a neutralizing anti-VI antibody was significantly reduced (Fig. 3h,i, S3e). These observations are in accordance with previous reports showing a capacity of uncoating competent viruses to permeabilize

cellular membranes (Di Paolo et al., 2013; Wickham et al., 1994). Collectively, our data establish a model for how an incoming non-enveloped virus harnesses Ca^{2+} signaling to hijack host lipid metabolism, produces specific lipid signatures and effectively overcomes the host cell membrane (Fig. 4).

Figure 1:

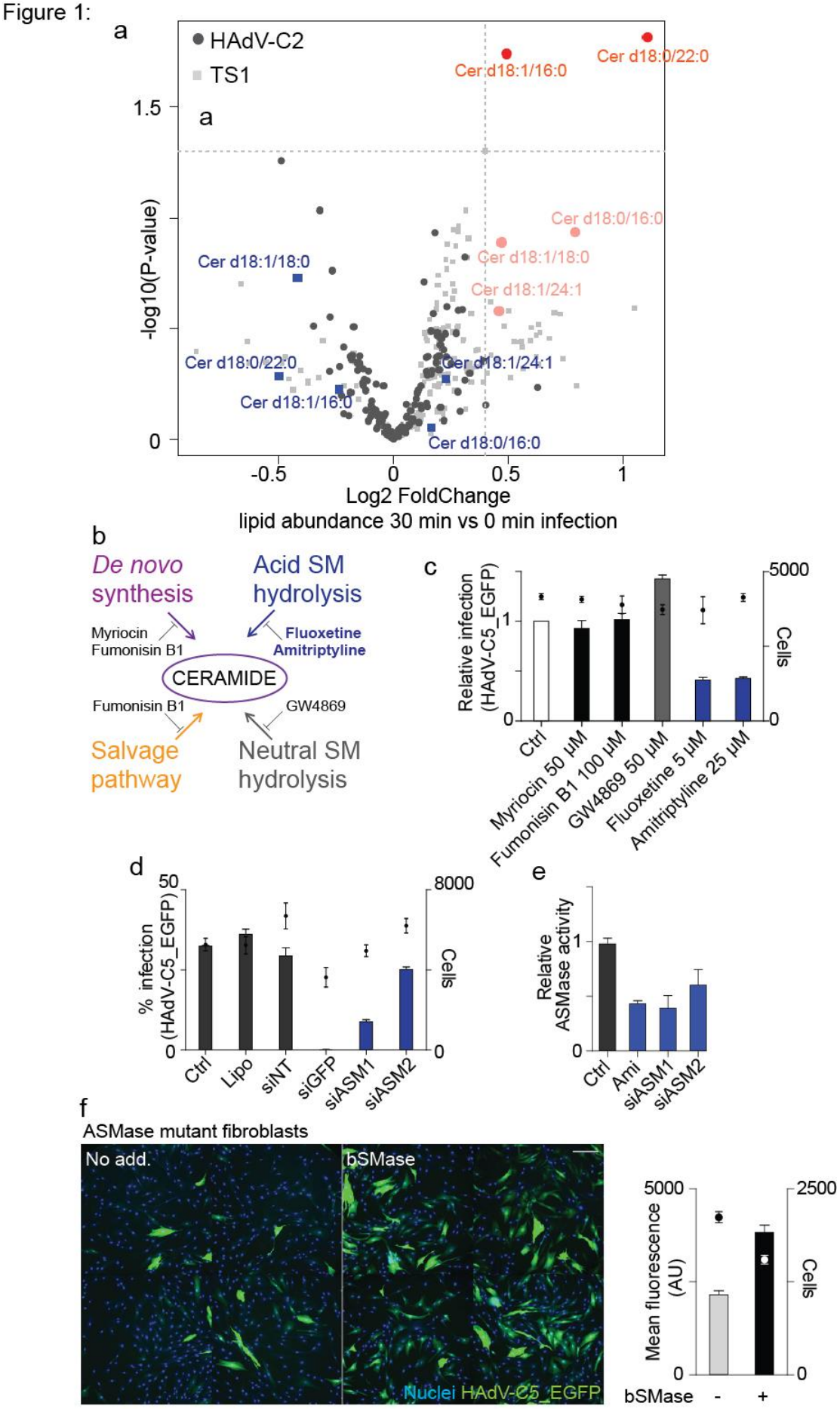
a
HAdV-C2
TS1
a
Cer d18:1/16:0
Cer d18:0/22:0
Cer d18:0/16:0
Cer d18:1/18:0
Cer d18:1/24:1
Cer d18:1/18:0
Cer d18:0/22:0
Cer d18:1/24:1
Cer d18:1/16:0
Cer d18:0/16:0
1.5
0
-log10(P-value)
-0.5
0
0.5
1
Log2 FoldChange
lipid abundance 30 min vs 0 min infection
b
De novo synthesis
Acid SM hydrolysis
Myriocin
Fumonisin B1
Fluoxetine
Amitriptyline
CERAMIDE
Fumonisin B1
GW4869
Salvage pathway
Neutral SM hydrolysis
c
Relative infection (HAdV-C5_EGFP)
Cells
5000
1
0
Ctrl
Myriocin 50 µM
Fumonisin B1 100 µM
GW4869 50 µM
Fluoxetine 5 µM
Amitriptyline 25 µM
d
% infection (HAdV-C5_EGFP)
Cells
50
8000
0
Ctrl
Lipo
siNT
siGFP
siASM1
siASM2
e
Relative ASMase activity
1
0
Ctrl
Ami
siASM1
siASM2
f
ASMase mutant fibroblasts
No add.
bSMase
Nuclei HAdV-C5_EGFP
Mean fluorescence (AU)
Cells
5000
2500
0
bSMase
-
+

Figure 1: Ceramides generated by acid sphingomyelinase are selectively enriched by incoming adenovirus and support infection

a) Comparative lipidomics of HeLa Ohio cells infected for 30 min with either HAdV-C2 or TS1 is shown. Ceramide species are highlighted.

b) Schematic representation of selected ceramide generating pathways and respective inhibitors.

c,d,e) Chemical inhibition and silencing of ASMase reduced infection and ASMase cellular activity. HeLa Ohio cells were treated with the indicated drugs for 4h before and 16h during infection or transfected using lipofectamine (Lipo) with siRNA sequences specific for ASMase (siASM1, siASM2), GFP (siGFP), or non targeted sequences (siNT) for 72h before infection. Lysates of treated cells were incubated with HMU-PC, a fluorogenic substrate of ASMase.

f) Addition of bSMase to the inoculum enhanced infection of GM00112 cells. Scale bar=200 μM.

Figure 2:

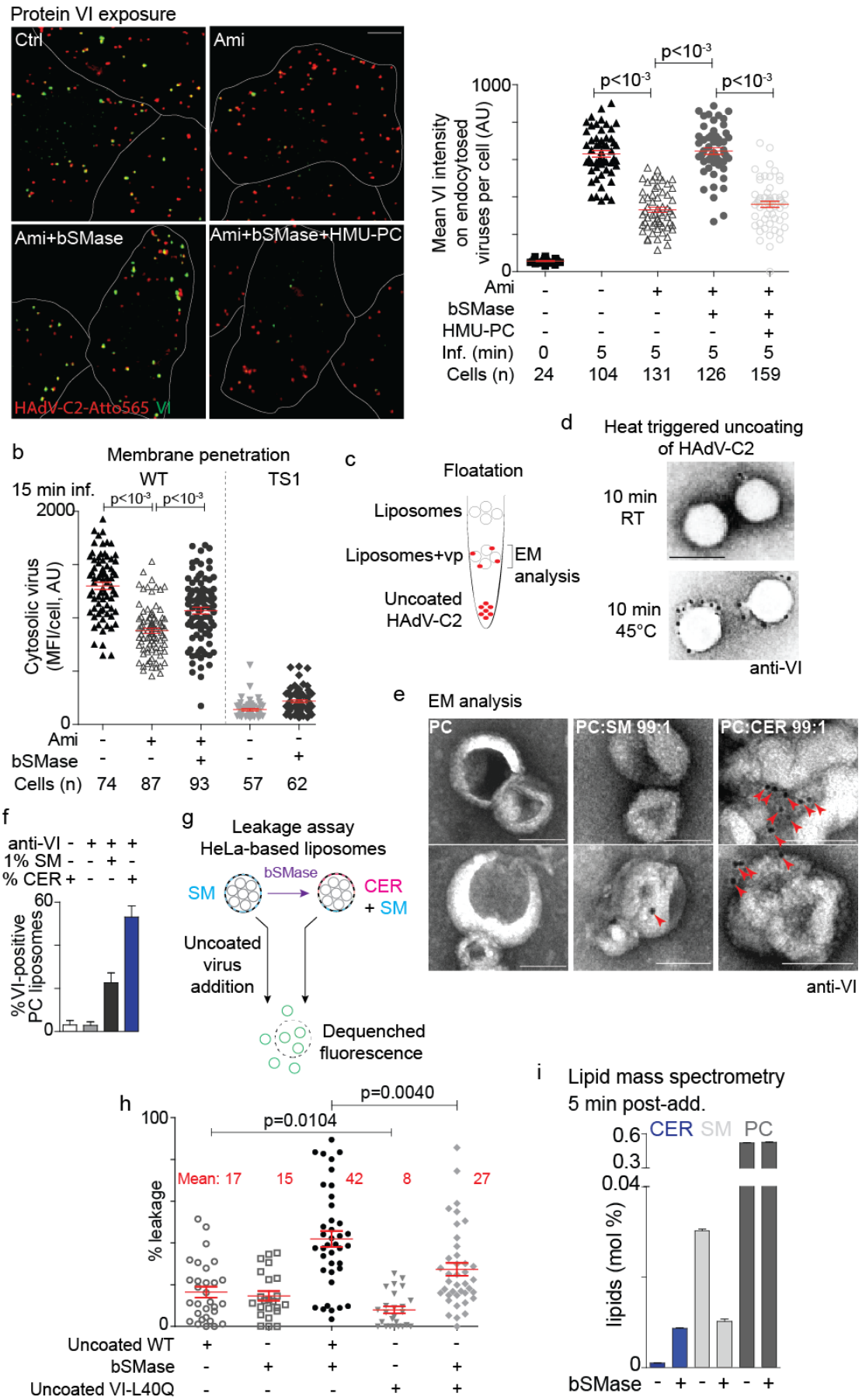
a
Protein VI exposure
Ctrl
Ami
Ami+bSMase
Ami+bSMase+HMU-PC
HAdV-C2-Atto565 VI
Mean VI intensity on endocytosed viruses per cell (AU)
p<10-3
Ami
bSMase
HMU-PC
Inf. (min)
Cells (n)
b
Membrane penetration
15 min inf.
WT
TS1
Cytosolic virus (MFI/cell, AU)
c
Floatation
Liposomes
Liposomes+vp
Uncoated HAdV-C2
EM analysis
d
Heat triggered uncoating of HAdV-C2
10 min RT
10 min 45°C
anti-VI
e
EM analysis
PC
PC:SM 99:1
PC:CER 99:1
anti-VI
f
anti-VI
1% SM
1% CER
%VI-positive PC liposomes
g
Leakage assay
HeLa-based liposomes
bSMase
SM
CER + SM
Uncoated virus addition
Dequenched fluorescence
h
p=0.0104
p=0.0040
Mean: 17
15
42
8
27
% leakage
Uncoated WT
bSMase
Uncoated VI-L40Q
i
Lipid mass spectrometry
5 min post-add.
CER
SM
PC
lipids (mol %)
bSMase

Figure 2: ceramide interacts with the capsid protein VI to mediate efficient endosomal escape

a) ASMase inhibition reduced VI exposure. Cells were pre-treated 4h with either DMEM-0.2% FAF BSA or 25 µM Ami, then exposed to cold-binding with HAdV-C5-Atto565. The samples were incubated for 5 min at 37°C in medium supplemented either with Ami, 0.012 U/ml bSMase or bSMase mixed with a 150-fold excess of its *in vitro* substrate HMU-PC. Surface viruses were recognized by incubation at 4°C with the 9C12 anti-hexon antibody in unfixed, unpermeabilized cells. Viruses positive for Atto565 but negative for 9C12 staining were scored as internalized, and VI exposure on internalized particles was evaluated. Scale bar=5 µm.

b) ASMase inhibition reduced escape to the cytosol. Infection was performed as described above. Cytosolic but not endosomal HAdV-C2-Alexa488 or TS1-Alexa488 were accessible to immunofluorescence labeling in SLO-treated cells after virus internalization.

c) Schematic representation of a liposome binding assay. Top fractions were subjected to immunogold labeling of VI and analyzed by EM.

d) *In vitro* virus uncoating, immunogold labeling of VI and EM analysis showed VI exposure on heat treated capsids.

e,f) VI preferentially binds to liposomes containing ceramide, as shown by EM micrographs of liposomes bound to VI and quantification of % positive liposomes (a minimum of 250 liposomes were analyzed per condition). Scale bar=100 nm.

g,h) Leakage is enhanced in ceramide-rich liposomes. Schematic representation of a liposome leakage assay. 6-carboxyfluorescein entrapped liposomes were exposed to bSMase or left untreated. Liposomes were further incubated with uncoated HAdV-C5-EGFP or uncoated HAdV-C5-L40Q. 100% liposomes leakage was determined by incubation with Triton X-100.

i) BSMase exogenously added to the supernatant rapidly increased ceramide levels in HeLa Ohio cells.

Figure 3:

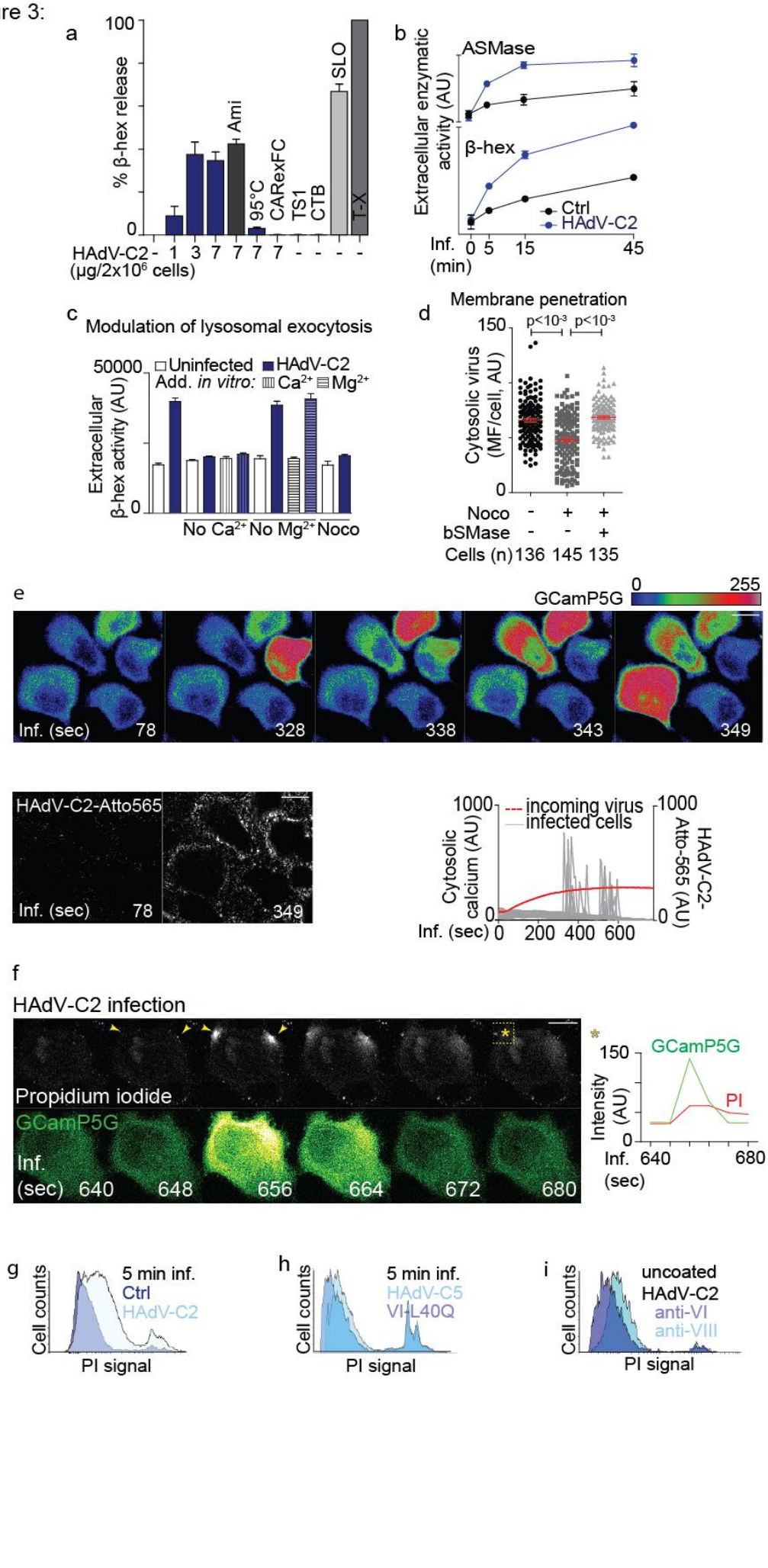
a
% β-hex release
100
0
Ami
95°C
CARexFC
TS1
CTB
SLO
T-X
HAdV-C2 - 1 3 7 7 7 7 - - - -
(µg/2x10^6 cells)
b
ASMase
β-hex
Extracellular enzymatic activity (AU)
Ctrl
HAdV-C2
Inf. 0 5 15 45
(min)
c
Modulation of lysosomal exocytosis
50000
Uninfected
HAdV-C2
Add. in vitro: Ca2+ Mg2+
Extracellular β-hex activity (AU)
0
No Ca2+ No Mg2+ Noco
d
Membrane penetration
150
p<10-3 p<10-3
Cytosolic virus (MF/cell, AU)
0
Noco - + +
bSMase - - +
Cells (n) 136 145 135
e
GCamP5G
0 255
Inf. (sec) 78 328 338 343 349
HAdV-C2-Atto565
Inf. (sec) 78 349
1000
incoming virus
infected cells
Cytosolic calcium (AU)
HAdV-C2-Atto-565 (AU)
0
Inf. (sec) 0 200 400 600
f
HAdV-C2 infection
Propidium iodide
GCamP5G
Inf. (sec) 640 648 656 664 672 680
150
GCamP5G
PI
Intensity (AU)
0
Inf. 640 680
(sec)
g
5 min inf.
Ctrl
HAdV-C2
Cell counts
PI signal
h
5 min inf.
HAdV-C5
VI-L40Q
Cell counts
PI signal
i
uncoated
HAdV-C2
anti-VI
anti-VIII
Cell counts
PI signal

Figure 3: Incoming adenovirus permeabilizes the plasma membrane to harness calcium signaling and trigger lysosomal exocytosis

a-c) Incoming adenovirus induces calcium-dependent lysosomal exocytosis. The activity of either the lysosomal enzymes β-hexosaminidase or ASMase in the supernatant of cells exposed to the indicated ligands in the specified media was determined at 45 min warm infection in a, and at various time points or at 15 min of a cold-synchronized infection in b and c respectively.

d) Lysosomal exocytosis accelerated endosomal escape. Cells were pre-treated with nocodazole and exposed to bSMase during 20 min of infection. Cytosolic but not endosomal HAdV-C2-Alexa488 was stained by immunofluorescence labeling in SLO-treated cells after virus internalization.

e-g) Incoming adenovirus permeabilizes the PM. Cytosolic Ca^{2+} transients and propidium iodide influx were analyzed in cells expressing GCamP5G during the first minutes of infection, either by confocal microscopy or by flow cytometry. Scale bar=10 µM.

h,i) VI contributes to PM permeabilization. In presence of propidium iodide, cells were exposed either to intact HAdV-C5 and the mutant VI-L40Q or to heat-uncoated HAdV-C2 pre-incubated with the indicated antibodies.

Figure 4:

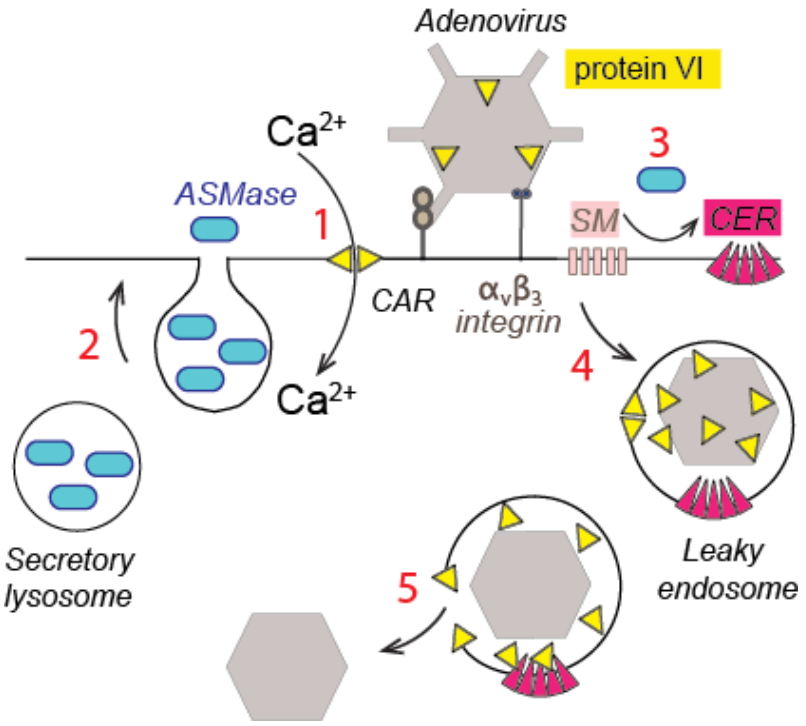

Figure 4: Working model

1. Uncoating competent adenovirus induces transient PM permeabilization mediated by VI. This leads to the influx of extracellular Ca^{2+} in the cytosol.

2. Increase in cytosolic Ca^{2+} triggers lysosomal exocytosis and delivers ASMase to the outer leaflet of the PM.

3,4. ASMase converts sphingomyelin (SM) to ceramide (CER). Ceramide increase supports virus endocytosis.

5. Protein VI interacts with CER to enhance endosomal lysis.

Figure S1:

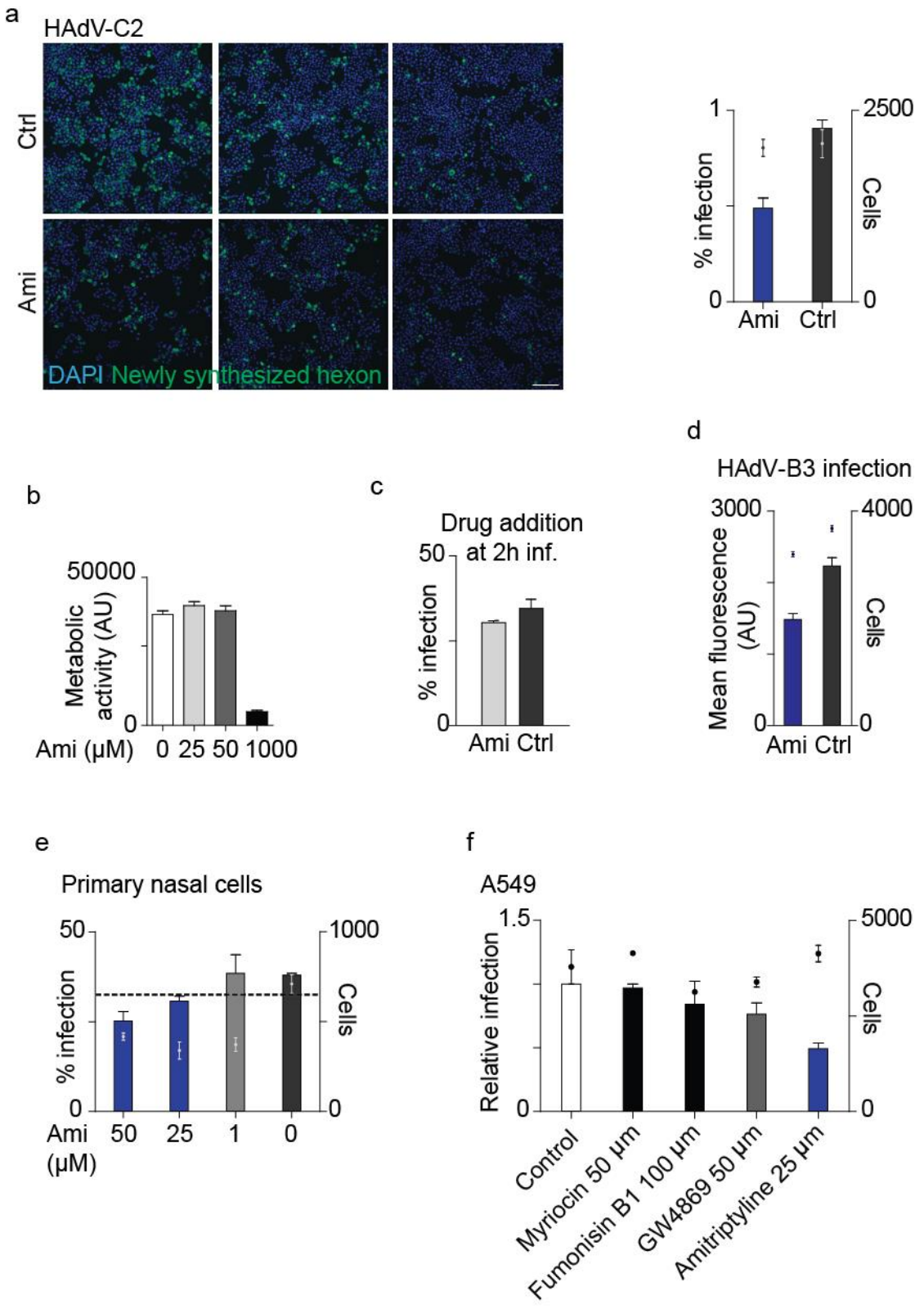
a
HAdV-C2
Ctrl
Ami
DAPI Newly synthesized hexon
1
0
% infection
2500
0
Cells
Ami Ctrl
b
50000
0
Metabolic activity (AU)
Ami (µM) 0 25 50 1000
c
Drug addition at 2h inf.
50
0
% infection
Ami Ctrl
d
HAdV-B3 infection
3000
0
Mean fluorescence (AU)
4000
0
Cells
Ami Ctrl
e
Primary nasal cells
50
0
% infection
1000
0
Cells
Ami (µM) 50 25 1 0
f
A549
1.5
0
Relative infection
5000
0
Cells
Control
Myriocin 50 µm
Fumonisin B1 100 µm
GW4869 50 µm
Amitriptyline 25 µm

Figure S1: The ASMase inhibitor amitriptyline (Ami) reduces infection and is not toxic to cells

a) HeLa Ohio cells were pre-treated with 25 µM with Ami in DMEM-0.2% FAF BSA and infected with HAdV-C2 for 18 h in presence of the drug. Newly synthesized hexon was stained in fixed cells and the percent of infection was evaluated. Scale bar=200 µM.

b) HeLa Ohio cells were incubated with Ami in DMEM-0.2% FAF BSA for 24 h and metabolic activity was assessed by resazurin assay.

c) Late addition of Ami does not reduce HAdV-C5_EGFP infection in HeLa Ohio cells.

d) Ami inhibits infection of a B-specie adenovirus. HeLa Ohio cells were pre-treated with 25 µM with Ami in DMEM-0.2% FAF BSA and infected with HAdV-B3_EGFP for 22 h in presence of the drug.

e,f) Ami treatment reduces infection of HAdV-C5_EGFP in primary nasal cells and A549.

Figure S2:

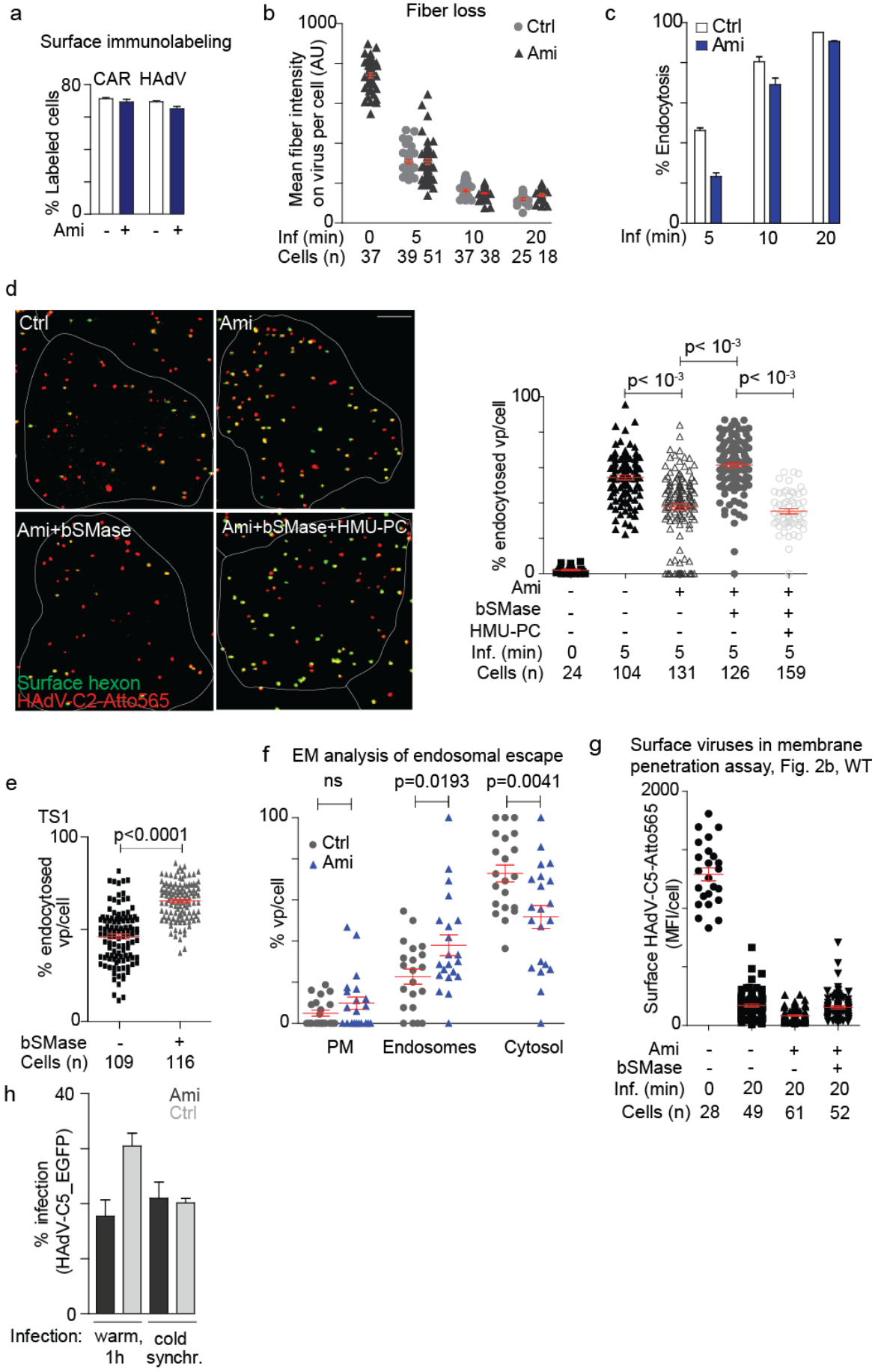
a
Surface immunolabeling
CAR HAdV
% Labeled cells
80
0
Ami - + - +
b
Fiber loss
Ctrl
Ami
Mean fiber intensity on virus per cell (AU)
1000
0
Inf (min) 0 5 10 20
Cells (n) 37 39 51 37 38 25 18
c
Ctrl
Ami
% Endocytosis
100
0
Inf (min) 5 10 20
d
Ctrl
Ami
Ami+bSMase
Ami+bSMase+HMU-PC
Surface hexon
HAdV-C2-Atto565
p< 10-3
p< 10-3
p< 10-3
% endocytosed vp/cell
100
0
Ami - - + + +
bSMase - - - + +
HMU-PC - - - - +
Inf. (min) 0 5 5 5 5
Cells (n) 24 104 131 126 159
e
TS1
p<0.0001
% endocytosed vp/cell
100
0
bSMase - +
Cells (n) 109 116
f
EM analysis of endosomal escape
ns
p=0.0193
p=0.0041
Ctrl
Ami
% vp/cell
100
0
PM
Endosomes
Cytosol
g
Surface viruses in membrane penetration assay, Fig. 2b, WT
Surface HAdV-C5-Atto565 (MFI/cell)
2000
0
Ami - - + +
bSMase - - - +
Inf. (min) 0 20 20 20
Cells (n) 28 49 61 52
h
Ami
Ctrl
% infection (HAdV-C5_EGFP)
40
0
Infection: warm, 1h
cold synchr.

Figure S2: ASMase inhibition does not affect binding and fiber loss, but delays the kinetics of endocytosis

a) Binding is intact. Unpermeabilized cells treated 4h with 25 µM Ami were either stained for surface CAR or exposed to HAdV-C5-Atto488 for 1h at 4°C to allow virus binding and analyzed by flow cytometry.

b) A time course of fiber release in a cold-synchronized infection was performed. Fixed cells were stained with R72 anti-fiber antibody and processed for confocal microscopy. The intensity of the antibody staining on the position of the viruses in a single cell-based analysis was determined.

c) Endocytosis is delayed. A time course of endocytosis following a cold-synchronized infection with HAdV-C5-Atto565 was performed. Surface viruses were recognized by incubation at 4°C with the 9C12 anti-hexon antibody in unfixed, unpermeabilized cells. The particles positive for Atto565 but negative for 9C12 staining were considered endocytosed. The % of endocytosis per cell was evaluated by confocal microscopy and Matlab.

d,e) bSMAse accelerated endocytosis of HAdV-C5-Atto565 and TS1-Atto488. Endocytosis was evaluated as described in c. Cells treated with Ami or untreated were exposed to HAdV-C2-Atto565 at 4°C. Warm medium supplemented with Ami, 0.012 U/ml bSMase or bSMase mixed with a 150-fold excess of its *in vitro* substrate HMU-PC was added to cells for 5 min at 37°C. Endocytosis of TS1 was evaluated at a time point of 10 min. Scale bar=5 µm.

f) Endosomal escape is reduced. At a time point of 20 min of infection, when all viruses were internalized, the number of viruses at the PM, in endosomes or in the cytosol per cell were counted by EM.

g) The SLO assay (Fig. 2b) does not allow distinction between surface and cytosolic virus. Therefore, surface HAdV-C5-Atto565 viruses were stained with the anti-hexon antibody 9C12 in parallel, unpermeabilized samples. Most viruses were internalized at the moment of SLO treatment.

h) The delay in endocytosis and endosomal escape affects infection levels during 16h of continuous infection. However, the infection levels after 16h of a cold synchronized infection were not affected by Ami treatment.

Figure S3:

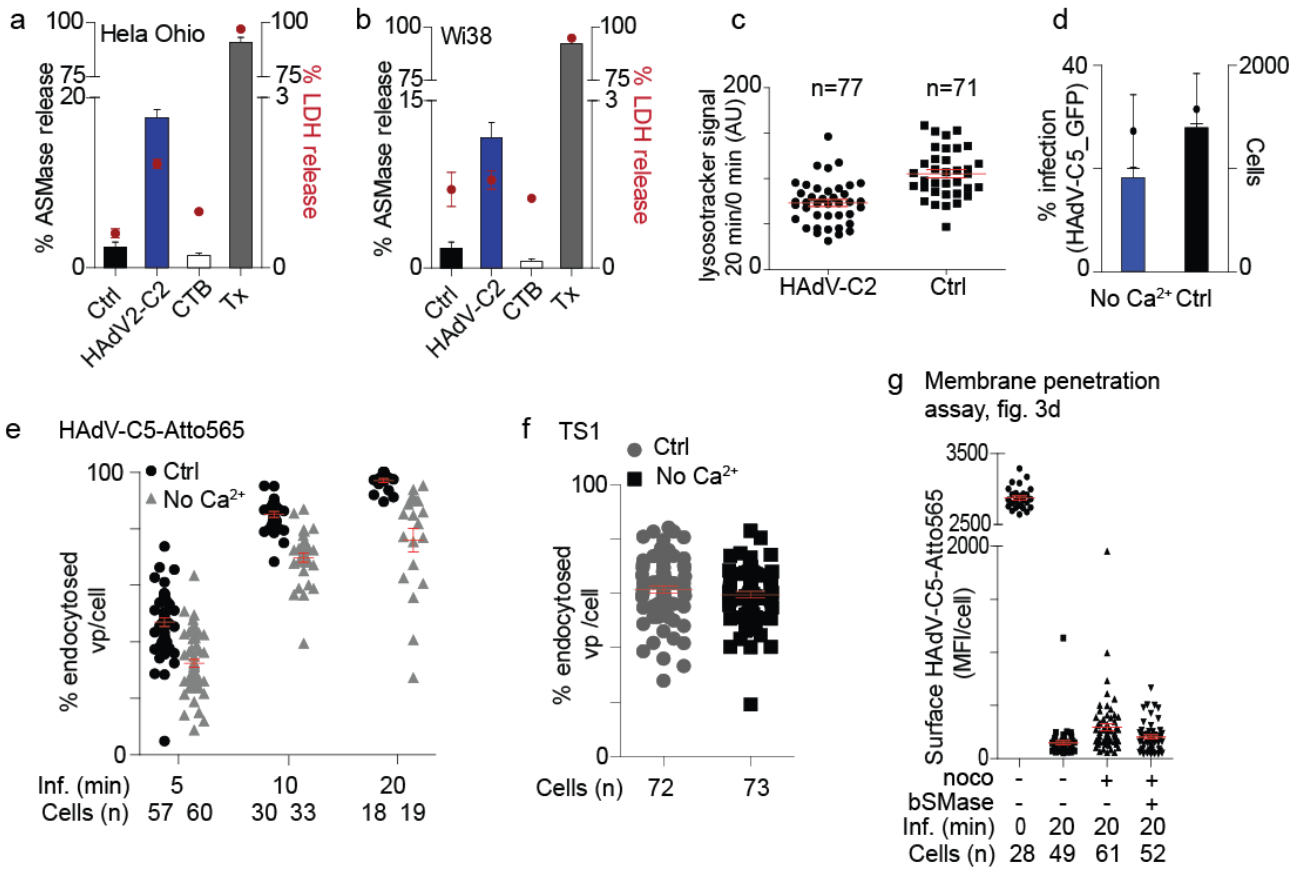

Figure S3: HAdV-C2/5 but not Ts1 induced Ca^{2+}-dep. lysosomal exocytosis to enhance endocytosis and escape

a,b) The supernatants of cells exposed to a synchronized infection with the indicated ligands were collected after 15 min and 45 min for HeLa Ohio and Wi38 respectively (the kinetics of HAdV-C2/5 endocytosis in Wi38 cells is slower compared to HeLa Ohio, data not shown). The enzymatic activity of the released lysosomal ASMase and cytosolic LDH was evaluated.

c) Cells were loaded with fluorescent lysotracker, then infected and subjected to live imaging. The intensity of the lysotracker signal per cell was determined at 0 and 20 min post-infection. The ratio of the signal at 20 min over 0 min is shown.

d) Infection of HAdV-C5_EGFP placed in medium devoid of extracellular Ca^{2+} for 2 h and subsequently in normal medium for 14 h was reduced. Virus binding w/wo calcium was equally efficient (data not shown).

e-f) Endocytosis of HAdV-C5-Atto565 but not of TS1 is delayed in absence of extracellular Ca^{2+}. Viruses were cold-bound to cells in full medium. Unbound viruses were washed away in media w/wo calcium. The time course of infection was performed in medium w/wo calcium.

g) The SLO assay (Fig. 3d) does not allow distinction between surface and cytosolic virus. Therefore, surface HAdV-C5-Atto565 viruses were stained in parallel, unpermeabilized samples with 9C12. Most viruses were internalized at the moment of SLO treatment.

Figure S4:

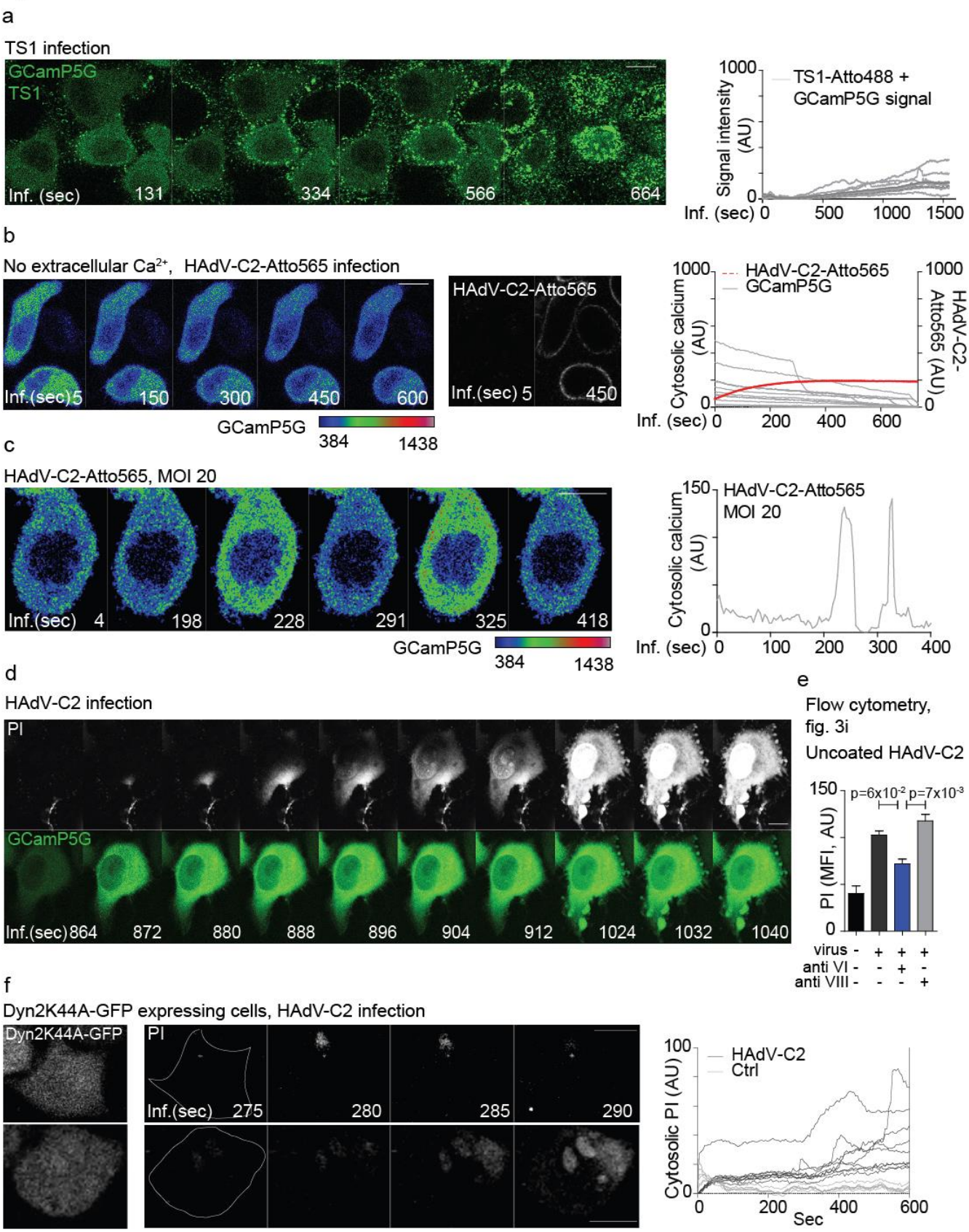
a
TS1 infection
GCamP5G
TS1
Inf. (sec) 131 334 566 664
TS1-Atto488 +
GCamP5G signal
Signal intensity (AU)
Inf. (sec) 0 500 1000 1500
b
No extracellular Ca2+, HAdV-C2-Atto565 infection
Inf.(sec)5 150 300 450 600
GCamP5G
384 1438
HAdV-C2-Atto565
Inf.(sec) 5 450
HAdV-C2-Atto565
GCamP5G
Cytosolic calcium (AU)
HAdV-C2-Atto565 (AU)
Inf. (sec) 0 200 400 600
c
HAdV-C2-Atto565, MOI 20
Inf.(sec) 4 198 228 291 325 418
GCamP5G
384 1438
HAdV-C2-Atto565
MOI 20
Cytosolic calcium (AU)
Inf. (sec) 0 100 200 300 400
d
HAdV-C2 infection
PI
GCamP5G
Inf.(sec) 864 872 880 888 896 904 912 1024 1032 1040
e
Flow cytometry,
fig. 3i
Uncoated HAdV-C2
p=6x10-2 p=7x10-3
PI (MFI, AU)
virus - + + +
anti VI - - + -
anti VIII - - - +
f
Dyn2K44A-GFP expressing cells, HAdV-C2 infection
Dyn2K44A-GFP
PI
Inf.(sec) 275 280 285 290
HAdV-C2
Ctrl
Cytosolic PI (AU)
Sec

Figure S4: Incoming, uncoating competent HAdV induces cytosolic calcium transients that depend on extracellular calcium

a-d) HeLa Ohio cells expressing the cytosolic calcium sensor GCamp5G were infected with the indicated HAdVs in medium w/wo either extracellular calcium or propidium iodide. Confocal time-lapse imaging was performed and the cytosolic signal intensity profile is shown.

e) Uncoated HAdV-C2 causes permeability to PI in a VI-dependent manner. An additional quantification of PI intensity from Fig. 3i is shown. The neutralization of VI with a specific antibody reduced cell permeability to PI.

f) Endocytosis is not a pre-requisite for cytosolic calcium transients. HeLa Ohio cells expressing Dyn2K44A-GFP, a dominant negative dynamin-2 mutant incapable of vesicle scission, were imaged by time-lapse confocal microscopy in presence of propidium iodide. The expression of Dyn2K44A-GFP was reported to allow fiber shedding but block endocytosis (Nakano et al., 2000). The influx of PI was visualized, suggesting that virus uncoating but not endocytosis trigger these events. All scale bars are 10 μM.

Figure S5:

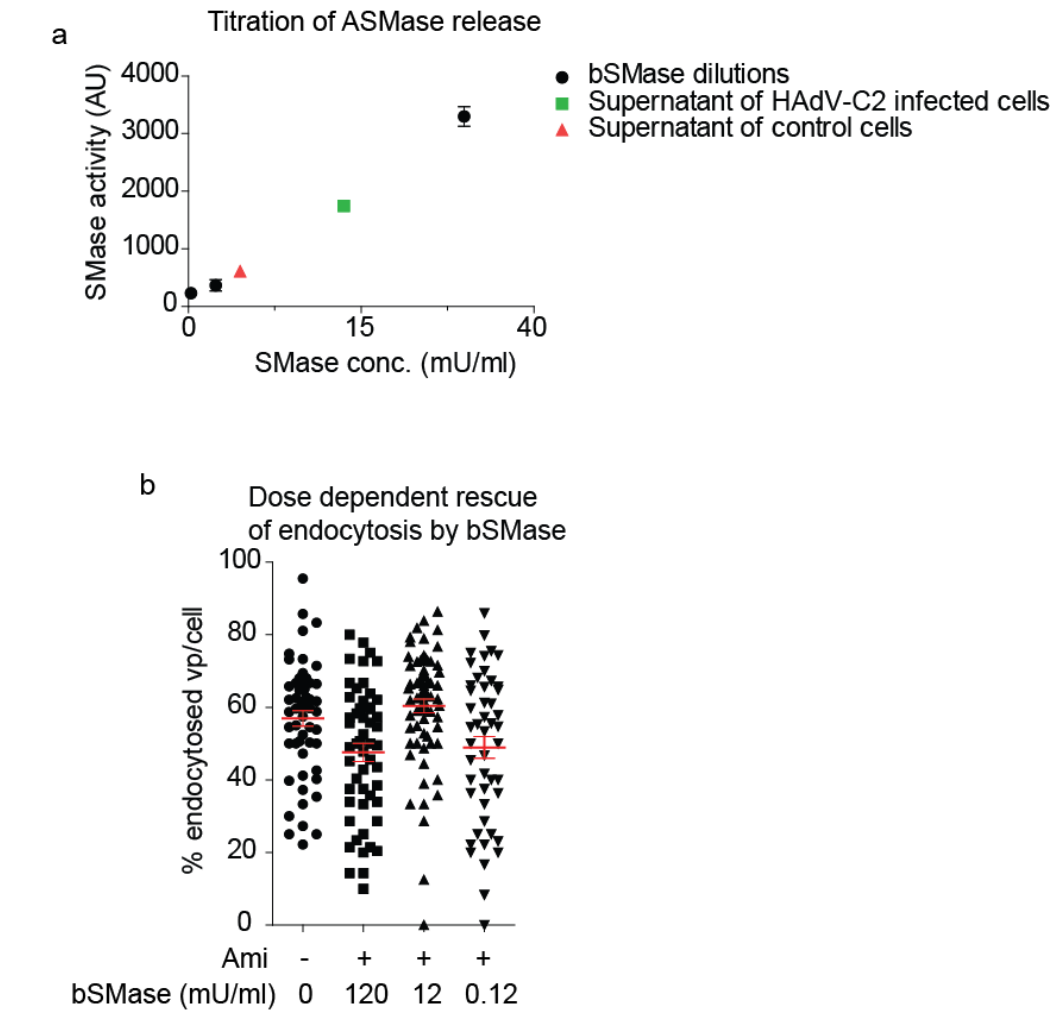

Figure S5: bSMase rescues endocytosis in a dose-dependent manner

a) A titration curve with bSMase was performed and the activity of ASMase released from cells infected with HAdV-C2 (like for Fig. 2a) was evaluated.

b) Endocytosis of HAdV-C5-Atto565 in amitriptyline treated cells was rescued by supplementing the media with a concentration of bSMase similar to what is released during infection (Fig. S5a) for 5 min. A 10-fold higher/lower concentration did not enhance endocytosis.

DISCUSSION

Early remodeling of the host lipid landscape

Cellular lipids are essential at various stages of the viral life cycle. While several viruses actively remodel membranes during replication and egress, for binding and invasion they are thought to depend on the pre-existing lipid landscape (Mazzon and Mercer, 2014). Previous lipidomic analysis revealed a profound reprogramming of host lipid metabolism during influenza (Tanner et al., 2014) and dengue virus (DENV) infection (Perera et al., 2012) at the earliest time point of 12h and 36h respectively. Interestingly, the entry process of UV treated, replication incompetent DENV is sufficient to alter cellular lipid landscape (Perera et al., 2012). Still, it is difficult to identify the function of such changes: they might support virus entry or be part of a cellular antiviral response. Here, we provide a snapshot of the lipid landscape during the first 30 min of virus infection. We found that infectious HAdV-C2 actively remodeled the host lipid landscape and intriguingly, over the 159 lipids profiled, only few ceramide species were selectively increased. Notably, entry of the mutant Ts1 did not trigger ceramide increase, indicating that this phenomenon is specific for uncoating competent adenovirus. All in all, we report the novel finding that HAdVs modulate specific lipid pathways already from the first minutes of interaction with the host.

ASMase in infection

Perturbation of selected ceramide generating pathways revealed that early ceramide increase supports infection and is mediated by acid sphingomyelinase. Acid sphingomyelinase facilitates the infection of several pathogens, including Japanese Encephalitis virus (JEV) and Ebola virus (Avota et al., 2011a; Grassmé et al., 1997; Grassmé et al., 2003; Grassmé et al., 2005; Miller et al., 2012; Steinhart et al., 1984; Tani et al., 2010). Infection levels of the enveloped JEV and Ebola virus are reduced by drug inhibition of cellular ASMase. Interestingly, addition of exogenous bSMase to the culture medium enhances JEV in Huh-7 (Tani et al., 2010), but inhibits Ebola virus infection in HeLa cells (Miller et al., 2012). This discrepancy suggests multiple functions for ASMase in infection.

Lysosomal ASMase is a key factor in maintaining lipid homeostasis and membrane trafficking. It is conceivable that by exerting its constitutive function, ASMase provides a membrane environment permissive for virus infection. Alternatively, an imbalance of SM/CER on cell membranes might interfere with PM biophysical integrity and signaling properties. Along this line, surface bSMase inhibits Hepatitis C (HCV) infection in Huh-7 cells by enhancing internalization of the surface entry factor CD-81, thus by modulating PM dynamics (Voisset et al., 2008).

Ceramide in endosomal escape: a role for membrane deformation and specific binding to VI?

Ceramide facilitated VI exposure on endocytosed viruses and supported membrane penetration *in vitro* and *in vivo*. Notably, VI preferentially bound to enriched ceramide containing liposomes. Reduced VI exposure

on endocytosed viruses might indicate a role for ceramide in viral uncoating, already during PM events. CAR-directed surface driftings and binding to immobile integrins lead to mechanical shedding of fibers (Burckhardt et al., 2011). SM/ceramide enriched domains might influence these dynamics, and identical kinetic of fiber release was observed by immunofluorescence during ASMase inhibition (Fig. S2b). Since the fiber release assay by immunofluorescence has a low dynamic range, further investigations are needed to determine if ceramide does influence the shedding of the fibers. Based on our observation that VI binds preferentially to ceramide-containing liposomes than ceramide-free liposomes, it is likely, however, that surface ceramide stabilizes the binding of VI to the plasma membrane.

Membrane permeabilization as a consequence of membrane deformation

Membranes are often referred to as inert bilayers that are subjected to active modifications by proteins and passively accommodate the formation of pores. Yet, the biophysical properties of lipids and the dynamic nature of the membrane itself are factors that cooperate with proteins and influence the poration process (Wimley, 2010). Membrane responses to interferences by proteins are governed by thermodynamic principles and maintain the most favorable energetic state.

A role for membrane curvature

Strong membrane curvature can lead to leakage events. Several membrane penetrating peptides either preferentially bind to curved membranes, or actively induce membrane curvature. The induction of highly positive or negative curvatures favors the binding of pre-amyloid amphiphiles such as islet amyloid polypeptide IAPP (Smith et al., 2009), Aβ (Matsuzaki and Horikiri, 1999) and α-synuclein (Middleton and Rhoades, 2010), the AMPs magainin 2 (Matsuzaki et al., 1998b) and LL-37 (Henzler-Wildman et al., 2004), the CPP HIV TAT (Mishra et al., 2011), as well as the α-helical VI of adenovirus (Maier et al., 2010). During the transition from a disordered state to an amphipathic structure, the peptide shapes the membrane to fit its geometry. Membrane distortion in turn causes an energetically unfavorable rearrangement of the lipid landscape. To resolve such membrane deformations, a possibility is the flipping of phospholipids from a leaflet to the other, a process that offers the opportunity of leakage events (Last et al., 2013).

In endosomes, ceramide might play a role alone in destabilizing membranes by its virtue of inducing membrane curvature. As shown in Fig. 2h, bSMase incubation with liposomes triggered leakage of the liposomes also in absence of viral proteins. Natural ceramides have an inverted cone shape given by the two long hydrophobic tails and a very small polar head (Goñi and Alonso, 2006). Assembly of ceramides leads to the negative curvature of the leaflet where they are inserted. Spontaneous flip-flop of ceramide is possible but occurs at low rates (estimated rate: 22 min; Bai and Pagano, 1997). Instead, this possibly leads to the spontaneous flip-flop of phospholipids, and consequently to membrane leakage event.

A role for membrane tension

SM conversion to ceramide increases surface area and membrane tension (López-Montero et al., 2007). While the PM benefits from exocytosis/endocytosis and cytoskeletal pulling forces to equilibrate membrane deformation (Groulx et al., 2006), endosomes might be more vulnerable and prone to poration. The membrane lytic factor of parvoviruses for example exploits uniquely lipid remodeling to induce membrane curvature and trigger endosomal escape (Farr et al., 2005; Filippone et al., 2008; Stahnke et al., 2011; Zádori et al., 2001). The membrane lytic factor of Rotaviruses increases membrane curvature and endosomal surface tension (Abdelhakim et al., 2014). As a consequence of membrane tension, membrane poration likely occurs. Unperturbed membranes are stable and the formation of pores is a highly unfavorable event. However, when external perturbations increase membrane tension, the spontaneous generation of pores becomes energetically favorable. Such perturbations include the binding of amphipathic peptides. The hydrophobic sides of the peptides initially displace the head groups of the lipids to access the core of the membrane. If the lipid tails are not simultaneously expanded (Huang et al., 2004; Lee et al., 2004), acyl chains are forced into an unfavorable packaging, which leads to surface tension (Lee et al., 2004). In this context, the formation of pores decreases the membrane surface area, allows lipids to return to the initial conformation and thereby ultimately releases the membrane tension. The energetic penalty of pore formation is therefore strongly decreased by the presence of membrane bound peptides. Biophysical studies of pore forming peptides interacting with liposomes allowed the modeling of a common principle for several poration mechanisms proposed by Last, Schlamadinger and Miranker:

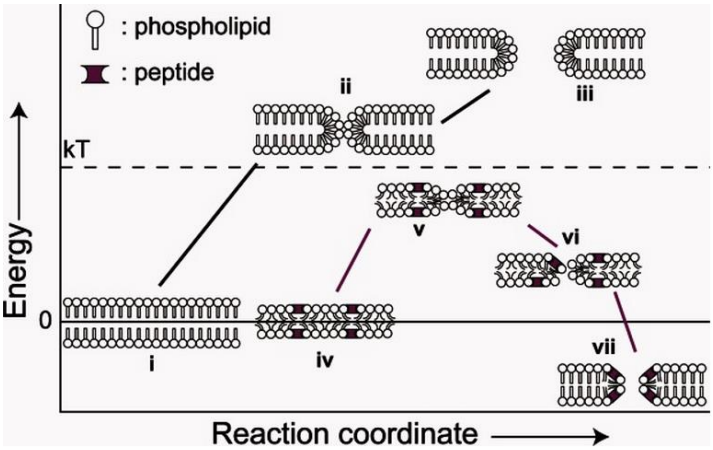

Fig. 5: Schematic representation of the energetic landscape during membrane poration.

(i) In these energetic considerations, the intact phospholipid bilayer is considered as a reference point. (ii) Spontaneous thermal fluctuations have marginal impacts long as they remain below kT. (iii) Additional energy is required to extend membrane defects leading to membrane rupture. (iv) The partitioning of amphipathic proteins onto the surface of the lipid bilayer induces membrane tensions and increases the occurrence of membrane defects

> (v). Stochastic and transient pores form spontaneously to relax the surface tension. If small enough, they immediately reseal. In other cases, pores further assemble and grow (vi). (vii) Finally, some peptides are capable of stabilizing the rim of the pores. Thereby a full release of membrane tensions and further drop of the global energy level occurs. (Last et al., 2013)

The energetic aspect of pore formation has been mathematically described in model lipid bilayers:

$$E_P = \gamma 2\pi R - \sigma \pi R^2$$

where E_P is the energy of pore formation, R is the radius of the pore, σ is the membrane tension and γ is the line tension. The line tension opposes pore formation and results from the attraction between hydrophobic groups at interphase between aqueous and hydrocarbon phase (Israelachvili et al., 1980; Taupin et al., 1975). Notably, the increase of one single parameter, the membrane tension σ, is sufficient to trigger spontaneous pore formation.

To summarize, according to this model membrane permeabilization does not require specific protein sequences that bind to specific lipids in a "key-lock" fashion. Instead, it fully relies on the amphipathic nature of the peptides and their capacity to induce membrane changes. Membrane tension is the primary and only trigger that renders membrane permeabilization energetically favorable. Also, the tension resulting from the binding of various peptides to a single membrane has additive effects. As a result, the peptides cooperate in the process of tension-induced membrane permeabilization without the need to oligomerize into pore structures.

Of note, VI itself induces membrane positive curvature (Maier et al., 2010) and ceramide enrichment in the inner leaflet of endosomes induces membrane outward budding. VI and ceramide might therefore cooperate in destabilizing endosomes by a cumulative effect of independent membrane curvature and tension induction. Indeed, our *in vitro* liposome studies showed enhanced leakage when VI was exposed to ceramide-enriched liposomes.

Specific binding of VI to ceramide

EM analysis suggested that VI bound better to ceramide-containing liposomes than ceramide-free liposomes, indicating a specific ceramide-VI interaction. VI associates to membranes in a planar fashion (Maier et al., 2010). Accessing the hydrophobic core of the membrane implies that the hydrophilic heads of several lipids have to be displaced (discussed in the introduction). It is tempting to imagine that the lipophilic side of VI more easily displaces the small hydroxyl-head of ceramides compared to the phosphorylcholine-head of PC and SM. Also, VI preferentially binds to a sphingoid-backbone compared to a glycerol-based lipid, as suggested by the increased binding to SM compared to PC (Fig. 2e,f).

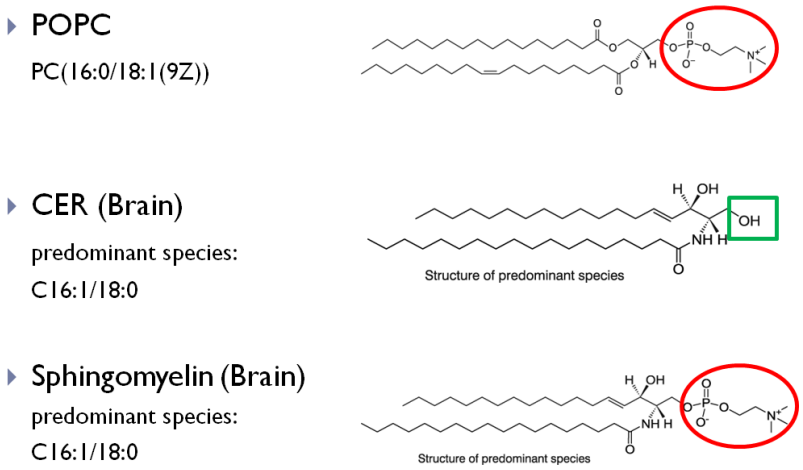

Fig. 16: structure of the PC, CER and SM species used in this study (Avanti). The head group of the lipids is highlighted. Red indicates phosphorylcholine and green the hydroxyl-group.

Efficient VI binding increments the protein/lipids ratio and might enhance membrane permeabilization events by carpet model (described in the introduction). That the protein/lipid ratio is critical in such events was previously shown for several membrane lytic factors, including the AMPs cecropin A, melittin and gamma of FHV (Maia et al., 2006; Shai, 1999). These factors share with VI a short alpha-helical domain, amphipathic properties and planar association to membranes (Last et al., 2013; Maier et al., 2010). Similarly to VI, gamma has been shown to efficiently permeabilize liposomes with specific lipid compositions and low cholesterol (Maia et al., 2006). Analogous effects were seen for other AMPs (Mason et al., 2007; Nicol et al., 1996; Won et al., 2012), suggesting that membrane composition influences the efficiency of permeabilization.

Ceramide might also dictate the modality by which VI perforates membranes. Magainin 2 and melittin switch from detergent-like permeabilization to the formation of stable pores depending on membrane lipid composition (Ladokhin and White, 2001; Lee et al., 2008; Ludtke et al., 1996). Recombinant VI aggregates in solution (personal communication, M. Suomalainen), yet to our knowledge VI assembly into pore-structures has never been characterized. Together, these findings emphasize how membrane composition can influence protein mediated leakage.

VI might carry a specific binding site to ceramide or its sphingoid base. Previous studies identified a sphingomyelin binding motif conserved in the transmembrane (TMD) domain of several integral membrane proteins (Björkholm et al., 2014; Contreras et al., 2012). SM 18 specifically binds to the TMD of p24 but not p23, two proteins involved in COPI vesicle budding in the Golgi. The binding involves both head group and backbone of SM, and is of higher affinity towards SM 18 compared to for example SM 16, SM 20, PC 18 and CER 18. Crucial for this is the signature sequence VXXTLXXIY. VXXTL packs the C18 chain and mutation of L

completely abrogated binding to the lipids, while Y interacts with the polar head of SM (Contreras et al., 2012). VI of HAdV-C5 partially shares this signature: WXXTLXXIV (position 229-237, Uniprot annotation: Q2KS09). This signature is highly conserved among human adenovirus species and groups. Tryptophane (W) has a considerably bigger side chain than valine (V), but it is as well hydrophobic and might therefore still interact with the hydrocarbon chain of sphingolipids. Studies with mutant VI attributed the full capacity of membrane lysis to the N-term amphipathic domain, but sphingolipids were never included in the synthetic membranes used for the *in vitro* experiments (Maier et al., 2010). Moreover, studies with mutants are difficult, as the VI sequence 231-242 contains a nuclear localization signal, essential for nuclear import of newly synthesized hexons during viral assembly (Wodrich et al., 2003).

We can propose a speculative two step model of VI interaction with ceramide: first, the low polarity of the ceramide head group facilitates adsorption of the N-term amphipathic-alpha helix in a planar fashion. Second, the sphingoid backbone offers the opportunity of inserting the C-term domain of VI into the bilayer by high affinity binding. The determination of tryptophan depths into membranes containing ceramide might clarify whether VI insertion indeed occurs.

Changes in the curvature of the endosomal membrane, leakage events or altered lipid composition might be sensed by cytosolic proteins and attract cellular machineries that further contribute to efficient escape. The ESCRT protein CHMP4B immediately localizes to lysed PM (Jimenez et al., 2014), SphK associates with ceramide-rich endocytosed structures (Shen et al., 2014), and galectins cluster on ruptured membranes (Martinez et al., 2013). Yet, although bSMase treatment enhanced TS1 endocytosis, it was not sufficient to rescue TS1 escape. Together with the observation that TS1 does not efficiently shed its fibers and does not expose protein VI, this observation underlines the importance of viral uncoating and a cooperation between lipids and viral factors in coordinating membrane lysis.

For HAdV-C2/5, we propose a multistep endosomal leakage process. Ceramide-induced membrane curvature and tension combined with occasional VI binding to membranes triggers minor leakage events (phospholipids flip-flop, spontaneous and short-lived membrane poration) that initially interfere with endosomal osmotic balance and render endosomes fragile. Next, further capsid uncoating and full VI exposure locally generate high concentrations of proteins that efficiently bind to ceramides. In the context of a small, highly curved endosome devoid of the stabilizing clathrin coat, this triggers the final leakage event and permits the escape of a 90 nm capsid.

PM permeabilization triggers calcium-dependent lipid remodeling

Intriguingly HAdVs actively modified the lipid landscape to ensure ceramide production in host membranes. Early release of VI by incoming HAdVs transiently permeabilized the plasma membrane to trigger calcium-dependent lysosomal exocytosis and delivery of ASMase to the cell surface. ASMase exocytosis was previously observed for other pathogens, such as rhinovirus (Grassme et al., 2005; Grassmé et al., 2005), measles virus (Avota et al., 2011b), *Neisseria gonorrhoe* (Grassme et al., 1997), and *Pseudomonas aeruginosa* (Grassme et al., 2003). Incoming rhinovirus and measles virus cause the formation of PM ceramide-enriched domains to which viruses co-localized. However, this was visualized by immunofluorescence and concerns regarding specificity of the ceramide antibody and reliability of fixations techniques have been raised (see introduction). HRV binding and the activation by measles virus of surface cell signaling via DC-SIGN on dendritic cells or an unidentified factor on T-cells (Gassert et al., 2009) were the trigger for ASMase re-localization (Dreschers et al., 2007; Grassme et al., 2005). During HAdV entry, the key stimulus was unexpectedly direct plasma membrane permeabilization. That HAdVs induce PM permeabilization was previously suggested (Di Paolo et al., 2013; Wickham et al., 1994). Studies in artificial systems where viruses were blocked at the cell surface and acidified, initially identified penton base as the lytic factor (Seth, 1994; Wickham et al., 1994). In these studies the readout for membrane permeabilization was the release of radioactive choline from either cells or liposomes. Antibodies against penton base (Seth, 1994) or soluble penton base (Wickham et al., 1994) blocked membrane permeabilization. Another possible interpretation of these results is that blocking penton base prevents viral uncoating. As a consequence, VI is not released and membrane lysis can not occur.

How to harness calcium signaling?

PM permeabilization resulted in cytosolic influx of extracellular calcium. Calcium is a ubiquitous and highly versatile ion sensed by a wide variety of cellular factors. Within the lifetime of an organism, it is not degraded. To control its activity, the cell compartmentalizes calcium ions and expresses for example proteins that carry functions depending on calcium binding. Calcium is involved in the regulation of fundamental biological processes such as fertilization, proliferation, development, learning and memory, contraction and secretion (Berridge et al., 2000). It is not surprising that calcium signaling is harnessed by a variety of viruses at different replication stages. Adenovirus itself was already known to depend on extracellular calcium for virus uptake and penetration (Greber et al., 1997; Nemerow and Stewart, 1999; Wu et al., 2006).

Calcium homeostasis is tightly regulated; extracellular calcium concentrations are around 1 mM, cytosolic calcium concentrations are kept at approximately 100 nM and ER stores contain about 100 µM Ca^{2+} (Syntichaki and Tavernarakis, 2003). In this work, we showed that incoming HAdVs induced short-lived calcium transients and PI influx. This indicated minor lesions that spontaneously resealed, or were efficiently repaired.

How are small lesions formed? Surface events during adenovirus entry, such as the binding of integrins to penton base, lead to the clockwise untwisting of the penton base (Lindert et al., 2009) and partial uncoating. Disassembly of the first vertices likely allows release of few copies of VI. The release of just a few molecules of VI from multiple vertices may lead to a local high concentration of VI on the membrane, and possibly transient membrane lysis. Considering that the extracellular calcium concentration is about 10'000 fold higher than intracellular, even short-lived PM lesions offer the opportunity of a dramatic increase in cytosolic calcium. Calcium increase might be locally limited, but still sufficient to trigger the fusion of PM proximal lysosomes (Jaiswal et al., 2002).

Similarly to HAdV, other viruses induce calcium transients during entry. Coxsackie virus B (CVB), a non-enveloped virus that binds to CAR, induces a depletion of intracellular calcium stores. This occurs via virus mediated clustering of the Decay Accelerating factor (DAF), and subsequent activation of Src, PLC and Ins3P signaling. CVB exploits calcium signaling to activate calpain and thereby promote intracellular virus trafficking (Bozym et al., 2010). Influenza induced calcium transients very early after binding to cells, by unknown mechanisms that involve release of ER calcium stores. Cytosolic calcium transients initiate a positive-feedback loop that activates Rho- and Ras-signaling for efficient endocytosis (Fujioka et al., 2013). HSV entry showed a two-step regulation of calcium fluxes. First, virus binding to syndecan-2 and nectin-1 and shifting cells to 37°C increased PM calcium levels. Second, an $\alpha_v\beta$ integrins-dependent signal and Akt activation triggered the release of calcium from the ER (Cheshenko et al., 2007; Cheshenko et al., 2013).
Different viruses harness calcium signaling by multiple strategies that converge into the instantaneous enhancement of endocytosis, and Ca^{2+}-dependent lipid remodeling might be a common feature.

Immediate consequences of calcium influx depend on amplitude, duration and localization of such event. The bacterial pore forming toxin SLO rapidly induces lysosomal exocytosis and consequent endocytosis of the lesions (Idone et al., 2008; Tam et al., 2010), but also triggers the formation of PM blebs. The blebs might contain lesions and can be shed extracellularly via an annexin-5 dependent mechanism (Babiychuk et al., 2009; Keyel et al., 2011). Similar blebbing phenotypes are also observed after laser-mediated PM damage, and involves ESCRT components (Jimenez et al., 2014). Cellular responses to HAdV infection find agreement with both conflicting observations. Short-lived lesions did not affect cell morphology and survival, but when openings failed to be resealed, events of membrane blebbing were visualized. While bacterial toxins mostly form stable, long-lived pores with dramatic consequences on cell survival (Bischofberger et al., 2012), HAdVs finely control PM integrity to induce selected PM repair mechanisms, but avoid detrimental lesions.

Immediate consequences of PM permeabilization?

The multiple downstream effects of calcium signaling might include the activation of p38/MAPK pathway. Incoming HAdV, but not TS1, induces calcium influx (Fig. S4a) and activates p38/MAP kinase by mechanisms independent of integrins signaling (Suomalainen et al., 2001; Tibbles et al., 2002). Activation of p38 facilitates nuclear targeting and the adenoviral nuclear life (van der Houven van Oordt et al., 2000). Of note, most pore forming toxins, besides inducing calcium influx also activate p38 (Porta et al., 2011). Similarly, PM permeabilization might be the underlining mechanism for p38 activation by HAdV. A direct correlation between these events might be addressed in the future.

P38 signaling has recently been related to ASMase activity. ASMase inhibition with an amitriptyline analogue abrogated activation of p38 as well as IL-6 synthesis and release (Perry et al., 2014). Incoming adenovirus is known to rapidly induce IL-6 release, together with a cocktail of other cytokines. When released by infected macrophages, these cytokines act in favor of infection, by re-localizing integrins to the apical surface of polarized epithelial cells (Lütschg et al., 2011). Therefore, targeting ASMase in a natural infection might be anti-adenoviral at two levels: first by confining entry receptors to the basolateral side of the target tissue and second by inhibiting endocytosis, escape and infection. However, the involvement of ASMase in releasing inflammatory cytokines during a natural infection remains controversial, as ASMase-/- mice were shown to efficiently secrete IL-1beta, IL-6, TNF and IFN-gamma (Manthey and Schuchman, 1998; Utermöhlen et al., 2003). Also, precise kinetics of p38 activation and which p38 isoforms are involved remains to be characterized.

Ceramide in endocytosis, biophysical or signalling role?

Exogenous bacterial sphingomyelinase readily increased cellular ceramide levels and rescued HAdV-C2 endocytosis in amitriptyline treated cells (Fig. 2i, S2 d). Ceramide might favor endocytosis for two reasons, by inducing membrane inward budding or clustering PM signaling factors.

Although the abundance of ceramide in membranes is low (Castro et al., 2014), ceramide profoundly impacts the biophysical properties of membranes. Ceramides influence lateral segregation of membrane factors, tend to aggregate and induce membrane curvature, provoke inward budding and support membrane permeabilization. Few but crucial reports highlighting these features were selected among a copious literature and are briefly discussed here. Studies employing bacterial sphingomyelinase (bSMase) to generate ceramide from sphingomyelin were preferred over studies using synthetic ceramides.

An influence of ceramide on membrane partitioning was initially observed in model membranes by Ira and collaborators (Ira and Johnston, 2008). In these experiments, the fluorescent compound TR-DHPE was used as a marker for the fluid phase and cholera-toxin B-647 was employed to detect GM1 containing rafts. The acquisition of the samples was done by TIRFM and AFM. When bSMAse was added to the supported bilayers, the segregation of the membrane markers into platforms rapidly occurred (Ira and Johnston,

2008). In a similar assay, Chiantia and colleagues demonstrated that the partitioning of proteins interacting with membranes, such as synaptobrevin2 and GPI-PLAP was differentially regulated in synthetic lipid bilayers (DOPC, cholesterol, CER) containing increasing ceramide levels (Chiantia et al., 2008; Christensen et al., 1988).

Lateral segregation induced by ceramide in biological membranes was recently investigated by Pinto and colleagues (Pinto et al., 2014). To mimic physiological conditions, ceramide was produced via sphingomyelin hydrolysis by bSMase. Ceramide production was measured by TLC and occurred very rapidly, within 0 to 5 min post incubation of HEK cells with bSMase. The segregation behavior of the anisotropy markers NBD-DPPE and t-PnA indicated that the level of order in membranes as well rapidly increased. Within 15 min of incubation the formation of gel-like domains was visualized. Since high concentrations of ceramide have been implicated in pore formation (Siskind et al., 2002), the authors addressed the integrity of the plasma membrane by lactate dehydrogenase (LDH) assay. Of note, HEK cells were intact during the course of the whole experiment indicating that bSMase alone was not capable to induce membrane permeabilization (Pinto et al., 2014).

Ceramide association also influences membrane budding. Ceramide aggregates generated by bSMase might result in inward budding of membrane portions, as observed in model liposomes (Holopainen et al., 2000; Trajkovic et al., 2008). Interestingly, Zha and collaborators observed that exogenous addition of bSMAse to endocytosis incompetent fibroblasts and macrophages (by deoxyglucose and sodium azide treatment) rescued the uptake of FITC-dextran. Results suggested a function for PM ceramide in inward budding of endocytic vesicles (Zha et al., 1998) independently of additional cellular factors. Ceramides support endocytosis also in unperturbed cell culture conditions. This was verified for cargos of various sizes that bound to different receptors. Cellular ASMase has been implicated in the phagocytosis of *Neisseria gonorrhoeae* (Hauck et al., 2000) and *Neisseria menigitidis* (Simonis et al., 2014) and in the uptake of polystyrene-beads targeted to ICAM-1 (Serrano et al., 2012).

Endocytosis requires extensive membrane rearrangements, orchestrated by tight protein-lipid interactions (Doherty and McMahon, 2009). Lipid-regulated lateral segregation of membrane factors generate microdomains that coordinate protein localization and activity (Breslow and Weissman, 2010; Simons and Sampaio, 2011). SM is a major player in PM organization (Simons and Sampaio, 2011), is particularly enriched on the outer leaflet of the PM (Slotte et al., 1990) and about 10 times more abundant than ceramide (Bielawski et al., 2006). Visualization of nanoscale membrane domains revealed the co-existence of SM and $PI(4,5)P_2$ (PIP2) (Abe and Kobayashi, 2014). PIP2 is enriched at sites of endocytosis and plays a fundamental role in the nucleation of clathrin-mediated endocytic pits (Doherty and McMahon, 2009). The

addition of bSMase triggered the dispersion of these SM domains (Abe and Kobayashi, 2014), suggesting a possible impact of ceramide increase in endocytic processes.

Enhanced endocytosis might require generation of ceramide metabolites. For example, sphingolipid homeostasis is necessary for endocytic trafficking of rhodopsin and the integrity of photoreceptor cells in flies (Acharya and Acharya, 2005; Yonamine et al., 2011). In particular, ceramidase was shown to facilitate the endocytosis of the G protein receptor rhodopsin 1 (Acharya et al., 2004). Furthermore, S1P increased endocytosis of FITC-dextran in mature dendritic cells (Maeda et al., 2007). Remarkably, a sub-population of neutral ceramidases is found on the PM (Ito et al., 2014). Thus, following SM conversion to ceramide by bSMase, neutral ceramidases might readily convert ceramide into sphingosine. While ceramide flip-flop is rare, sphingosine can spontaneously switch lipid bilayer (Hannun and Obeid, 2008) and be metabolized into S1P by cytosolic sphingosine kinase. Indeed, sphingosine kinase is enriched on tubular endocytic structures triggered by bSMase (Shen et al., 2014). Unfortunately, the abundance of sphingosine and S1P in our samples was below the detection limit of the lipid profiling experiments. Further analysis are required to identify sphingosine and S1P requirements during infection.

Intriguingly, S1P and ceramide have opposing roles in regulating the ERM proteins ezrin, radixin and moesin. The ERM proteins physically link the PM to the actin cytoskeleton and have been localized on clathrin coated vesicles (Barroso-González et al., 2009) and early/recycling endosomes (Harder et al., 1997; Morel and Gruenberg, 2009; Stanasila et al., 2006). By regulating vesicle trafficking (Cha et al., 2006; Tamma et al., 2005; Zhou et al., 2003), endosome maturation (Chirivino et al., 2011) and actin cytoskeleton dynamics (Adada et al., 2014), ERM proteins widely impact endocytic processes. Exposure of HeLa cells to bSMAse acutely inactivated ezrin via protein-phosphatase 1 (Canals et al., 2010), an event likely to occur also in our experimental conditions. How ERM tune adenovirus infection remains obscure, but their regulation by sphingolipids might be important for virus endocytosis.

In addition, an increase of PM ceramide profoundly impacts cell signaling. The impressive variety of cellular processes affected by ceramide proposes a general role of ceramide in clustering membrane signaling factors (Kolesnick, Alonso 2000). Such clustering might involve factors required for endocytosis (Hauck et al., 2000; Serrano et al., 2012; Simonis et al., 2014). Yet, depletion of sphingomyelin without ceramide production might be sufficient to alter endocytic pathways. SM coalesce into PM rafts with cholesterol (Simons and Sampaio, 2011) and cholesterol depletion by methyl-beta-cyclodextrin (MβCD) phenocopies bSMAse treatment in terms of massive, tubular endocytosis (Shen et al., 2014). Cholesterol is required for membrane homeostasis, trafficking, or signaling during adenovirus endocytosis and escape (Imelli et al., 2004). Of note, acute MβCD treatment also depletes SM (Giocondi et al., 2004). The acute depletion of cholesterol (50 mM MβCD, 20 min) employed during HAdV entry was reported to delay endocytosis.

Accordingly, an acute depletion of SM mediated by highly concentrated bSMase inhibited HAdV endocytosis (Fig. S5b). Also, a prolonged incubation with increasing bSMase concentrations interfered with HeLa cell survival (data not shown), in agreement with a role for ceramide in cell death (Obeid et al., 1993). Harsh perturbations have adverse consequences for virus entry, but what happens under 'physiological' conditions? For rescue experiments, we estimated the amount of ASMase released during HAdV-C2 entry (Fig. S5a), and observed that add-back of similar concentrations accelerated both HAdV-C2 and TS1 endocytosis (Fig. S2d,e). Together, the available data highlight how ceramide potentially modulates HAdV endocytosis at multiple levels, including physical membrane curvature, initiation of endocytosis, segregation of signaling factors and as a substrate for other sphingolipids.

Targeting ceramide metabolism: a clinical perspective

Amitriptyline was introduced by Merck in the early sixties to treat depressive disorder (Beckmann et al., 2014) and continues to be FDA-approved for this application. During this long clinical history, an extensive knowledge of pharmacokinetics, benefits and side-effects was gained and essentially documented the safety of this compound. Amitriptyline and other ASMase inhibitors meanwhile showed efficacy against cystic fibrosis and cardiovascular, metabolic, inflammatory, liver and infectious diseases (Beckmann et al., 2014). Targeting ASMase could be a valid strategy against a broad number of pathogens. Yet, ASMase activity needs to be fine-tuned. Knockout of ASMase blocks phagocytosis and thereby confers high susceptibility to some bacterial infections (Utermöhlen et al., 2003). Also, too low ASMase activity in plasma leads to thrombus formation (Münzer et al., 2014). Moreover, long term ASMase inhibition is not conceivable as it would mimic Niemann-Pick disease symptoms. All in all, future developments in ASMase research might offer drugs for acute and highly specific ASMase inhibition. Administration by aerosol would specifically inhibit infectious diseases of the upper respiratory tract. Yet, although reduction of ASMase in lungs improved survival of CFTR patients (Becker et al., 2012), cells of the immune system might be less effective in survey (Utermöhlen et al., 2003) and activation of innate immunity responses such as inflammasome. Comprehensive lipidomics of infections in a physiological context, as previously done for influenza in mice (Tam et al., 2013b), might help clarifying the complexity of the lipid contribution to pro- and anti-viral events.

MATERIALS AND METHODS

Cells and viruses: HeLa cervical carcinoma cells, subline Ohio (from L. Kaiser, University Hospital, Geneva, Switzerland) (Greber et al., 1993), human bronchial epithelial A549 cells, and primary human embryonic lung Wi-38 cells (both American Type Culture Collection) cells were grown at 37°C under 5% CO_2 in Dulbecco's modified Eagle's medium (DMEM; Sigma) supplemented with 7.5% fetal calf serum (FCS; Life Technologies) and 1% nonessential amino acids (Sigma). Human Niemann-Pick disease A fibroblasts GM00112 (Coriell Institute for Medical Research (Camden, NJ) were cultured in Eagle's Minimum Essential Medium with Earle's salts, 1% non-essential amino acids and 10% fetal calf serum and human airway epithelial cells from nasal biopsies (hAECN) in hAEC medium (both Epithelix). HAdV-C2, the penetration-deficient mutant TS1, and HAdV-C5 were grown in A549 cells, isolated, and labeled with Alexa Fluor 488 (Alexa488; Life Technologies) or Atto-565 (Atto-tec, Germany) as previously described (Greber et al., 1996; Greber et al., 1993). HAdV-C5_EGFP, an E1/E3 deletion mutant virus containing the enhanced green fluorescent protein (EGFP) gene in the E1 region under the control of cytomegalovirus major immediate early promoter (Fleischli et al., 2007; Nagel et al., 2003) and the HAdV-C5_EGFP-VI_L40Q (VI-L40Q) (Moyer et al., 2011) were grown in 911 cells.

Lipid extraction and mass spectrometry: for lipid profiling, $8x10^6$ HeLa Ohio cells were infected for 30 min with 6.8-ml inocula containing 2 µg of either HAdV-C2 or TS1. Total lipid extracts were collected according to a modified Bligh and Dyer protocol and quantitative analysis of lipids was performed by HPLC MS/MS. The detailed procedure is described in (Tanner et al., 2014). The log2 fold change of lipid abundance at 0 and 30 min pi is plotted. Statistical significance was evaluated by unpaired student's t-test (two-tailed, $p<0.05$). For ceramide quantification in bSMase treated samples, $2x10^6$ HeLa Ohio cells were incubated for 5 min with 0.2 U bacterial sphingomyelinase from *S. Aureus* (bSMase; Sigma). Total lipid extracts were collected similarly to a previously described protocol (Guan et al., 2013). $0.75x10^6$ cells were grown overnight in 6-cm plates. 0.2 U bSMase in 4 ml culture medium were incubated with cells for 5 min at 37°C, 5% CO_2 . For lipid extraction, cells were placed on ice and further processed with ice cold reagents. Cells were scraped in total 4 ml PBS and carefully re-suspended. 200 µl of cell suspension was used for cell counting with CASY (Roche) and determination of protein concentration (Micro BCA kit ; Thermo Scientific). Cells were centrifuged at 5'000 rpm for 5 min at 4°C, the pellet was re-suspended in 30 µl PBS, transferred into fresh 1.7 ml tubes (Axygen), shock-frozen and stored at -20°C until further processing. For lipid extraction, 600 µl of chloroform : methanol 1 : 2 (chloroform: CHROMASOLV® Plus, ref.: 650471-1L; Sigma) were added to the cell pellet. The suspension was vortexed 1 min and put on ice for 4 min. This step was repeated in total three times, then 300 µl chloroform + 200 µl H_2O were added. The samples were vortexed 30 sec and put on ice 1 min*, in total 3 times, before being centrifuged at 9'000 rpm for 5 min at

4°C. The lower phase containing lipids was pipetted into a clean tube with a 200 µl tip resistant to chloroform dissolution (ref.: 070000; Greiner Bio-One). Special care was taken in avoiding to contaminate the organic phase with the proteins and ions precipitates at the interphase. The aqueous phase was re-extracted by adding 500 µl chloroform and repeating the procedure from*. The two organic phases were pooled and dried in the Speedvac (Thermo Scientific) at maximal 30°C. Samples were sealed and stored at -20°C. Ceramide and sphingomyelin were quantified using LC-MS (Guan et al., 2013).

Infection assays: Cells grown on 96-well imaging plates (Greiner Bio-one) were infected in DMEM-0.2% fatty acid free bovine serum albumin fraction V (FAF BSA; Roche) for 16-24 h to reach an infection level of 20-40%. Cells were fixed, stained with DAPI and anti-VI (Burckhardt et al., 2011) or anti-hexon (mab 8052; Millipore) and imaged by automated fluorescence microscopy with ImageXpress Micro (Molecular Devices). Mean fluorescence intensity of the nuclear GFP signal and percentage of either GFP expressing or VI stained cells was evaluated using a custom programmed Matlab routine. For drug interference, cells were treated with 50 µM myriocin(He et al., 2004) (Enzo Life Sciences), 100 µM fumonisin B1 (Tocris; Wang et al., 1991), 50 µM GW4869 (Luberto et al., 2002) , 25 µM amitriptyline (Kornhuber et al., 2008) and 5 µM fluoxetine (Kornhuber et al., 2008) (all Sigma) for 4h before and during infection with either HAdV-C5_EGFP or HAdV-C5. For siRNA mediated knockdown of ASMase, HeLa Ohio cells were subjected to reverse-transfection with 10 nM siRNA using lipofectamine RNAiMAX (LifeTechnologies) and cells were infected after 72 h. ON-TARGET *Plus* siRNA sequences against human SMPD1 (J006676-05; J-006676-06) and Non targeting sequences were obtained from Thermo Scientific Dharmacon ; siRNA against GFP from Microsynth. For rescue experiments in GM00112 cells, inocula were supplemented with 0.024 U/ml of bacterial sphingomyelinase (bSMase) from *S. Aureus* (Sigma). For calcium-free infection assays, cells were exposed to the inoculum w/wo calcium (lysosomal exocytosis buffer) for 2h, then placed for further 14h into DMEM-0.2% FAF BSA to avoid cell detachment.

Fiber loss, endocytosis and VI exposure: fluorescently labeled HAdVs were exposed for 1h at 4°C to cells pre-treated for 4h with 25 µm Ami or DMEM-0.2% FAF BSA, to yield 50-200 viruses per cell. Bound viruses were internalized at 37°C for the indicated time. For rescue experiments, medium was supplemented with either Ami, 0.012 U/ml bSMase or bSMase mixed with a 150-fold excess of its *in vitro* substrate HMU-PC and added to cells for 5 min at 37°C. For the endocytosis assay, surface viruses were stained with 9C12 anti-hexon antibody (Varghese et al., 2004) at 4°C in intact cells. For fiber loss and VI exposure, fixed and permeabilized samples were stained with R72 anti-fiber antibody (Baum et al., 1972) and anti-VI antibody (Burckhardt et al., 2011). Samples were processed for fluorescence microscopy and images acquired with Leica SP5 equipped with 63×objective (oil immersion, numerical aperture 1.4). Maximum projection images of Z-stacks (11x 0.5 µm steps, 16× frame averaging) were analyzed using a customized Matlab routine

(available upon request). Fluorescence intensity of the antibody staining on the position of each virus was determined and mean values per cell are shown. Endocytosed viruses were identified as positive for the fluorescent tag but negative for surface staining with 9C12. Intensity of VI staining was evaluated on endocytosed viruses only, to exclude effects due to internalization delay. For further details, please refer to (Burckhardt et al., 2011; Suomalainen et al., 2013).

Detection of cytosolic viruses: cytosolic viruses were distinguished from endosomal viruses using SLO-penetration assay and EM analysis. Both procedures were performed exactly as described in (Suomalainen et al., 2013). Briefly, cells were pre-treated for 4h with 25 µm Ami or 1h 10 µM nocodazole or left untreated and exposed to a cold-synchronized infection for various times. For rescue experiments, medium was supplemented with either Ami, 0.012 U/ml bSMase or bSMase mixed with a 150-fold excess of its *in vitro* substrate HMU-PC and added to cells for 20 min at 37°C. For SLO-assay, streptolysin O (SLO; kindly provided by M. Husmann and S. Bhakdi, University Medical Center, Johannes Gutenberg-University Mainz) was used to selectively permeabilize plasma membranes and allow perfusion of antibodies to the cytosol but not to the lumen of intracellular organelles. HAdV-C5-Alexa488 and TS1-Alexa488 were immuno-stained for 1h at 4°C with rabbit anti-Alexa Fluor 488 antibodies (Life Technologies). Samples were processed as described in the previous section. Mean signal intensities of anti-Alexa Fluor 488 associated to viruses per cell are indicated. For quantification of EM sections, the number of viruses at the plasma membrane, in endosomes and in the cytosol was determined by manual counting (K. Boucke, IMLS Zürich).

Liposome floatation: 1-palmitoyl-2-oleoylphosphatidylcholine (PC), N-octadecanoyl-D-erythro-sphingosine (CER), N-octadecanoyl-D-erythro-sphingosylphosphorylcholine (SM) and extruder were obtained from Avanti Polar Lipids. Lipids were dissolved in ice cold chloroform as indicated in Table 2 and conserved at -20°C in sealed glass containers.

Lipid	Full name	Origin	Product nr.	Amount (mg)	Vol. (ml)	Conc. (mg/ml)
PC (16:0/18:1)	1-palmitoyl-2-oleoyl-*sn*-glycero-3-phosphocholine	Synthetic	850457P	25	3.78	6.6
SM (mainly C18)	N-octadecanoyl-D-*erythro*-sphingosylphosphorylcholine	Brain, porcine	860062	25	3.43	7.24
Cer (mainly C18)	N-octadecanoyl-D-*erythro*-sphingosine	Brain, porcine	860052P	25	5	5

Table 2: informations concerning the lipids ordered by Avanti used in this study are summarized.

Lipids were mixed as indicated in table 3 and dryed in a Speedvac (Thermo Scientific). To avoid plastic contaminations in the samples, tubes and tips resistant to organic solvents were exclusively employed (Axygen and Greiner Bio-One). Dried lipid films composed of PC, PC:CER 99:1 mol% and PC:SM 99:1 mol% were hydrated in liposomes buffer (10 mM Hepes, 150 mM NaCl, 2 mM $CaCl_2$, pH 7.5) to a final concentration of 1 mg/ml. Ceramide and sphingomyelin containing samples were hydrated by incubation in the water bath at 42°C and vortexing. To achieve an homogeneous size of the liposomes and mimic endosomal dimensions, lipid suspensions were subjected to 20 freeze-thaw cycles and extruded 11 times through a 100 nm polycarbonate-membrane (Avanti). Liposomes suspensions were shock-frozen and stored at -20°C.

Mol %	**POPC** (µl of a 6.6 mg/ml stock)	**Cer** (µl of a 0.5 mg/ml stock)	**SM** (µl of a 0.724 mg/ml stock)
100/0/0	151.5	-	-
99/1/0	150	37	-
99/0/1	150	-	27

Table 3: lipid mix to prepare 1 ml of 1 mg/ml liposomes. The stock solutions were prepared as indicated in table CC, except for cer and SM that were further diluted 1:10.

Viruses were incubated 10 min at 45°C to induce uncoating (Wiethoff et al., 2005) (Fig. 2d). Uncoated viruses (4 µg) were incubated for 15 min at 37°C with liposomes (100 µg). Samples were put on ice and mixed with Optiprep (Sigma) to a final concentration of 15%. Each 600 µl sample was overlayed with a density gradient of Optiprep (1.5 ml of 10%, 1 ml of 2.5% and 0% in liposomes buffer, ice cold) and centrifuged at 100'000 g for 2h at 4°C. Low density, empty liposomes floated to the top fraction of the gradient, while liposomes bound to viral proteins concentrated into a lower band (Fig. 2c). Fractions (400 µl) were immediately collected, subjected to immuno-gold labeling of VI and analyzed by EM negative staining with uranyl acetate. Images were acquired with magnification 25'000x, where the gold signal is indistinguishable. Each image was further magnified (80'000x) and the total number of liposomes and liposomes bound to gold were counted. To avoid underestimation of binding, when one liposome bound to n+1 gold, n liposomes with 100% binding (meaning one liposome bound to one VI-gold) were included in the statistics.

Liposomes leakage: Total lipid extracts of $5x10^6$ HeLa Ohio cells were collected according to a modified Bligh & Dyer method (Tanner et al., 2014), dried and re-hydrated in 0.2M 6-carboxyfluorescein (6-CF; Sigma). Liposomes were produced as described for the liposome binding assay. To remove unincorporated 6-CF, a 1 ml gravity flow column (Biorad) filled with Sephadex-G50 (Pharmacia Biotech; hydrated overnight at 4°C) and centrifuged 2 min at 2'000 g was used. 100 µl liposomes were loaded on the gel and centrifuged 2 min at 2'000g. The eluate was further cleared by a second step of centrifugation on a new column and the final volume brought to 200 µl with liposomes buffer. For each new liposomes solution, linear range of

the leakage was first established. The concentration of viral proteins and bSMAse that induced 10-20% leakage were employed. Cleared liposomes (8-10 µl, resulting from approximately $5x10^4$ cells) were immediately pre-incubated for 15 min with 5-10 µl of 0.48 U/ml bSMase dissolved in liposomes buffer or liposomes buffer, then further incubated for 15 min at 37°C with 5-10 µl of 5 µg/ml uncoated HAdV-C5-EGFP or VI-L40Q. All incubations were carried in a transparent round bottom 96-well plate (Greiner Bio-One) containing 50 µl of liposomes buffer, in a M200 Infinite Plate Reader pre-warmed to 37°C (Tecan). 100% liposomes leakage was determined by adding Triton X-100 to a final concentration of 0.5%. Fluorescence was measured at 485 nm excitation/530 nm emission wavelength. The percentage leakage was calculated using the formula: 100 -[(Fmeas _ F0)/(Ftx100 _ F0)], where Fmeas is the maximum fluorescence intensity measured, F0 is fluorescence intensity before adding viral proteins, and Ftx100 is the fluorescence intensity in the presence of 0.5% Triton X-100, as described in (Wiethoff et al., 2005).

ASMase activity: activity of ASMase was determined as described in (van Diggelen et al., 2005). For extracellular ASMase activity, $1x10^6$ cells were grown overnight in 6-cm plates. The next day, cells were exposed to cold binding with the indicated ligands in RPMI-0.2% FAF BSA (cholera toxin subunit B; CTB; Crucell; CARexFC (Ebbinghaus et al., 2001); 1 mg/ml; kindly provided by S. Hemmi, University of Zürich). Unbound ligands were removed and cells placed at 37°C in 600 µl exocytosis buffer (25 mM Hepes, 125mM NaCl, 5 mM KCl, 1.2 mM $MgSO_4$, 1 mM $CaCl_2$, 1.2 mM KH_2PO_4, 6 mM D-glucose) for 5, 15 or 45 min. For calcium- and magnesium-free media, exocytosis buffer devoid of $CaCl_2$ and $MgSO_4$ were used for the washing steps after cold binding (ice cold) and for the incubation at 37°C (pre-warmed). Supernatants were collected and cleared by centrifugation at 11'000 g for 5 min. For total ASMase activity, lysates of cells treated with drugs and siRNA were re-suspended in 1 mM PMSF (Sigma) in ddH_2O and the protein concentration was determined using the Micro BCA kit (Thermo Scientifics). Lysates were diluted to a final concentration of 1 µg/µl. 10 µl of cell lysates in a 96-well plate (transparent, round bottom; Greiner Bio-One) or 300 µl of the supernatants (in eppendorf tubes) were incubated with 20 µl or 80 µl respectively of 0.4 mg/ml 6-hexadecanoylamino-4-methylumbelliferylphosphorylcholine (HMU-PC; Moscerdam Substrates) in substrate buffer (0.1 M sodium acetate buffer, 0.2% (w/v), synthetic sodium taurocholate (Sigma), pH 5.2) for 3h at 37°C. The reaction was blocked by adding 200 µl stop buffer (0.5 M sodium carbonate buffer, 0.25% Triton X-100, pH 10.7) for 15 min at RT in the dark. Fluorescence was recorded with M200 Infinite Plate Reader (Tecan) at 404 nm excitation/460 nm emission wavelength.

β-hexosaminidase:

Supernatants were collected as described in the previous section (ASMase activity) and processed as described in (Rodríguez et al., 1997). 350 µl samples were incubated with 50 µl of 6 mM 4-methyl-umbellyferyl-*N*-acetylb-d-glucosaminide (Sigma) in sodium citrate-phosphate buffer (prepared by mixing 557.5 ml of 0.2 M Na_2HPO_4 with 442.5 ml of 0.1 M citric acid, and adjusting the pH to 4.5) for 1 h at 37°C.

The reaction was stopped by adding 100 µl of stop buffer 2 (2 M Na_2CO_3, 1.1 M glycine). Samples were gently shaked for 15 min at RT in the dark. Fluorescence was recorded with M200 Infinite Plate Reader (Tecan) at 404 nm excitation/460 nm emission wavelength.

Lactate dehydrogenase activity:

Supernatants were collected as described in the previous section (ASMase activity) and processed as described in (Rodríguez et al., 1997). 300 µl of freshly prepared, ice cold substrate (0.23 mM NADH, 1 mM sodium pyruvate, 0.1% Triton X-100, 0.2 M Tris-HCl (all Sigma), pH 7.3) were added to a 96-well plate (transparent, round bottom; Greiner Bio-One) on ice. Triton-X treated samples were diluted 1:10. 30 µl of supernatant was mixed with the substrate and the plate placed at 37°C in the M200 Infinite Plate Reader (Tecan). A time course of NADH conversion into NAD^+ by LDH was immediately started by measuring the decrease in absorbance at 340 nm every 2 min.

Live imaging of calcium sensing and propidium iodide influx: $0.5x10^6$ HeLa Ohio cells were transfected with 6 µg of either pCMV_GCamP5G (Addgene) (Akerboom et al., 2012) or Dyn2K44A-GFP (Gastaldelli et al., 2008) using Neon technology (100 µl tip, 1005 V, 35 ms, 2 pulses; Life Technologies). Cells were grown in 96-well imaging plates (Greiner Bio-one) for 24h. Cells were exposed to 1-10 µg/ml HAdV-C2-Atto565 or 1-10 µg/ml HAdV-C2 in presence of 0.2 mg/ml propidium iodide (Molecular Probes) or absence of calcium where indicated. Imaging was performed between 0 and 15 min infection at 37°C with a Leica Sp5 confocal microscope equipped with 40× objective (oil immersion, numerical aperture 1.25). Z-stacks composed of 4x 0.5 µm steps were recorded at a frequency of 8000 Hz applying bidirectional scan, line averaging 32x and minimized acquisition time. Total fluorescence intensity per cell or per indicated area was quantified with MacBiophotonics ImageJ (McMaster University).

Flow cytometry: sub-confluent cells were harvested in PBS-20 mM EDTA and washed 2 times in cell medium to fully remove EDTA. 75'000 cells were incubated with 2 µg HAdV-C2/5, VI-L40Q, heat-treated HAdV-C2/5, HAdV-C5-Atto488 and anti-CAR antibody for 1h at 4°C, in a total volume of 100 µl. For PI accessibility, cells were placed 5 min at 37°C in RPMI-0.2% FAF BSA containing 0.2 mg/ml PI. For surface profiling, unbound antibodies or viruses were washed away and cells were fixed and stained with anti CAR antibody E1-1 (kindly provided by S. Hemmi, University of Zürich). For VI immunodepletion, 2 µg heat treated viruses were incubated for 1h with 12 µg of either anti-VI IgG (Burckhardt et al., 2011) or an anti-VIII IgG control (D. Püntener, unpublished) before incubation with cells for 20 min at 37°C in presence of 0.2 mg/ml PI. Samples were analyzed with FACSCanto II (BD Biosciences). 5'000 cells per sample were analyzed, with FSC=319 V, SSC=33 V and PE=260 V.

Lysotracker signal quantification: HeLa Ohio cells were loaded with LysoTracker Red DND99 (Invitrogen) as indicated by the manufacturer. Time-lapse imaging of infection was performed as described above, except that Z-stacks were composed of 11x 0.5 µM steps and were acquired at 0 min and 20 min post-infection. The total lysotracker signal on maximal projections was quantified using MacBiophotonics ImageJ. The ratio lysotracker signal at 20 min/0 min per cell is plotted.

Resazurin assay: cell toxicity was evaluated using the resazurin fluorometric assay (Czekanska, 2011). Briefly, after 24h of drug treatment, cells were placed into sterile filtered 0.002% resazurin (Sigma) in PBS for 1h and 30 min in a 37°C, 5% CO_2 incubator. The reduction of resazurin to the fluorescent resorufin by several mitochondrial enzymes was measured using M200 Infinite Plate Reader (Tecan) at excitation 550/9 nm and emission 590/20 nm wavelength.

Statistical analysis: statistical analysis were performed using GraphPad Prism software (GraphPad Software, Inc. La Jolla). Population analysis are plotted as bars or symbols and single-cell based analysis are represented as scatter dot plot, where the horizontal bar indicates the mean value and the vertical bars show the standard error of the mean. Two-tailed P-values were calculated by unpaired t-test with confidence interval 95%.

CONCLUDING REMARKS

With this study, we propose a mechanism for how incoming HAdV, a non-enveloped virus, tunes cellular sphingolipids for efficient invasion.

In recent years, it became increasingly clear that cellular lipids play fundamental roles at different stages of the viral life cycle. Viruses have evolved various mechanisms to hijack lipid signaling, metabolism and synthesis for own purposes. Much about these strategies remains to be characterized, both during the host cell-virus interaction, and also at the physiological level. The great technical advances in the field of lipid research provided many valuable tools to study lipid regulations and importantly contributed to our basic understanding of viral infections. Moreover, gaining further insights into how host lipid remodeling occurs might offer new perspectives for anti-viral treatments.

ABBREVIATIONS

aa	amino acids
AFM	atomic force microscopy
AMPs	antimicrobial peptides
ASMase	human acid sphingomyelinase
Aβ	amyloid beta
bSMase	bacterial sphingomyelinase
C1PP	ceramide-1-phosphate phosphatase
CAR	coxsackievirus B and adenovirus receptor
CDase	ceramidase
cer	ceramide
CERT	ceramide transfer proteins
CHMP	charged multivesicular body protein
CK	ceramide kinase
CPPs	cell penetrating peptides
CRS	cerebrosidase
CS	ceramide synthase
CVB	Coxsackie virus B
DAF	decay-accelerating factor
DAG	diacylglycerol
DES	dihydroceramidedesaturase
DOPC	1,2-Dioleoyl-sn-glycero-3-phosphocholine
EM	electron microscopy
ESCRT	endosomal sorting complexes required for transport
FHV	flock house virus
GCS	glucosylceramide synthase
GPI-PLAP	GPI-anchored placental alkaline phosphatase

HAdV	human adenovirus
HCV	Hepatitis C virus
HIV TAT	HIV trans-activating protein
IAPP	islet amyloid polypeptide
IFN	interferon
IL	interleukin
Ins3P	inositol 1,4,5-trisphosphate
ISVPs	intermediate subviral particles
JEV	japanese encephalitic virus
LDH	lactate dehydrogenase
MVM	minute virus of mice
NBD-DPPE	7-nitrobenz-2-oxa-1,3-diazol-4-yl - 1,2-Dipalmitoyl-sn-glycero-3-phosphoethanolamine
NPD	Niemann-Pick disease
PC	phosphatidylcholine
PIP2	$PI(4,5)P_2$, phosphatidylinositol 4,5-bisphosphate
PLA2	phospholipase A2
PLC	phospholipase C
PM	plasma membrane
POPC	1-palmitoyl-2-oleoyl-sn-glycero-3-phosphocholine
ROS	reactive oxygen species
S1P	sphingosine-1-phosphate
S1PP	S1P phosphatase
SLO	streptolysin-O
SM	sphingomyelin
SMase	sphingomyelinase
SMS	sphingomyelin synthase
SPT	serine-palmitoyltransferase
syt	synaptotagmin

TIRFM	total internal reflection fluorescence microscopy
TLC	thin layer chromatography
TNF	tumor necrosis factor
t-PnA	trans-parinaric acid
TR-DHPE	Texas Red-1,2-dihexadecanoyl-sn-glycero-3-phophoethanolamine
VP	viral protein
β-hex	β-hexosaminidase

REFERENCES

Abdelhakim, A. H., E. N. Salgado, X. Fu, M. Pasham, D. Nicastro, T. Kirchhausen, and S. C. Harrison, 2014, Structural correlates of rotavirus cell entry: PLoS Pathog, v. 10, p. e1004355.

Abe, M., and T. Kobayashi, 2014, Imaging local sphingomyelin-rich domains in the plasma membrane using specific probes and advanced microscopy: Biochim Biophys Acta, v. 1841, p. 720-6.

Acharya, U., and J. K. Acharya, 2005, Enzymes of sphingolipid metabolism in Drosophila melanogaster: Cell Mol Life Sci, v. 62, p. 128-42.

Acharya, U., M. B. Mowen, K. Nagashima, and J. K. Acharya, 2004, Ceramidase expression facilitates membrane turnover and endocytosis of rhodopsin in photoreceptors: Proc Natl Acad Sci U S A, v. 101, p. 1922-6.

Adada, M., D. Canals, Y. A. Hannun, and L. M. Obeid, 2014, Sphingolipid regulation of ezrin, radixin, and moesin proteins family: implications for cell dynamics: Biochim Biophys Acta, v. 1841, p. 727-37.

Agosto, M. A., T. Ivanovic, and M. L. Nibert, 2006, Mammalian reovirus, a nonfusogenic nonenveloped virus, forms size-selective pores in a model membrane: Proc Natl Acad Sci U S A, v. 103, p. 16496-501.

Agosto, M. A., J. K. Middleton, E. C. Freimont, J. Yin, and M. L. Nibert, 2007, Thermolabilizing pseudoreversions in reovirus outer-capsid protein micro 1 rescue the entry defect conferred by a thermostabilizing mutation: J Virol, v. 81, p. 7400-9.

Akerboom, J., T. W. Chen, T. J. Wardill, L. Tian, J. S. Marvin, S. Mutlu, N. C. Calderón, F. Esposti, B. G. Borghuis, X. R. Sun, A. Gordus, M. B. Orger, R. Portugues, F. Engert, J. J. Macklin, A. Filosa, A. Aggarwal, R. A. Kerr, R. Takagi, S. Kracun, E. Shigetomi, B. S. Khakh, H. Baier, L. Lagnado, S. S. Wang, C. I. Bargmann, B. E. Kimmel, V. Jayaraman, K. Svoboda, D. S. Kim, E. R. Schreiter, and L. L. Looger, 2012, Optimization of a GCaMP calcium indicator for neural activity imaging: J Neurosci, v. 32, p. 13819-40.

Andersson, E., V. Rydengård, A. Sonesson, M. Mörgelin, L. Björck, and A. Schmidtchen, 2004, Antimicrobial activities of heparin-binding peptides: Eur J Biochem, v. 271, p. 1219-26.

Andrews, N. W., 2000, Regulated secretion of conventional lysosomes: Trends Cell Biol, v. 10, p. 316-21.

Andrews, N. W., P. E. Almeida, and M. Corrotte, 2014, Damage control: cellular mechanisms of plasma membrane repair: Trends Cell Biol, v. 24, p. 734-742.

Apostolidou, M., S. A. Jayasinghe, and R. Langen, 2008, Structure of alpha-helical membrane-bound human islet amyloid polypeptide and its implications for membrane-mediated misfolding: J Biol Chem, v. 283, p. 17205-10.

Atanassoff, A. P., H. Wolfmeier, R. Schoenauer, A. Hostettler, A. Ring, A. Draeger, and E. B. Babiychuk, 2014, Microvesicle shedding and lysosomal repair fulfill divergent cellular needs during the repair of streptolysin O-induced plasmalemmal damage: PLoS One, v. 9, p. e89743.

Avota, E., E. Gassert, and S. Schneider-Schaulies, 2011a, Cytoskeletal dynamics: concepts in measles virus replication and immunomodulation: Viruses, v. 3, p. 102-17.

Avota, E., E. Gulbins, and S. Schneider-Schaulies, 2011b, DC-SIGN mediated sphingomyelinase-activation and ceramide generation is essential for enhancement of viral uptake in dendritic cells: PLoS Pathog, v. 7, p. e1001290.

Babiychuk, E. B., K. Monastyrskaya, and A. Draeger, 2008, Fluorescent annexin A1 reveals dynamics of ceramide platforms in living cells: Traffic, v. 9, p. 1757-75.

Babiychuk, E. B., K. Monastyrskaya, S. Potez, and A. Draeger, 2009, Intracellular Ca(2+) operates a switch between repair and lysis of streptolysin O-perforated cells: Cell Death Differ, v. 16, p. 1126-34.

Bai, J., and R. E. Pagano, 1997, Measurement of spontaneous transfer and transbilayer movement of BODIPY-labeled lipids in lipid vesicles: Biochemistry, v. 36, p. 8840-8.

Banerjee, M., and J. E. Johnson, 2008, Activation, exposure and penetration of virally encoded, membrane-active polypeptides during non-enveloped virus entry: Curr Protein Pept Sci, v. 9, p. 16-27.

Barranger-Mathys, M., and D. S. Cafiso, 1994, Collisions between helical peptides in membranes monitored using electron paramagnetic resonance: evidence that alamethicin is monomeric in the absence of a membrane potential: Biophys J, v. 67, p. 172-6.

Barroso-González, J., J. D. Machado, L. García-Expósito, and A. Valenzuela-Fernández, 2009, Moesin regulates the trafficking of nascent clathrin-coated vesicles: J Biol Chem, v. 284, p. 2419-34.

Bartke, N., and Y. A. Hannun, 2009, Bioactive sphingolipids: metabolism and function: J Lipid Res, v. 50 Suppl, p. S91-6.

Bartlett, J. S., R. Wilcher, and R. J. Samulski, 2000, Infectious entry pathway of adeno-associated virus and adeno-associated virus vectors: J Virol, v. 74, p. 2777-85.

Barton, E. S., J. L. Connolly, J. C. Forrest, J. D. Chappell, and T. S. Dermody, 2001a, Utilization of sialic acid as a coreceptor enhances reovirus attachment by multistep adhesion strengthening: J Biol Chem, v. 276, p. 2200-11.

Barton, E. S., J. C. Forrest, J. L. Connolly, J. D. Chappell, Y. Liu, F. J. Schnell, A. Nusrat, C. A. Parkos, and T. S. Dermody, 2001b, Junction adhesion molecule is a receptor for reovirus: Cell, v. 104, p. 441-51.

Baum, S. G., M. S. Horwitz, and J. V. Maizel, 1972, Studies of the mechanism of enhancement of human adenovirus infection in monkey cells by simian virus 40: J Virol, v. 10, p. 211-9.

Becker, K. A., B. Henry, R. Ziobro, B. Tümmler, E. Gulbins, and H. Grassmé, 2012, Role of CD95 in pulmonary inflammation and infection in cystic fibrosis: J Mol Med (Berl), v. 90, p. 1011-23.

Beckmann, N., D. Sharma, E. Gulbins, K. A. Becker, and B. Edelmann, 2014, Inhibition of acid sphingomyelinase by tricyclic antidepressants and analogons: Front Physiol, v. 5, p. 331.

Benevento, M., S. Di Palma, J. Snijder, C. L. Moyer, V. S. Reddy, G. R. Nemerow, and A. J. Heck, 2014, Adenovirus composition, proteolysis, and disassembly studied by in-depth qualitative and quantitative proteomics: J Biol Chem, v. 289, p. 11421-30.

Bergelson, J. M., J. A. Cunningham, G. Droguett, E. A. Kurt-Jones, A. Krithivas, J. S. Hong, M. S. Horwitz, R. L. Crowell, and R. W. Finberg, 1997, Isolation of a common receptor for Coxsackie B viruses and adenoviruses 2 and 5.: Science, v. 275, p. 1320-3.

Bergsbaken, T., S. L. Fink, A. B. den Hartigh, W. P. Loomis, and B. T. Cookson, 2011, Coordinated host responses during pyroptosis: caspase-1-dependent lysosome exocytosis and inflammatory cytokine maturation: J Immunol, v. 187, p. 2748-54.

Berridge, M. J., P. Lipp, and M. D. Bootman, 2000, The versatility and universality of calcium signalling: Nat Rev Mol Cell Biol, v. 1, p. 11-21.

Bielawski, J., Z. M. Szulc, Y. A. Hannun, and A. Bielawska, 2006, Simultaneous quantitative analysis of bioactive sphingolipids by high-performance liquid chromatography-tandem mass spectrometry: Methods, v. 39, p. 82-91.

Bilkova, E., J. Forstova, and L. Abrahamyan, 2014, Coat as a dagger: the use of capsid proteins to perforate membranes during non-enveloped DNA viruses trafficking: Viruses, v. 6, p. 2899-937.

Bischofberger, M., I. Iacovache, and F. G. van der Goot, 2012, Pathogenic pore-forming proteins: function and host response: Cell Host Microbe, v. 12, p. 266-75.

Bischoff, J. R., D. H. Kirn, A. Williams, C. Heise, S. Horn, M. Muna, L. Ng, J. A. Nye, A. Sampson-Johannes, A. Fattaey, and F. McCormick, 1996, An adenovirus mutant that replicates selectively in p53-deficient human tumor cells.: Science, v. 274, p. 373-6.

Björkholm, P., A. M. Ernst, M. Hacke, F. Wieland, B. Brügger, and G. von Heijne, 2014, Identification of novel sphingolipid-binding motifs in mammalian membrane proteins: Biochim Biophys Acta, v. 1838, p. 2066-70.

Bonilla, E., K. Fischbeck, and D. L. Schotland, 1981, Freeze-fracture studies of muscle caveolae in human muscular dystrophy: Am J Pathol, v. 104, p. 167-73.

Borsa, J., B. D. Morash, M. D. Sargent, T. P. Copps, P. A. Lievaart, and J. G. Szekely, 1979, Two modes of entry of reovirus particles into L cells: J Gen Virol, v. 45, p. 161-70.

Bothner, B., X. F. Dong, L. Bibbs, J. E. Johnson, and G. Siuzdak, 1998, Evidence of viral capsid dynamics using limited proteolysis and mass spectrometry: J Biol Chem, v. 273, p. 673-6.

Boulant, S., M. Stanifer, C. Kural, D. K. Cureton, R. Massol, M. L. Nibert, and T. Kirchhausen, 2013, Similar uptake but different trafficking and escape routes of reovirus virions and infectious subvirion particles imaged in polarized Madin-Darby canine kidney cells: Mol Biol Cell, v. 24, p. 1196-207.

Bouter, A., C. Gounou, R. Bérat, S. Tan, B. Gallois, T. Granier, B. L. d'Estaintot, E. Pöschl, B. Brachvogel, and A. R. Brisson, 2011, Annexin-A5 assembled into two-dimensional arrays promotes cell membrane repair: Nat Commun, v. 2, p. 270.

Bozym, R. A., S. A. Morosky, K. S. Kim, S. Cherry, and C. B. Coyne, 2010, Release of intracellular calcium stores facilitates coxsackievirus entry into polarized endothelial cells: PLoS Pathog, v. 6, p. e1001135.

Breslow, D. K., and J. S. Weissman, 2010, Membranes in balance: mechanisms of sphingolipid homeostasis: Mol Cell, v. 40, p. 267-79.

Brogden, K. A., 2005, Antimicrobial peptides: pore formers or metabolic inhibitors in bacteria?: Nat Rev Microbiol, v. 3, p. 238-50.

Burckhardt, C. J., M. Suomalainen, P. Schoenenberger, K. Boucke, S. Hemmi, and U. F. Greber, 2011, Drifting motions of the adenovirus receptor CAR and immobile integrins initiate virus uncoating and membrane lytic protein exposure: Cell Host Microbe, v. 10, p. 105-17.

Burnett, R. M., 1985, The structure of the adenovirus capsid. II. The packing symmetry of hexon and its implications for viral architecture: J Mol Biol, v. 185, p. 125-43.

Błachnio-Zabielska, A., M. Baranowski, P. Zabielski, and J. Górski, 2008, Effect of exercise duration on the key pathways of ceramide metabolism in rat skeletal muscles: J Cell Biochem, v. 105, p. 776-84.

Cafiso, D. S., 1994, Alamethicin: a peptide model for voltage gating and protein-membrane interactions: Annu Rev Biophys Biomol Struct, v. 23, p. 141-65.

Callahan, J. W., C. S. Jones, D. J. Davidson, and P. Shankaran, 1983, The active site of lysosomal sphingomyelinase: evidence for the involvement of hydrophobic and ionic groups: J Neurosci Res, v. 10, p. 151-63.

Canals, D., R. W. Jenkins, P. Roddy, M. J. Hernández-Corbacho, L. M. Obeid, and Y. A. Hannun, 2010, Differential effects of ceramide and sphingosine 1-phosphate on ERM phosphorylation: probing sphingolipid signaling at the outer plasma membrane: J Biol Chem, v. 285, p. 32476-85.

Carpinteiro, A., C. Dumitru, M. Schenck, and E. Gulbins, 2008, Ceramide-induced cell death in malignant cells: Cancer Lett, v. 264, p. 1-10.

Cashikar, A. G., S. Shim, R. Roth, M. R. Maldazys, J. E. Heuser, and P. I. Hanson, 2014, Structure of cellular ESCRT-III spirals and their relationship to HIV budding: Elife, v. 3.

Castro, B. M., M. Prieto, and L. C. Silva, 2014, Ceramide: a simple sphingolipid with unique biophysical properties: Prog Lipid Res, v. 54, p. 53-67.

Cha, B., M. Tse, C. Yun, O. Kovbasnjuk, S. Mohan, A. Hubbard, M. Arpin, and M. Donowitz, 2006, The NHE3 juxtamembrane cytoplasmic domain directly binds ezrin: dual role in NHE3 trafficking and mobility in the brush border: Mol Biol Cell, v. 17, p. 2661-73.

Chalfant, C. E., B. Ogretmen, S. Galadari, B. J. Kroesen, B. J. Pettus, and Y. A. Hannun, 2001, FAS activation induces dephosphorylation of SR proteins; dependence on the de novo generation of ceramide and activation of protein phosphatase 1: J Biol Chem, v. 276, p. 44848-55.

Chandran, K., D. L. Farsetta, and M. L. Nibert, 2002, Strategy for nonenveloped virus entry: a hydrophobic conformer of the reovirus membrane penetration protein micro 1 mediates membrane disruption: J Virol, v. 76, p. 9920-33.

Chandran, K., and M. L. Nibert, 1998, Protease cleavage of reovirus capsid protein mu1/mu1C is blocked by alkyl sulfate detergents, yielding a new type of infectious subvirion particle: J Virol, v. 72, p. 467-75.

Chandran, K., S. B. Walker, Y. Chen, C. M. Contreras, L. A. Schiff, T. S. Baker, and M. L. Nibert, 1999, In vitro recoating of reovirus cores with baculovirus-expressed outer-capsid proteins mu1 and sigma3: J Virol, v. 73, p. 3941-50.

Charras, G. T., C. K. Hu, M. Coughlin, and T. J. Mitchison, 2006, Reassembly of contractile actin cortex in cell blebs: J Cell Biol, v. 175, p. 477-90.

Chen, F. Y., M. T. Lee, and H. W. Huang, 2002, Sigmoidal concentration dependence of antimicrobial peptide activities: a case study on alamethicin: Biophys J, v. 82, p. 908-14.

Chen, F. Y., M. T. Lee, and H. W. Huang, 2003, Evidence for membrane thinning effect as the mechanism for peptide-induced pore formation: Biophys J, v. 84, p. 3751-8.

Chen, J. Z., E. C. Settembre, S. T. Aoki, X. Zhang, A. R. Bellamy, P. R. Dormitzer, S. C. Harrison, and N. Grigorieff, 2009, Molecular interactions in rotavirus assembly and uncoating seen by high-resolution cryo-EM: Proc Natl Acad Sci U S A, v. 106, p. 10644-8.

Cheng, R. H., V. S. Reddy, N. H. Olson, A. J. Fisher, T. S. Baker, and J. E. Johnson, 1994, Functional implications of quasi-equivalence in a T = 3 icosahedral animal virus established by cryo-electron microscopy and X-ray crystallography: Structure, v. 2, p. 271-82.

Cheshenko, N., W. Liu, L. M. Satlin, and B. C. Herold, 2007, Multiple receptor interactions trigger release of membrane and intracellular calcium stores critical for herpes simplex virus entry: Mol Biol Cell, v. 18, p. 3119-30.

Cheshenko, N., J. B. Trepanier, M. Stefanidou, N. Buckley, P. Gonzalez, W. Jacobs, and B. C. Herold, 2013, HSV activates Akt to trigger calcium release and promote viral entry: novel candidate target for treatment and suppression: FASEB J, v. 27, p. 2584-99.

Chiantia, S., J. Ries, G. Chwastek, D. Carrer, Z. Li, R. Bittman, and P. Schwille, 2008, Role of ceramide in membrane protein organization investigated by combined AFM and FCS: Biochim Biophys Acta, v. 1778, p. 1356-64.

Chirivino, D., L. Del Maestro, E. Formstecher, P. Hupé, G. Raposo, D. Louvard, and M. Arpin, 2011, The ERM proteins interact with the HOPS complex to regulate the maturation of endosomes: Mol Biol Cell, v. 22, p. 375-85.

Chiu, C. Y., P. Mathias, G. R. Nemerow, and P. L. Stewart, 1999, Structure of adenovirus complexed with its internalization receptor, alphavbeta5 integrin: J Virol, v. 73, p. 6759-68.

Christensen, B., J. Fink, R. B. Merrifield, and D. Mauzerall, 1988, Channel-forming properties of cecropins and related model compounds incorporated into planar lipid membranes: Proc Natl Acad Sci U S A, v. 85, p. 5072-6.

Coffey, M. C., J. E. Strong, P. A. Forsyth, and P. W. Lee, 1998, Reovirus therapy of tumors with activated Ras pathway: Science, v. 282, p. 1332-4.

Contreras, F. X., A. M. Ernst, P. Haberkant, P. Björkholm, E. Lindahl, B. Gönen, C. Tischer, A. Elofsson, G. von Heijne, C. Thiele, R. Pepperkok, F. Wieland, and B. Brügger, 2012, Molecular recognition of a single sphingolipid species by a protein's transmembrane domain: Nature, v. 481, p. 525-9.

Corrotte, M., P. E. Almeida, C. Tam, T. Castro-Gomes, M. C. Fernandes, B. A. Millis, M. Cortez, H. Miller, W. Song, T. K. Maugel, and N. W. Andrews, 2013, Caveolae internalization repairs wounded cells and muscle fibers: Elife, v. 2, p. e00926.

Cowart, L. A., Z. Szulc, A. Bielawska, and Y. A. Hannun, 2002, Structural determinants of sphingolipid recognition by commercially available anti-ceramide antibodies: J Lipid Res, v. 43, p. 2042-8.

Creutz, C. E., C. J. Pazoles, and H. B. Pollard, 1978, Identification and purification of an adrenal medullary protein (synexin) that causes calcium-dependent aggregation of isolated chromaffin granules: J Biol Chem, v. 253, p. 2858-66.

Czekanska, E. M., 2011, Assessment of cell proliferation with resazurin-based fluorescent dye: Methods Mol Biol, v. 740, p. 27-32.

D'Halluin, J. C., M. Milleville, P. A. Boulanger, and G. R. Martin, 1978, Temperature-sensitive mutant of adenovirus type 2 blocked in virion assembly: accumulation of light intermediate particles: J Virol, v. 26, p. 344-56.

del Pozo, M. A., N. Balasubramanian, N. B. Alderson, W. B. Kiosses, A. Grande-García, R. G. Anderson, and M. A. Schwartz, 2005, Phospho-caveolin-1 mediates integrin-regulated membrane domain internalization: Nat Cell Biol, v. 7, p. 901-8.

Denisova, E., W. Dowling, R. LaMonica, R. Shaw, S. Scarlata, F. Ruggeri, and E. R. Mackow, 1999, Rotavirus capsid protein VP5* permeabilizes membranes: J Virol, v. 73, p. 3147-53.

Di Paolo, N. C., K. Doronin, L. K. Baldwin, T. Papayannopoulou, and D. M. Shayakhmetov, 2013, The transcription factor IRF3 triggers "defensive suicide" necrosis in response to viral and bacterial pathogens: Cell Rep, v. 3, p. 1840-6.

Dickson, R. C., 2008, Thematic review series: sphingolipids. New insights into sphingolipid metabolism and function in budding yeast: J Lipid Res, v. 49, p. 909-21.

Ding, B., and Z. Chen, 2012, Molecular interactions between cell penetrating peptide Pep-1 and model cell membranes: J Phys Chem B, v. 116, p. 2545-52.

Dobrzyń, A., and J. Górski, 2002, Ceramides and sphingomyelins in skeletal muscles of the rat: content and composition. Effect of prolonged exercise: Am J Physiol Endocrinol Metab, v. 282, p. E277-85.

Doherty, G. J., and H. T. McMahon, 2009, Mechanisms of endocytosis: Annu Rev Biochem, v. 78, p. 857-902.

Dormitzer, P. R., H. B. Greenberg, and S. C. Harrison, 2000, Purified recombinant rotavirus VP7 forms soluble, calcium-dependent trimers: Virology, v. 277, p. 420-8.

Dormitzer, P. R., E. B. Nason, B. V. Prasad, and S. C. Harrison, 2004, Structural rearrangements in the membrane penetration protein of a non-enveloped virus: Nature, v. 430, p. 1053-8.

Dorsch, S., G. Liebisch, B. Kaufmann, P. von Landenberg, J. H. Hoffmann, W. Drobnik, and S. Modrow, 2002, The VP1 unique region of parvovirus B19 and its constituent phospholipase A2-like activity: J Virol, v. 76, p. 2014-8.

Draeger, A., K. Monastyrskaya, and E. B. Babiychuk, 2011, Plasma membrane repair and cellular damage control: the annexin survival kit: Biochem Pharmacol, v. 81, p. 703-12.

Draeger, A., R. Schoenauer, A. P. Atanassoff, H. Wolfmeier, and E. B. Babiychuk, 2014, Dealing with damage: Plasma membrane repair mechanisms: Biochimie, v. 107 Pt A, p. 66-72.

Drayna, D., and B. N. Fields, 1982, Genetic studies on the mechanism of chemical and physical inactivation of reovirus: J Gen Virol, v. 63 (Pt 1), p. 149-59.

Díaz-Salinas, M. A., D. Silva-Ayala, S. López, and C. F. Arias, 2014, Rotaviruses reach late endosomes and require the cation-dependent mannose-6-phosphate receptor and the activity of cathepsin proteases to enter the cell: J Virol, v. 88, p. 4389-402.

Ebbinghaus, C., A. Al-Jaibaji, E. Operschall, A. Schöffel, I. Peter, U. F. Greber, and S. Hemmi, 2001, Functional and selective targeting of adenovirus to high-affinity Fcgamma receptor I-positive cells by using a bispecific hybrid adapter: J Virol, v. 75, p. 480-9.

Ebert, D. H., J. Deussing, C. Peters, and T. S. Dermody, 2002, Cathepsin L and cathepsin B mediate reovirus disassembly in murine fibroblast cells: J Biol Chem, v. 277, p. 24609-17.

Eddleman, C. S., M. L. Ballinger, M. E. Smyers, H. M. Fishman, and G. D. Bittner, 1998, Endocytotic formation of vesicles and other membranous structures induced by Ca2+ and axolemmal injury: J Neurosci, v. 18, p. 4029-41.

el Bawab, S., C. Mao, L. M. Obeid, and Y. A. Hannun, 2002, Ceramidases in the regulation of ceramide levels and function: Subcell Biochem, v. 36, p. 187-205.

Estes, M. K., D. Y. Graham, and B. B. Mason, 1981, Proteolytic enhancement of rotavirus infectivity: molecular mechanisms: J Virol, v. 39, p. 879-88.

Evans, M. J., M. Eddy, and J. Plummer, 1985, A comparative assessment of lactate dehydrogenase isozymes, LDHk and LDH5: J Biol Chem, v. 260, p. 306-14.

Farr, G. A., S. F. Cotmore, and P. Tattersall, 2006, VP2 cleavage and the leucine ring at the base of the fivefold cylinder control pH-dependent externalization of both the VP1 N terminus and the genome of minute virus of mice: J Virol, v. 80, p. 161-71.

Farr, G. A., L. G. Zhang, and P. Tattersall, 2005, Parvoviral virions deploy a capsid-tethered lipolytic enzyme to breach the endosomal membrane during cell entry: Proc Natl Acad Sci U S A, v. 102, p. 17148-53.

Ferlinz, K., R. Hurwitz, G. Vielhaber, K. Suzuki, and K. Sandhoff, 1994, Occurrence of two molecular forms of human acid sphingomyelinase: Biochem J, v. 301 (Pt 3), p. 855-62.

Filippone, C., N. Zhi, S. Wong, J. Lu, S. Kajigaya, G. Gallinella, L. Kakkola, M. Söderlund-Venermo, N. S. Young, and K. E. Brown, 2008, VP1u phospholipase activity is critical for infectivity of full-length parvovirus B19 genomic clones: Virology, v. 374, p. 444-52.

Fleischli, C., D. Sirena, G. Lesage, M. J. Havenga, R. Cattaneo, U. F. Greber, and S. Hemmi, 2007, Species B adenovirus serotypes 3, 7, 11 and 35 share similar binding sites on the membrane cofactor protein CD46 receptor: J Gen Virol, v. 88, p. 2925-34.

Forrest, J. C., J. A. Campbell, P. Schelling, T. Stehle, and T. S. Dermody, 2003, Structure-function analysis of reovirus binding to junctional adhesion molecule 1. Implications for the mechanism of reovirus attachment: J Biol Chem, v. 278, p. 48434-44.

Frisch, S. M., and J. S. Mymryk, 2002, Adenovirus-5 E1A: paradox and paradigm.: Nat Rev Mol Cell Biol, v. 3, p. 441-52.

Fujioka, Y., M. Tsuda, A. Nanbo, T. Hattori, J. Sasaki, T. Sasaki, T. Miyazaki, and Y. Ohba, 2013, A Ca(2+)-dependent signalling circuit regulates influenza A virus internalization and infection: Nat Commun, v. 4, p. 2763.

Garrido, M., J. L. Abad, A. Alonso, F. M. Goñi, A. Delgado, and L. R. Montes, 2012, In situ synthesis of fluorescent membrane lipids (ceramides) using click chemistry: J Chem Biol, v. 5, p. 119-23.

Gassert, E., E. Avota, H. Harms, G. Krohne, E. Gulbins, and S. Schneider-Schaulies, 2009, Induction of membrane ceramides: a novel strategy to interfere with T lymphocyte cytoskeletal reorganisation in viral immunosuppression: PLoS Pathog, v. 5, p. e1000623.

Gastaldelli, M., N. Imelli, K. Boucke, B. Amstutz, O. Meier, and U. F. Greber, 2008, Infectious adenovirus type 2 transport through early but not late endosomes: Traffic, v. 9, p. 2265-78.

Gazit, E., A. Boman, H. G. Boman, and Y. Shai, 1995, Interaction of the mammalian antibacterial peptide cecropin P1 with phospholipid vesicles: Biochemistry, v. 34, p. 11479-88.

Gazzerro, E., F. Sotgia, C. Bruno, M. P. Lisanti, and C. Minetti, 2010, Caveolinopathies: from the biology of caveolin-3 to human diseases: Eur J Hum Genet, v. 18, p. 137-45.

Giocondi, M. C., P. E. Milhiet, P. Dosset, and C. Le Grimellec, 2004, Use of cyclodextrin for AFM monitoring of model raft formation: Biophys J, v. 86, p. 861-9.

Girod, A., C. E. Wobus, Z. Zádori, M. Ried, K. Leike, P. Tijssen, J. A. Kleinschmidt, and M. Hallek, 2002, The VP1 capsid protein of adeno-associated virus type 2 is carrying a phospholipase A2 domain required for virus infectivity: J Gen Virol, v. 83, p. 973-8.

Goldkorn, T., and S. Filosto, 2010, Lung injury and cancer: Mechanistic insights into ceramide and EGFR signaling under cigarette smoke: Am J Respir Cell Mol Biol, v. 43, p. 259-68.

Goñi, F. M., and A. Alonso, 2006, Biophysics of sphingolipids I. Membrane properties of sphingosine, ceramides and other simple sphingolipids: Biochim Biophys Acta, v. 1758, p. 1902-21.

Goñi, F. M., and A. Alonso, 2009, Effects of ceramide and other simple sphingolipids on membrane lateral structure: Biochim Biophys Acta, v. 1788, p. 169-77.

Graham, D. Y., and M. K. Estes, 1980, Proteolytic enhancement of rotavirus infectivity: biology mechanism: Virology, v. 101, p. 432-9.

Grassme, H., E. Gulbins, B. Brenner, K. Ferlinz, K. Sandhoff, K. Harzer, F. Lang, and T. F. Meyer, 1997, Acidic sphingomyelinase mediates entry of N. gonorrhoeae into nonphagocytic cells: Cell, v. 91, p. 605-15.

Grassme, H., V. Jendrossek, A. Riehle, G. von Kurthy, J. Berger, H. Schwarz, M. Weller, R. Kolesnick, and E. Gulbins, 2003, Host defense against Pseudomonas aeruginosa requires ceramide-rich membrane rafts: Nat Med, v. 9, p. 322-30.

Grassme, H., A. Riehle, B. Wilker, and E. Gulbins, 2005, Rhinoviruses infect human epithelial cells via ceramide-enriched membrane platforms: J Biol Chem, v. 280, p. 26256-62.

Grassmé, H., E. Gulbins, B. Brenner, K. Ferlinz, K. Sandhoff, K. Harzer, F. Lang, and T. F. Meyer, 1997, Acidic sphingomyelinase mediates entry of N. gonorrhoeae into nonphagocytic cells: Cell, v. 91, p. 605-15.

Grassmé, H., V. Jendrossek, A. Riehle, G. von Kürthy, J. Berger, H. Schwarz, M. Weller, R. Kolesnick, and E. Gulbins, 2003, Host defense against Pseudomonas aeruginosa requires ceramide-rich membrane rafts: Nat Med, v. 9, p. 322-30.

Grassmé, H., A. Riehle, B. Wilker, and E. Gulbins, 2005, Rhinoviruses infect human epithelial cells via ceramide-enriched membrane platforms: J Biol Chem, v. 280, p. 26256-62.

Graziano, V., W. J. McGrath, M. Suomalainen, U. F. Greber, P. Freimuth, P. C. Blainey, G. Luo, X. S. Xie, and W. F. Mangel, 2013, Regulation of a viral proteinase by a peptide and DNA in one-dimensional space: I. binding to DNA AND to hexon of the precursor to protein VI, pVI, of human adenovirus: J Biol Chem, v. 288, p. 2059-67.

Greber, U. F., M. Suomalainen, R. P. Stidwill, K. Boucke, M. W. Ebersold, and A. Helenius, 1997, The role of the nuclear pore complex in adenovirus DNA entry: EMBO J, v. 16, p. 5998-6007.

Greber, U. F., P. Webster, J. Weber, and A. Helenius, 1996, The role of the adenovirus protease on virus entry into cells: EMBO J, v. 15, p. 1766-77.

Greber, U. F., M. Willetts, P. Webster, and A. Helenius, 1993, Stepwise dismantling of adenovirus 2 during entry into cells: Cell, v. 75, p. 477-86.

Gregory, S. M., A. Pokorny, and P. F. Almeida, 2009, Magainin 2 revisited: a test of the quantitative model for the all-or-none permeabilization of phospholipid vesicles: Biophys J, v. 96, p. 116-31.

Griffiths, G. M., 1996, Secretory lysosomes - a special mechanism of regulated secretion in haemopoietic cells: Trends Cell Biol, v. 6, p. 329-32.

Groulx, N., F. Boudreault, S. N. Orlov, and R. Grygorczyk, 2006, Membrane reserves and hypotonic cell swelling: J Membr Biol, v. 214, p. 43-56.

Guan, X. L., G. Cestra, G. Shui, A. Kuhrs, R. B. Schittenhelm, E. Hafen, F. G. van der Goot, C. C. Robinett, M. Gatti, M. Gonzalez-Gaitan, and M. R. Wenk, 2013, Biochemical membrane lipidomics during Drosophila development: Dev Cell, v. 24, p. 98-111.

Guillas, I., J. C. Jiang, C. Vionnet, C. Roubaty, D. Uldry, R. Chuard, J. Wang, S. M. Jazwinski, and A. Conzelmann, 2003, Human homologues of LAG1 reconstitute Acyl-CoA-dependent ceramide synthesis in yeast: J Biol Chem, v. 278, p. 37083-91.

Górska, M., A. Dobrzyń, M. Zendzian-Piotrowska, and Z. Namiot, 2002, Concentration and composition of free ceramides in human plasma: Horm Metab Res, v. 34, p. 466-8.

Hallock, K. J., D. K. Lee, and A. Ramamoorthy, 2003, MSI-78, an analogue of the magainin antimicrobial peptides, disrupts lipid bilayer structure via positive curvature strain: Biophys J, v. 84, p. 3052-60.

Hanada, K., K. Kumagai, S. Yasuda, Y. Miura, M. Kawano, M. Fukasawa, and M. Nishijima, 2003, Molecular machinery for non-vesicular trafficking of ceramide: Nature, v. 426, p. 803-9.

Hannan, C., L. H. Raptis, C. V. Déry, and J. Weber, 1983, Biological and structural studies with an adenovirus type 2 temperature-sensitive mutant defective for uncoating: Intervirology, v. 19, p. 213-23.

Hannun, Y. A., 1996, Functions of ceramide in coordinating cellular responses to stress: Science, v. 274, p. 1855-9.

Hannun, Y. A., and L. M. Obeid, 2008, Principles of bioactive lipid signalling: lessons from sphingolipids: Nat Rev Mol Cell Biol, v. 9, p. 139-50.

Hannun, Y. A., and L. M. Obeid, 2011, Many ceramides: J Biol Chem, v. 286, p. 27855-62.

Harder, T., R. Kellner, R. G. Parton, and J. Gruenberg, 1997, Specific release of membrane-bound annexin II and cortical cytoskeletal elements by sequestration of membrane cholesterol: Mol Biol Cell, v. 8, p. 533-45.

Harrison, S. C., 2010, Virology. Looking inside adenovirus: Science, v. 329, p. 1026-7.

Haselhorst, T., F. E. Fleming, J. C. Dyason, R. D. Hartnell, X. Yu, G. Holloway, K. Santegoets, M. J. Kiefel, H. Blanchard, B. S. Coulson, and M. von Itzstein, 2009, Sialic acid dependence in rotavirus host cell invasion: Nat Chem Biol, v. 5, p. 91-3.

Hassell, J. A., and J. Weber, 1978, Genetic analysis of adenovirus type 2. VIII. Physical locations of temperature-sensitive mutations: J Virol, v. 28, p. 671-8.

Hauck, C. R., H. Grassmé, J. Bock, V. Jendrossek, K. Ferlinz, T. F. Meyer, and E. Gulbins, 2000, Acid sphingomyelinase is involved in CEACAM receptor-mediated phagocytosis of Neisseria gonorrhoeae: FEBS Lett, v. 478, p. 260-6.

He, K., S. J. Ludtke, D. L. Worcester, and H. W. Huang, 1996, Neutron scattering in the plane of membranes: structure of alamethicin pores: Biophys J, v. 70, p. 2659-66.

He, Q., V. J. Johnson, M. F. Osuchowski, and R. P. Sharma, 2004, Inhibition of serine palmitoyltransferase by myriocin, a natural mycotoxin, causes induction of c-myc in mouse liver: Mycopathologia, v. 157, p. 339-47.

Hebda, J. A., I. Saraogi, M. Magzoub, A. D. Hamilton, and A. D. Miranker, 2009, A peptidomimetic approach to targeting pre-amyloidogenic states in type II diabetes: Chem Biol, v. 16, p. 943-50.

Heinrich, M., J. Neumeyer, M. Jakob, C. Hallas, V. Tchikov, S. Winoto-Morbach, M. Wickel, W. Schneider-Brachert, A. Trauzold, A. Hethke, and S. Schütze, 2004, Cathepsin D links TNF-induced acid sphingomyelinase to Bid-mediated caspase-9 and -3 activation: Cell Death Differ, v. 11, p. 550-63.

Heller, W. T., K. He, S. J. Ludtke, T. A. Harroun, and H. W. Huang, 1997, Effect of changing the size of lipid headgroup on peptide insertion into membranes: Biophys J, v. 73, p. 239-44.

Hendrickx, R., N. Stichling, J. Koelen, L. Kuryk, A. Lipiec, and U. F. Greber, 2014, Innate immunity to adenovirus: Hum Gene Ther, v. 25, p. 265-84.

Henry, B., R. Ziobro, K. A. Becker, R. Kolesnick, and E. Gulbins, 2013, Acid sphingomyelinase: Handb Exp Pharmacol, p. 77-88.

Henzler-Wildman, K. A., G. V. Martinez, M. F. Brown, and A. Ramamoorthy, 2004, Perturbation of the hydrophobic core of lipid bilayers by the human antimicrobial peptide LL-37: Biochemistry, v. 43, p. 8459-69.

Hindley, C. E., F. J. Lawrence, and D. A. Matthews, 2007, A role for transportin in the nuclear import of adenovirus core proteins and DNA.: Traffic, v. 8, p. 1313-22.

Holopainen, J. M., M. I. Angelova, and P. K. Kinnunen, 2000, Vectorial budding of vesicles by asymmetrical enzymatic formation of ceramide in giant liposomes: Biophys J, v. 78, p. 830-8.

Hooper, J. W., and B. N. Fields, 1996, Role of the mu 1 protein in reovirus stability and capacity to cause chromium release from host cells: J Virol, v. 70, p. 459-67.

Howitt, J., C. W. Anderson, and P. Freimuth, 2003, Adenovirus interaction with its cellular receptor CAR.: Curr Top Microbiol Immunol, v. 272, p. 331-64.

Hristova, K., M. E. Selsted, and S. H. White, 1997, Critical role of lipid composition in membrane permeabilization by rabbit neutrophil defensins: J Biol Chem, v. 272, p. 24224-33.

Hu, L., S. E. Crawford, J. M. Hyser, M. K. Estes, and B. V. Prasad, 2012, Rotavirus non-structural proteins: structure and function: Curr Opin Virol, v. 2, p. 380-8.

Huang, H. W., 2000, Action of antimicrobial peptides: two-state model: Biochemistry, v. 39, p. 8347-52.

Huang, H. W., 2006, Molecular mechanism of antimicrobial peptides: the origin of cooperativity: Biochim Biophys Acta, v. 1758, p. 1292-302.

Huang, H. W., F. Y. Chen, and M. T. Lee, 2004, Molecular mechanism of Peptide-induced pores in membranes: Phys Rev Lett, v. 92, p. 198304.

Hultmark, D., H. Steiner, T. Rasmuson, and H. G. Boman, 1980, Insect immunity. Purification and properties of three inducible bactericidal proteins from hemolymph of immunized pupae of Hyalophora cecropia: Eur J Biochem, v. 106, p. 7-16.

Idone, V., C. Tam, J. W. Goss, D. Toomre, M. Pypaert, and N. W. Andrews, 2008, Repair of injured plasma membrane by rapid Ca2+-dependent endocytosis: J Cell Biol, v. 180, p. 905-14.

Imelli, N., O. Meier, K. Boucke, S. Hemmi, and U. F. Greber, 2004, Cholesterol is required for endocytosis and endosomal escape of adenovirus type 2: J Virol, v. 78, p. 3089-98.

Imelli, N., Z. Ruzsics, D. Puntener, M. Gastaldelli, and U. F. Greber, 2009, Genetic reconstitution of the human adenovirus type 2 temperature-sensitive 1 mutant defective in endosomal escape: Virol J, v. 6, p. 174.

Ira, and L. J. Johnston, 2008, Sphingomyelinase generation of ceramide promotes clustering of nanoscale domains in supported bilayer membranes: Biochim Biophys Acta, v. 1778, p. 185-97.

Israelachvili, J. N., S. Marcelja, and R. G. Horn, 1980, Physical principles of membrane organization: Q Rev Biophys, v. 13, p. 121-200.

Ito, M., N. Okino, and M. Tani, 2014, New insight into the structure, reaction mechanism, and biological functions of neutral ceramidase: Biochim Biophys Acta, v. 1841, p. 682-91.

Ivanovic, T., M. A. Agosto, K. Chandran, and M. L. Nibert, 2007, A role for molecular chaperone Hsc70 in reovirus outer capsid disassembly: J Biol Chem, v. 282, p. 12210-9.

Ivanovic, T., M. A. Agosto, L. Zhang, K. Chandran, S. C. Harrison, and M. L. Nibert, 2008, Peptides released from reovirus outer capsid form membrane pores that recruit virus particles: EMBO J, v. 27, p. 1289-98.

Jaiswal, J. K., N. W. Andrews, and S. M. Simon, 2002, Membrane proximal lysosomes are the major vesicles responsible for calcium-dependent exocytosis in nonsecretory cells: J Cell Biol, v. 159, p. 625-35.

Janshoff, A., D. T. Bong, C. Steinem, J. E. Johnson, and M. R. Ghadiri, 1999, An animal virus-derived peptide switches membrane morphology: possible relevance to nodaviral transfection processes: Biochemistry, v. 38, p. 5328-36.

Jenkins, R. W., D. Canals, and Y. A. Hannun, 2009, Roles and regulation of secretory and lysosomal acid sphingomyelinase: Cell Signal, v. 21, p. 836-46.

Jimenez, A. J., P. Maiuri, J. Lafaurie-Janvore, S. Divoux, M. Piel, and F. Perez, 2014, ESCRT machinery is required for plasma membrane repair: Science, v. 343, p. 1247136.

Juvvadi, P., S. Vunnam, E. L. Merrifield, H. G. Boman, and R. B. Merrifield, 1996, Hydrophobic effects on antibacterial and channel-forming properties of cecropin A-melittin hybrids: J Pept Sci, v. 2, p. 223-32.

Kagan, B. L., M. E. Selsted, T. Ganz, and R. I. Lehrer, 1990, Antimicrobial defensin peptides form voltage-dependent ion-permeable channels in planar lipid bilayer membranes: Proc Natl Acad Sci U S A, v. 87, p. 210-4.

Karttunen, A. J., M. Linnolahti, and T. A. Pakkanen, 2008, Structural principles of polyhedral allotropes of phosphorus: Chemphyschem, v. 9, p. 2550-8.

Keefe, D., L. Shi, S. Feske, R. Massol, F. Navarro, T. Kirchhausen, and J. Lieberman, 2005, Perforin triggers a plasma membrane-repair response that facilitates CTL induction of apoptosis: Immunity, v. 23, p. 249-62.

Kelkar, S. A., K. K. Pfister, R. G. Crystal, and P. L. Leopold, 2004, Cytoplasmic dynein mediates adenovirus binding to microtubules.: J Virol, v. 78, p. 10122-32.

Keyel, P. A., L. Loultcheva, R. Roth, R. D. Salter, S. C. Watkins, W. M. Yokoyama, and J. E. Heuser, 2011, Streptolysin O clearance through sequestration into blebs that bud passively from the plasma membrane: J Cell Sci, v. 124, p. 2414-23.

Kirby, I., E. Davison, A. J. Beavil, C. P. Soh, T. J. Wickham, P. W. Roelvink, I. Kovesdi, B. J. Sutton, and G. Santis, 2000, Identification of contact residues and definition of the CAR-binding site of adenovirus type 5 fiber protein.: J Virol, v. 74, p. 2804-13.

Kitatani, K., and C. Luberto, 2010, Introduction to tools and techniques for ceramide-centered research: Adv Exp Med Biol, v. 688, p. 276-85.

Koivusalo, M., M. Jansen, P. Somerharju, and E. Ikonen, 2007, Endocytic trafficking of sphingomyelin depends on its acyl chain length: Mol Biol Cell, v. 18, p. 5113-23.

Konopka-Anstadt, J. L., B. A. Mainou, D. M. Sutherland, Y. Sekine, S. M. Strittmatter, and T. S. Dermody, 2014, The Nogo receptor NgR1 mediates infection by mammalian reovirus: Cell Host Microbe, v. 15, p. 681-91.

Kornhuber, J., P. Tripal, M. Reichel, L. Terfloth, S. Bleich, J. Wiltfang, and E. Gulbins, 2008, Identification of new functional inhibitors of acid sphingomyelinase using a structure-property-activity relation model: J Med Chem, v. 51, p. 219-37.

Ladokhin, A. S., and S. H. White, 2001, 'Detergent-like' permeabilization of anionic lipid vesicles by melittin: Biochim Biophys Acta, v. 1514, p. 253-60.

Lansmann, S., K. Ferlinz, R. Hurwitz, O. Bartelsen, G. Glombitza, and K. Sandhoff, 1996, Purification of acid sphingomyelinase from human placenta: characterization and N-terminal sequence: FEBS Lett, v. 399, p. 227-31.

Lariccia, V., M. Fine, S. Magi, M. J. Lin, A. Yaradanakul, M. C. Llaguno, and D. W. Hilgemann, 2011, Massive calcium-activated endocytosis without involvement of classical endocytic proteins: J Gen Physiol, v. 137, p. 111-32.

Last, N. B., D. E. Schlamadinger, and A. D. Miranker, 2013, A common landscape for membrane-active peptides: Protein Sci, v. 22, p. 870-82.

Lee, M. T., F. Y. Chen, and H. W. Huang, 2004, Energetics of pore formation induced by membrane active peptides: Biochemistry, v. 43, p. 3590-9.

Lee, M. T., W. C. Hung, F. Y. Chen, and H. W. Huang, 2008, Mechanism and kinetics of pore formation in membranes by water-soluble amphipathic peptides: Proc Natl Acad Sci U S A, v. 105, p. 5087-92.

Lehmberg, E., J. A. Traina, J. A. Chakel, R. J. Chang, M. Parkman, M. T. McCaman, P. K. Murakami, V. Lahidji, J. W. Nelson, W. S. Hancock, E. Nestaas, and E. Pungor, 1999, Reversed-phase high-performance liquid chromatographic assay for the adenovirus type 5 proteome: J Chromatogr B Biomed Sci Appl, v. 732, p. 411-23.

Levran, O., R. J. Desnick, and E. H. Schuchman, 1992, Identification and expression of a common missense mutation (L302P) in the acid sphingomyelinase gene of Ashkenazi Jewish type A Niemann-Pick disease patients: Blood, v. 80, p. 2081-7.

Li, Z., M. L. Baker, W. Jiang, M. K. Estes, and B. V. Prasad, 2009, Rotavirus architecture at subnanometer resolution: J Virol, v. 83, p. 1754-66.

Lichtenstein, D. L., K. Toth, K. Doronin, A. E. Tollefson, and W. S. Wold, 2004, Functions and mechanisms of action of the adenovirus E3 proteins.: Int Rev Immunol, v. 23, p. 75-111.

Lindert, S., M. Silvestry, T. M. Mullen, G. R. Nemerow, and P. L. Stewart, 2009, Cryo-electron microscopy structure of an adenovirus-integrin complex indicates conformational changes in both penton base and integrin: J Virol, v. 83, p. 11491-501.

Liu, H., L. Jin, S. B. Koh, I. Atanasov, S. Schein, L. Wu, and Z. H. Zhou, 2010, Atomic structure of human adenovirus by cryo-EM reveals interactions among protein networks: Science, v. 329, p. 1038-43.

Lopez, S., and C. F. Arias, 2006, Early steps in rotavirus cell entry: Curr Top Microbiol Immunol, v. 309, p. 39-66.

Los, F. C., C. Y. Kao, J. Smitham, K. L. McDonald, C. Ha, C. A. Peixoto, and R. V. Aroian, 2011, RAB-5- and RAB-11-dependent vesicle-trafficking pathways are required for plasma membrane repair after attack by bacterial pore-forming toxin: Cell Host Microbe, v. 9, p. 147-57.

Los, F. C., T. M. Randis, R. V. Aroian, and A. J. Ratner, 2013, Role of pore-forming toxins in bacterial infectious diseases: Microbiol Mol Biol Rev, v. 77, p. 173-207.

Luberto, C., D. F. Hassler, P. Signorelli, Y. Okamoto, H. Sawai, E. Boros, D. J. Hazen-Martin, L. M. Obeid, Y. A. Hannun, and G. K. Smith, 2002, Inhibition of tumor necrosis factor-induced cell death in MCF7 by a novel inhibitor of neutral sphingomyelinase: J Biol Chem, v. 277, p. 41128-39.

Ludtke, S. J., K. He, W. T. Heller, T. A. Harroun, L. Yang, and H. W. Huang, 1996, Membrane pores induced by magainin: Biochemistry, v. 35, p. 13723-8.

López-Montero, I., M. Vélez, and P. F. Devaux, 2007, Surface tension induced by sphingomyelin to ceramide conversion in lipid membranes: Biochim Biophys Acta, v. 1768, p. 553-61.

Lütschg, V., K. Boucke, S. Hemmi, and U. F. Greber, 2011, Chemotactic antiviral cytokines promote infectious apical entry of human adenovirus into polarized epithelial cells.: Nat Commun, v. 2, p. 391.

Maeda, Y., H. Matsuyuki, K. Shimano, H. Kataoka, K. Sugahara, and K. Chiba, 2007, Migration of CD4 T cells and dendritic cells toward sphingosine 1-phosphate (S1P) is mediated by different receptor subtypes: S1P regulates the functions of murine mature dendritic cells via S1P receptor type 3: J Immunol, v. 178, p. 3437-46.

Maginnis, M. S., J. C. Forrest, S. A. Kopecky-Bromberg, S. K. Dickeson, S. A. Santoro, M. M. Zutter, G. R. Nemerow, J. M. Bergelson, and T. S. Dermody, 2006, Beta1 integrin mediates internalization of mammalian reovirus: J Virol, v. 80, p. 2760-70.

Maia, L. F., M. R. Soares, A. P. Valente, F. C. Almeida, A. C. Oliveira, A. M. Gomes, M. S. Freitas, A. Schneemann, J. E. Johnson, and J. L. Silva, 2006, Structure of a membrane-binding domain from a non-enveloped animal virus: insights into the mechanism of membrane permeability and cellular entry: J Biol Chem, v. 281, p. 29278-86.

Maier, O., D. L. Galan, H. Wodrich, and C. M. Wiethoff, 2010, An N-terminal domain of adenovirus protein VI fragments membranes by inducing positive membrane curvature: Virology, v. 402, p. 11-9.

Maier, O., S. A. Marvin, H. Wodrich, E. M. Campbell, and C. M. Wiethoff, 2012, Spatiotemporal dynamics of adenovirus membrane rupture and endosomal escape: J Virol, v. 86, p. 10821-8.

Mainou, B. A., and T. S. Dermody, 2012, Transport to late endosomes is required for efficient reovirus infection: J Virol, v. 86, p. 8346-58.

Mainou, B. A., P. F. Zamora, A. W. Ashbrook, D. C. Dorset, K. S. Kim, and T. S. Dermody, 2013, Reovirus cell entry requires functional microtubules: MBio, v. 4.

Mangel, W. F., W. J. McGrath, D. L. Toledo, and C. W. Anderson, 1993, Viral DNA and a viral peptide can act as cofactors of adenovirus virion proteinase activity: Nature, v. 361, p. 274-5.

Mani, B., C. Baltzer, N. Valle, J. M. Almendral, C. Kempf, and C. Ros, 2006, Low pH-dependent endosomal processing of the incoming parvovirus minute virus of mice virion leads to externalization of the

VP1 N-terminal sequence (N-VP1), N-VP2 cleavage, and uncoating of the full-length genome: J Virol, v. 80, p. 1015-24.

Manthey, C. L., and E. H. Schuchman, 1998, Acid sphingomyelinase-derived ceramide is not required for inflammatory cytokine signalling in murine macrophages: Cytokine, v. 10, p. 654-61.

Mao, C., R. Xu, Z. M. Szulc, A. Bielawska, S. H. Galadari, and L. M. Obeid, 2001, Cloning and characterization of a novel human alkaline ceramidase. A mammalian enzyme that hydrolyzes phytoceramide: J Biol Chem, v. 276, p. 26577-88.

Marassi, F. M., S. J. Opella, P. Juvvadi, and R. B. Merrifield, 1999, Orientation of cecropin A helices in phospholipid bilayers determined by solid-state NMR spectroscopy: Biophys J, v. 77, p. 3152-5.

Marion, D., M. Zasloff, and A. Bax, 1988, A two-dimensional NMR study of the antimicrobial peptide magainin 2: FEBS Lett, v. 227, p. 21-6.

Martin-Fernandez, M., S. V. Longshaw, I. Kirby, G. Santis, M. J. Tobin, D. T. Clarke, and G. R. Jones, 2004, Adenovirus type-5 entry and disassembly followed in living cells by FRET, fluorescence anisotropy, and FLIM: Biophys J, v. 87, p. 1316-27.

Martinez, R., A. M. Burrage, C. M. Wiethoff, and H. Wodrich, 2013, High temporal resolution imaging reveals endosomal membrane penetration and escape of adenoviruses in real time: Methods Mol Biol, v. 1064, p. 211-26.

Mason, A. J., A. Marquette, and B. Bechinger, 2007, Zwitterionic phospholipids and sterols modulate antimicrobial peptide-induced membrane destabilization: Biophys J, v. 93, p. 4289-99.

Matsuzaki, K., and C. Horikiri, 1999, Interactions of amyloid beta-peptide (1-40) with ganglioside-containing membranes: Biochemistry, v. 38, p. 4137-42.

Matsuzaki, K., Y. Mitani, K. Y. Akada, O. Murase, S. Yoneyama, M. Zasloff, and K. Miyajima, 1998a, Mechanism of synergism between antimicrobial peptides magainin 2 and PGLa: Biochemistry, v. 37, p. 15144-53.

Matsuzaki, K., O. Murase, N. Fujii, and K. Miyajima, 1996, An antimicrobial peptide, magainin 2, induced rapid flip-flop of phospholipids coupled with pore formation and peptide translocation: Biochemistry, v. 35, p. 11361-8.

Matsuzaki, K., K. Sugishita, N. Ishibe, M. Ueha, S. Nakata, K. Miyajima, and R. M. Epand, 1998b, Relationship of membrane curvature to the formation of pores by magainin 2: Biochemistry, v. 37, p. 11856-63.

Matthews, D. A., and W. C. Russell, 1998, Adenovirus core protein V is delivered by the invading virus to the nucleus of the infected cell and later in infection is associated with nucleoli: J Gen Virol, v. 79 (Pt 7), p. 1671-5.

Mazzon, M., and J. Mercer, 2014, Lipid interactions during virus entry and infection: Cell Microbiol, v. 16, p. 1493-502.

McGovern, M. M., N. Lippa, E. Bagiella, E. H. Schuchman, R. J. Desnick, and M. P. Wasserstein, 2013, Morbidity and mortality in type B Niemann-Pick disease: Genet Med, v. 15, p. 618-23.

McGovern, M. M., T. Pohl-Worgall, R. J. Deckelbaum, W. Simpson, D. Mendelson, R. J. Desnick, E. H. Schuchman, and M. P. Wasserstein, 2004, Lipid abnormalities in children with types A and B Niemann Pick disease: J Pediatr, v. 145, p. 77-81.

McGrath, W. J., J. Ding, A. Didwania, R. M. Sweet, and W. F. Mangel, 2003, Crystallographic structure at 1.6-A resolution of the human adenovirus proteinase in a covalent complex with its 11-amino-acid peptide cofactor: insights on a new fold: Biochim Biophys Acta, v. 1648, p. 1-11.

McIntosh, T. J., S. A. Simon, D. Needham, and C. H. Huang, 1992, Structure and cohesive properties of sphingomyelin/cholesterol bilayers: Biochemistry, v. 31, p. 2012-20.

McMahon, H. T., and J. L. Gallop, 2005, Membrane curvature and mechanisms of dynamic cell membrane remodelling: Nature, v. 438, p. 590-6.

McNeil, A. K., U. Rescher, V. Gerke, and P. L. McNeil, 2006, Requirement for annexin A1 in plasma membrane repair: J Biol Chem, v. 281, p. 35202-7.

McNeil, P. L., and T. Kirchhausen, 2005, An emergency response team for membrane repair: Nat Rev Mol Cell Biol, v. 6, p. 499-505.

McNeil, P. L., S. S. Vogel, K. Miyake, and M. Terasaki, 2000, Patching plasma membrane disruptions with cytoplasmic membrane: J Cell Sci, v. 113 (Pt 11), p. 1891-902.

Mecke, A., D. K. Lee, A. Ramamoorthy, B. G. Orr, and M. M. Banaszak Holl, 2005, Membrane thinning due to antimicrobial peptide binding: an atomic force microscopy study of MSI-78 in lipid bilayers: Biophys J, v. 89, p. 4043-50.

Medina, D. L., A. Fraldi, V. Bouche, F. Annunziata, G. Mansueto, C. Spampanato, C. Puri, A. Pignata, J. A. Martina, M. Sardiello, M. Palmieri, R. Polishchuk, R. Puertollano, and A. Ballabio, 2011, Transcriptional activation of lysosomal exocytosis promotes cellular clearance: Dev Cell, v. 21, p. 421-30.

Meier, O., K. Boucke, S. V. Hammer, S. Keller, R. P. Stidwill, S. Hemmi, and U. F. Greber, 2002a, Adenovirus triggers macropinocytosis and endosomal leakage together with its clathrin-mediated uptake: J Cell Biol, v. 158, p. 1119-31.

Merrill, A. H., M. C. Sullards, J. C. Allegood, S. Kelly, and E. Wang, 2005, Sphingolipidomics: high-throughput, structure-specific, and quantitative analysis of sphingolipids by liquid chromatography tandem mass spectrometry: Methods, v. 36, p. 207-24.

Middleton, E. R., and E. Rhoades, 2010, Effects of curvature and composition on α-synuclein binding to lipid vesicles: Biophys J, v. 99, p. 2279-88.

Miller, M. E., S. Adhikary, A. A. Kolokoltsov, and R. A. Davey, 2012, Ebolavirus requires acid sphingomyelinase activity and plasma membrane sphingomyelin for infection: J Virol, v. 86, p. 7473-83.

Mishra, A., G. H. Lai, N. W. Schmidt, V. Z. Sun, A. R. Rodriguez, R. Tong, L. Tang, J. Cheng, T. J. Deming, D. T. Kamei, and G. C. Wong, 2011, Translocation of HIV TAT peptide and analogues induced by multiplexed membrane and cytoskeletal interactions: Proc Natl Acad Sci U S A, v. 108, p. 16883-8.

Monastyrskaya, K., E. B. Babiychuk, A. Hostettler, U. Rescher, and A. Draeger, 2007, Annexins as intracellular calcium sensors: Cell Calcium, v. 41, p. 207-19.

Morel, E., and J. Gruenberg, 2009, Annexin A2 binding to endosomes and functions in endosomal transport are regulated by tyrosine 23 phosphorylation: J Biol Chem, v. 284, p. 1604-11.

Morgan, B. P., 1989, Complement membrane attack on nucleated cells: resistance, recovery and non-lethal effects: Biochem J, v. 264, p. 1-14.

Moyer, C. L., and G. R. Nemerow, 2011, Viral weapons of membrane destruction: variable modes of membrane penetration by non-enveloped viruses: Curr Opin Virol, v. 1, p. 44-9.

Moyer, C. L., and G. R. Nemerow, 2012, Disulfide-bond formation by a single cysteine mutation in adenovirus protein VI impairs capsid release and membrane lysis: Virology, v. 428, p. 41-7.

Moyer, C. L., C. M. Wiethoff, O. Maier, J. G. Smith, and G. R. Nemerow, 2011, Functional genetic and biophysical analyses of membrane disruption by human adenovirus: J Virol, v. 85, p. 2631-41.

Mueller, P., and D. O. Rudin, 1968, Action potentials induced in biomolecular lipid membranes: Nature, v. 217, p. 713-9.

Mullen, T. D., Y. A. Hannun, and L. M. Obeid, 2012, Ceramide synthases at the centre of sphingolipid metabolism and biology: Biochem J, v. 441, p. 789-802.

Murk, J. L., B. M. Humbel, U. Ziese, J. M. Griffith, G. Posthuma, J. W. Slot, A. J. Koster, A. J. Verkleij, H. J. Geuze, and M. J. Kleijmeer, 2003, Endosomal compartmentalization in three dimensions: implications for membrane fusion: Proc Natl Acad Sci U S A, v. 100, p. 13332-7.

Münzer, P., E. Schmid, B. Walker, A. Fotinos, M. Chatterjee, D. Rath, S. Vogel, S. M. Hoffmann, K. Metzger, P. Seizer, T. Geisler, M. Gawaz, O. Borst, and F. Lang, 2014, Sphingosine kinase 1 (Sphk1) negatively regulates platelet activation and thrombus formation: Am J Physiol Cell Physiol, v. 307, p. C920-7.

Nagel, H., S. Maag, A. Tassis, F. O. Nestlé, U. F. Greber, and S. Hemmi, 2003, The alphavbeta5 integrin of hematopoietic and nonhematopoietic cells is a transduction receptor of RGD-4C fiber-modified adenoviruses: Gene Ther, v. 10, p. 1643-53.

Nakano, M. Y., K. Boucke, M. Suomalainen, R. P. Stidwill, and U. F. Greber, 2000, The first step of adenovirus type 2 disassembly occurs at the cell surface, independently of endocytosis and escape to the cytosol: J Virol, v. 74, p. 7085-95.

Nemerow, G. R., and P. L. Stewart, 1999, Role of alpha(v) integrins in adenovirus cell entry and gene delivery: Microbiol Mol Biol Rev, v. 63, p. 725-34.

Nibert, M. L., 1998, Structure of mammalian orthoreovirus particles: Curr Top Microbiol Immunol, v. 233, p. 1-30.

Nicol, F., S. Nir, and F. C. Szoka, 1996, Effect of cholesterol and charge on pore formation in bilayer vesicles by a pH-sensitive peptide: Biophys J, v. 71, p. 3288-301.

Nikolova-Karakashian, M. N., and K. A. Rozenova, 2010, Ceramide in stress response: Adv Exp Med Biol, v. 688, p. 86-108.

Obeid, L. M., C. M. Linardic, L. A. Karolak, and Y. A. Hannun, 1993, Programmed cell death induced by ceramide: Science, v. 259, p. 1769-71.

Ogretmen, B., and Y. A. Hannun, 2004a, Biologically active sphingolipids in cancer pathogenesis and treatment: Nat Rev Cancer, v. 4, p. 604-16.

Ogretmen, B., and Y. A. Hannun, 2004b, Biologically active sphingolipids in cancer pathogenesis and treatment.: Nat Rev Cancer, v. 4, p. 604-16.

Ohanian, J., and V. Ohanian, 2001, Sphingolipids in mammalian cell signalling: Cell Mol Life Sci, v. 58, p. 2053-68.

Otterbach, B., and W. Stoffel, 1995, Acid sphingomyelinase-deficient mice mimic the neurovisceral form of human lysosomal storage disease (Niemann-Pick disease): Cell, v. 81, p. 1053-61.

Ouattara, L. A., F. Barin, M. A. Barthez, B. Bonnaud, P. Roingeard, A. Goudeau, P. Castelnau, G. Vernet, G. Paranhos-Baccalà, and F. Komurian-Pradel, 2011, Novel human reovirus isolated from children with acute necrotizing encephalopathy: Emerg Infect Dis, v. 17, p. 1436-44.

Pang, Z. P., and T. C. Südhof, 2010, Cell biology of Ca2+-triggered exocytosis: Curr Opin Cell Biol, v. 22, p. 496-505.

Parashar, U. D., E. G. Hummelman, J. S. Bresee, M. A. Miller, and R. I. Glass, 2003, Global illness and deaths caused by rotavirus disease in children: Emerg Infect Dis, v. 9, p. 565-72.

Parker, J. S., and C. R. Parrish, 2000, Cellular uptake and infection by canine parvovirus involves rapid dynamin-regulated clathrin-mediated endocytosis, followed by slower intracellular trafficking: J Virol, v. 74, p. 1919-30.

Parton, R. G., B. Joggerst, and K. Simons, 1994, Regulated internalization of caveolae: J Cell Biol, v. 127, p. 1199-215.

Parton, R. G., and K. Simons, 2007, The multiple faces of caveolae: Nat Rev Mol Cell Biol, v. 8, p. 185-94.

Pattingre, S., C. Bauvy, T. Levade, B. Levine, and P. Codogno, 2009, Ceramide-induced autophagy: to junk or to protect cells?: Autophagy, v. 5, p. 558-60.

Peng, T., X. Yuan, and H. C. Hang, 2014, Turning the spotlight on protein-lipid interactions in cells: Curr Opin Chem Biol, v. 21, p. 144-53.

Perera, R., C. Riley, G. Isaac, A. S. Hopf-Jannasch, R. J. Moore, K. W. Weitz, L. Pasa-Tolic, T. O. Metz, J. Adamec, and R. J. Kuhn, 2012, Dengue virus infection perturbs lipid homeostasis in infected mosquito cells: PLoS Pathog, v. 8, p. e1002584.

Perry, D. M., B. Newcomb, M. Adada, B. X. Wu, P. Roddy, K. Kitatani, L. Siskind, L. M. Obeid, and Y. A. Hannun, 2014, Defining a role for acid sphingomyelinase in the p38/interleukin-6 pathway: J Biol Chem, v. 289, p. 22401-12.

Pinto, S. N., E. L. Laviad, J. Stiban, S. L. Kelly, A. H. Merrill, M. Prieto, A. H. Futerman, and L. C. Silva, 2014, Changes in membrane biophysical properties induced by sphingomyelinase depend on the sphingolipid N-acyl chain: J Lipid Res, v. 55, p. 53-61.

Pokorny, A., and P. F. Almeida, 2004, Kinetics of dye efflux and lipid flip-flop induced by delta-lysin in phosphatidylcholine vesicles and the mechanism of graded release by amphipathic, alpha-helical peptides: Biochemistry, v. 43, p. 8846-57.

Porcelli, F., B. Buck, D. K. Lee, K. J. Hallock, A. Ramamoorthy, and G. Veglia, 2004, Structure and orientation of pardaxin determined by NMR experiments in model membranes: J Biol Chem, v. 279, p. 45815-23.

Porta, H., A. Cancino-Rodezno, M. Soberón, and A. Bravo, 2011, Role of MAPK p38 in the cellular responses to pore-forming toxins: Peptides, v. 32, p. 601-6.

Potez, S., M. Luginbühl, K. Monastyrskaya, A. Hostettler, A. Draeger, and E. B. Babiychuk, 2011, Tailored protection against plasmalemmal injury by annexins with different Ca2+ sensitivities: J Biol Chem, v. 286, p. 17982-91.

Prasad, B. V., G. J. Wang, J. P. Clerx, and W. Chiu, 1988, Three-dimensional structure of rotavirus: J Mol Biol, v. 199, p. 269-75.

Preiss, J. E., C. R. Loomis, R. M. Bell, and J. E. Niedel, 1987, Quantitative measurement of sn-1,2-diacylglycerols: Methods Enzymol, v. 141, p. 294-300.

Pérez-Berná, A. J., R. Marabini, S. H. Scheres, R. Menéndez-Conejero, I. P. Dmitriev, D. T. Curiel, W. F. Mangel, S. J. Flint, and C. San Martín, 2009, Structure and uncoating of immature adenovirus: J Mol Biol, v. 392, p. 547-57.

Rajab, A., V. Straub, L. J. McCann, D. Seelow, R. Varon, R. Barresi, A. Schulze, B. Lucke, S. Lützkendorf, M. Karbasiyan, S. Bachmann, S. Spuler, and M. Schuelke, 2010, Fatal cardiac arrhythmia and long-QT syndrome in a new form of congenital generalized lipodystrophy with muscle rippling (CGL4) due to PTRF-CAVIN mutations: PLoS Genet, v. 6, p. e1000874.

Rancourt, C., H. Keyvani-Amineh, S. Sircar, P. Labrecque, and J. M. Weber, 1995, Proline 137 is critical for adenovirus protease encapsidation and activation but not enzyme activity: Virology, v. 209, p. 167-73.

Reddy, V. S., S. K. Natchiar, P. L. Stewart, and G. R. Nemerow, 2010, Crystal structure of human adenovirus at 3.5 A resolution: Science, v. 329, p. 1071-5.

Reddy, V. S., and G. R. Nemerow, 2014, Structures and organization of adenovirus cement proteins provide insights into the role of capsid maturation in virus entry and infection: Proc Natl Acad Sci U S A, v. 111, p. 11715-20.

Reiss, K., J. E. Stencel, Y. Liu, B. S. Blaum, D. M. Reiter, T. Feizi, T. S. Dermody, and T. Stehle, 2012, The GM2 glycan serves as a functional coreceptor for serotype 1 reovirus: PLoS Pathog, v. 8, p. e1003078.

Repetto, S., M. Bado, P. Broda, G. Lucania, E. Masetti, F. Sotgia, I. Carbone, A. Pavan, E. Bonilla, G. Cordone, M. P. Lisanti, and C. Minetti, 1999, Increased number of caveolae and caveolin-3 overexpression in Duchenne muscular dystrophy: Biochem Biophys Res Commun, v. 261, p. 547-50.

Rizzo, V., S. Stankowski, and G. Schwarz, 1987, Alamethicin incorporation in lipid bilayers: a thermodynamic study: Biochemistry, v. 26, p. 2751-9.

Rodríguez, A., P. Webster, J. Ortego, and N. W. Andrews, 1997, Lysosomes behave as Ca2+-regulated exocytic vesicles in fibroblasts and epithelial cells: J Cell Biol, v. 137, p. 93-104.

Ros, C., C. Baltzer, B. Mani, and C. Kempf, 2006, Parvovirus uncoating in vitro reveals a mechanism of DNA release without capsid disassembly and striking differences in encapsidated DNA stability: Virology, v. 345, p. 137-47.

Rosen, H., M. Germana Sanna, P. J. Gonzalez-Cabrera, and E. Roberts, 2014, The organization of the sphingosine 1-phosphate signaling system: Curr Top Microbiol Immunol, v. 378, p. 1-21.

ROWE, W. P., R. J. HUEBNER, L. K. GILMORE, R. H. PARROTT, and T. G. WARD, 1953, Isolation of a cytopathogenic agent from human adenoids undergoing spontaneous degeneration in tissue culture: Proc Soc Exp Biol Med, v. 84, p. 570-3.

Russell, W. C., 2009, Adenoviruses: update on structure and function.: J Gen Virol, v. 90, p. 1-20.

Ruvolo, P. P., X. Deng, T. Ito, B. K. Carr, and W. S. May, 1999, Ceramide induces Bcl2 dephosphorylation via a mechanism involving mitochondrial PP2A: J Biol Chem, v. 274, p. 20296-300.

San Martín, C., 2012, Latest insights on adenovirus structure and assembly: Viruses, v. 4, p. 847-77.

San Martín, C., J. N. Glasgow, A. Borovjagin, M. S. Beatty, E. A. Kashentseva, D. T. Curiel, R. Marabini, and I. P. Dmitriev, 2008, Localization of the N-terminus of minor coat protein IIIa in the adenovirus capsid: J Mol Biol, v. 383, p. 923-34.

Sandhoff, R., 2010, Very long chain sphingolipids: tissue expression, function and synthesis: FEBS Lett, v. 584, p. 1907-13.

Saphire, A. C., T. Guan, E. C. Schirmer, G. R. Nemerow, and L. Gerace, 2000, Nuclear import of adenovirus DNA in vitro involves the nuclear protein import pathway and hsc70: J Biol Chem, v. 275, p. 4298-304.

Schissel, S. L., X. Jiang, J. Tweedie-Hardman, T. Jeong, E. H. Camejo, J. Najib, J. H. Rapp, K. J. Williams, and I. Tabas, 1998, Secretory sphingomyelinase, a product of the acid sphingomyelinase gene, can hydrolyze atherogenic lipoproteins at neutral pH. Implications for atherosclerotic lesion development: J Biol Chem, v. 273, p. 2738-46.

Schissel, S. L., E. H. Schuchman, K. J. Williams, and I. Tabas, 1996, Zn2+-stimulated sphingomyelinase is secreted by many cell types and is a product of the acid sphingomyelinase gene: J Biol Chem, v. 271, p. 18431-6.

Schneemann, A., W. Zhong, T. M. Gallagher, and R. R. Rueckert, 1992, Maturation cleavage required for infectivity of a nodavirus: J Virol, v. 66, p. 6728-34.

Schreiner, S., R. Martinez, P. Groitl, F. Rayne, R. Vaillant, P. Wimmer, G. Bossis, T. Sternsdorf, L. Marcinowski, Z. Ruzsics, T. Dobner, and H. Wodrich, 2012, Transcriptional activation of the adenoviral genome is mediated by capsid protein VI: PLoS Pathog, v. 8, p. e1002549.

Schuchman, E. H., and Desnick, R.J., 2001, Niemann–Pick disease types A and B: acid sphingomyelinase deficiencies: The Metabolic and Molecular Bases of Inherited Disease, 8th edition, p. pp. 3589.

.

Schulz, W. L., A. K. Haj, and L. A. Schiff, 2012, Reovirus uses multiple endocytic pathways for cell entry: J Virol, v. 86, p. 12665-75.

Serrano, D., T. Bhowmick, R. Chadha, C. Garnacho, and S. Muro, 2012, Intercellular adhesion molecule 1 engagement modulates sphingomyelinase and ceramide, supporting uptake of drug carriers by the vascular endothelium: Arterioscler Thromb Vasc Biol, v. 32, p. 1178-85.

Seth, P., 1994, Adenovirus-dependent release of choline from plasma membrane vesicles at an acidic pH is mediated by the penton base protein: J Virol, v. 68, p. 1204-6.

Settembre, E. C., J. Z. Chen, P. R. Dormitzer, N. Grigorieff, and S. C. Harrison, 2011, Atomic model of an infectious rotavirus particle: EMBO J, v. 30, p. 408-16.

Sezgin, E., I. Levental, M. Grzybek, G. Schwarzmann, V. Mueller, A. Honigmann, V. N. Belov, C. Eggeling, U. Coskun, K. Simons, and P. Schwille, 2012, Partitioning, diffusion, and ligand binding of raft lipid analogs in model and cellular plasma membranes: Biochim Biophys Acta, v. 1818, p. 1777-1784.

Shai, Y., 1999, Mechanism of the binding, insertion and destabilization of phospholipid bilayer membranes by alpha-helical antimicrobial and cell non-selective membrane-lytic peptides: Biochim Biophys Acta, v. 1462, p. 55-70.

Shai, Y., 2002, Mode of action of membrane active antimicrobial peptides: Biopolymers, v. 66, p. 236-48.

Shaner, R. L., J. C. Allegood, H. Park, E. Wang, S. Kelly, C. A. Haynes, M. C. Sullards, and A. H. Merrill, 2009, Quantitative analysis of sphingolipids for lipidomics using triple quadrupole and quadrupole linear ion trap mass spectrometers: J Lipid Res, v. 50, p. 1692-707.

Shayakhmetov, D. M., A. M. Eberly, Z. Y. Li, and A. Lieber, 2005, Deletion of penton RGD motifs affects the efficiency of both the internalization and the endosome escape of viral particles containing adenovirus serotype 5 or 35 fiber knobs: J Virol, v. 79, p. 1053-61.

Shen, H., F. Giordano, Y. Wu, J. Chan, C. Zhu, I. Milosevic, X. Wu, K. Yao, B. Chen, T. Baumgart, D. Sieburth, and P. De Camilli, 2014, Coupling between endocytosis and sphingosine kinase 1 recruitment: Nat Cell Biol, v. 16, p. 652-62.

Shin, H. W., H. Takatsu, and K. Nakayama, 2012, Mechanisms of membrane curvature generation in membrane traffic: Membranes (Basel), v. 2, p. 118-33.

Simonis, A., S. Hebling, E. Gulbins, S. Schneider-Schaulies, and A. Schubert-Unkmeir, 2014, Differential Activation of Acid Sphingomyelinase and Ceramide Release Determines Invasiveness of Neisseria meningitidis into Brain Endothelial Cells: PLoS Pathog, v. 10, p. e1004160.

Simons, K., and J. L. Sampaio, 2011, Membrane organization and lipid rafts: Cold Spring Harb Perspect Biol, v. 3, p. a004697.

Siskind, L. J., R. N. Kolesnick, and M. Colombini, 2002, Ceramide channels increase the permeability of the mitochondrial outer membrane to small proteins: J Biol Chem, v. 277, p. 26796-803.

Slotte, J. P., A. S. Härmälä, C. Jansson, and M. I. Pörn, 1990, Rapid turn-over of plasma membrane sphingomyelin and cholesterol in baby hamster kidney cells after exposure to sphingomyelinase: Biochim Biophys Acta, v. 1030, p. 251-7.

Smith, J. G., and G. R. Nemerow, 2008, Mechanism of adenovirus neutralization by Human alpha-defensins: Cell Host Microbe, v. 3, p. 11-9.

Smith, P. E., J. R. Brender, and A. Ramamoorthy, 2009, Induction of negative curvature as a mechanism of cell toxicity by amyloidogenic peptides: the case of islet amyloid polypeptide: J Am Chem Soc, v. 131, p. 4470-8.

Sonntag, F., S. Bleker, B. Leuchs, R. Fischer, and J. A. Kleinschmidt, 2006, Adeno-associated virus type 2 capsids with externalized VP1/VP2 trafficking domains are generated prior to passage through the cytoplasm and are maintained until uncoating occurs in the nucleus: J Virol, v. 80, p. 11040-54.

Stahnke, S., K. Lux, S. Uhrig, F. Kreppel, M. Hösel, O. Coutelle, M. Ogris, M. Hallek, and H. Büning, 2011, Intrinsic phospholipase A2 activity of adeno-associated virus is involved in endosomal escape of incoming particles: Virology, v. 409, p. 77-83.

Stanasila, L., L. Abuin, D. Diviani, and S. Cotecchia, 2006, Ezrin directly interacts with the alpha1b-adrenergic receptor and plays a role in receptor recycling: J Biol Chem, v. 281, p. 4354-63.

Stancevic, B., and R. Kolesnick, 2010, Ceramide-rich platforms in transmembrane signaling: FEBS Lett, v. 584, p. 1728-40.

Steinhart, W. L., J. S. Busch, J. P. Oettgen, and J. L. Howland, 1984, Sphingolipid metabolism during infection of human fibroblasts by herpes simplex virus type 1: Intervirology, v. 21, p. 70-6.

Stewart, P. L., S. D. Fuller, and R. M. Burnett, 1993, Difference imaging of adenovirus: bridging the resolution gap between X-ray crystallography and electron microscopy: EMBO J, v. 12, p. 2589-99.

Stiban, J., R. Tidhar, and A. H. Futerman, 2010, Ceramide synthases: roles in cell physiology and signaling: Adv Exp Med Biol, v. 688, p. 60-71.

Strelow, A., K. Bernardo, S. Adam-Klages, T. Linke, K. Sandhoff, M. Krönke, and D. Adam, 2000, Overexpression of acid ceramidase protects from tumor necrosis factor-induced cell death: J Exp Med, v. 192, p. 601-12.

Strunze, S., M. F. Engelke, I. H. Wang, D. Puntener, K. Boucke, S. Schleich, M. Way, P. Schoenenberger, C. J. Burckhardt, and U. F. Greber, 2011, Kinesin-1-mediated capsid disassembly and disruption of the nuclear pore complex promote virus infection: Cell Host Microbe, v. 10, p. 210-23.

Sugiura, M., K. Kono, H. Liu, T. Shimizugawa, H. Minekura, S. Spiegel, and T. Kohama, 2002, Ceramide kinase, a novel lipid kinase. Molecular cloning and functional characterization: J Biol Chem, v. 277, p. 23294-300.

Suikkanen, S., M. Antila, A. Jaatinen, M. Vihinen-Ranta, and M. Vuento, 2003, Release of canine parvovirus from endocytic vesicles: Virology, v. 316, p. 267-80.

Sullards, M. C., J. C. Allegood, S. Kelly, E. Wang, C. A. Haynes, H. Park, Y. Chen, and A. H. Merrill, 2007, Structure-specific, quantitative methods for analysis of sphingolipids by liquid chromatography-tandem mass spectrometry: "inside-out" sphingolipidomics: Methods Enzymol, v. 432, p. 83-115.

Suomalainen, M., and U. F. Greber, 2013, Uncoating of non-enveloped viruses: Curr Opin Virol, v. 3, p. 27-33.

Suomalainen, M., S. Luisoni, K. Boucke, S. Bianchi, D. A. Engel, and U. F. Greber, 2013, A direct and versatile assay measuring membrane penetration of adenovirus in single cells: J Virol, v. 87, p. 12367-79.

Suomalainen, M., M. Y. Nakano, K. Boucke, S. Keller, and U. F. Greber, 2001, Adenovirus-activated PKA and p38/MAPK pathways boost microtubule-mediated nuclear targeting of virus: EMBO J, v. 20, p. 1310-9.

Suomalainen, M., M. Y. Nakano, S. Keller, K. Boucke, R. P. Stidwill, and U. F. Greber, 1999, Microtubule-dependent plus- and minus end-directed motilities are competing processes for nuclear targeting of adenovirus: J Cell Biol, v. 144, p. 657-72.

Syntichaki, P., and N. Tavernarakis, 2003, The biochemistry of neuronal necrosis: rogue biology?: Nat Rev Neurosci, v. 4, p. 672-84.

Tam, C., A. R. Flannery, and N. Andrews, 2013a, Live imaging assay for assessing the roles of Ca2+ and sphingomyelinase in the repair of pore-forming toxin wounds: J Vis Exp, p. e50531.

Tam, C., V. Idone, C. Devlin, M. C. Fernandes, A. Flannery, X. He, E. Schuchman, I. Tabas, and N. W. Andrews, 2010, Exocytosis of acid sphingomyelinase by wounded cells promotes endocytosis and plasma membrane repair: J Cell Biol, v. 189, p. 1027-38.

Tam, V. C., O. Quehenberger, C. M. Oshansky, R. Suen, A. M. Armando, P. M. Treuting, P. G. Thomas, E. A. Dennis, and A. Aderem, 2013b, Lipidomic profiling of influenza infection identifies mediators that induce and resolve inflammation: Cell, v. 154, p. 213-27.

Tamma, G., E. Klussmann, J. Oehlke, E. Krause, W. Rosenthal, M. Svelto, and G. Valenti, 2005, Actin remodeling requires ERM function to facilitate AQP2 apical targeting: J Cell Sci, v. 118, p. 3623-30.

Tani, H., M. Shiokawa, Y. Kaname, H. Kambara, Y. Mori, T. Abe, K. Moriishi, and Y. Matsuura, 2010, Involvement of ceramide in the propagation of Japanese encephalitis virus: J Virol, v. 84, p. 2798-807.

Tanner, L. B., C. Chng, X. L. Guan, Z. Lei, S. G. Rozen, and M. R. Wenk, 2014, Lipidomics identifies a requirement for peroxisomal function during influenza virus replication: J Lipid Res, v. 55, p. 1357-1365.

Taupin, C., M. Dvolaitzky, and C. Sauterey, 1975, Osmotic pressure induced pores in phospholipid vesicles: Biochemistry, v. 14, p. 4771-5.

Tibbles, L. A., J. C. Spurrell, G. P. Bowen, Q. Liu, M. Lam, A. K. Zaiss, S. M. Robbins, M. D. Hollenberg, T. J. Wickham, and D. A. Muruve, 2002, Activation of p38 and ERK signaling during adenovirus vector cell entry lead to expression of the C-X-C chemokine IP-10: J Virol, v. 76, p. 1559-68.

Togo, T., T. B. Krasieva, and R. A. Steinhardt, 2000, A decrease in membrane tension precedes successful cell-membrane repair: Mol Biol Cell, v. 11, p. 4339-46.

Tollefson, A. E., A. Scaria, T. W. Hermiston, J. S. Ryerse, L. J. Wold, and W. S. Wold, 1996, The adenovirus death protein (E3-11.6K) is required at very late stages of infection for efficient cell lysis and release of adenovirus from infected cells.: J Virol, v. 70, p. 2296-306.

Trajkovic, K., C. Hsu, S. Chiantia, L. Rajendran, D. Wenzel, F. Wieland, P. Schwille, B. Brügger, and M. Simons, 2008, Ceramide triggers budding of exosome vesicles into multivesicular endosomes: Science, v. 319, p. 1244-7.

Trask, S. D., I. S. Kim, S. C. Harrison, and P. R. Dormitzer, 2010, A rotavirus spike protein conformational intermediate binds lipid bilayers: J Virol, v. 84, p. 1764-70.

Trotman, L. C., N. Mosberger, M. Fornerod, R. P. Stidwill, and U. F. Greber, 2001, Import of adenovirus DNA involves the nuclear pore complex receptor CAN/Nup214 and histone H1: Nat Cell Biol, v. 3, p. 1092-100.

Utermöhlen, O., U. Karow, J. Löhler, and M. Krönke, 2003, Severe impairment in early host defense against Listeria monocytogenes in mice deficient in acid sphingomyelinase: J Immunol, v. 170, p. 2621-8.

van der Houven van Oordt, W., M. T. Diaz-Meco, J. Lozano, A. R. Krainer, J. Moscat, and J. F. Cáceres, 2000, The MKK(3/6)-p38-signaling cascade alters the subcellular distribution of hnRNP A1 and modulates alternative splicing regulation: J Cell Biol, v. 149, p. 307-16.

van Diggelen, O. P., Y. V. Voznyi, J. L. Keulemans, K. Schoonderwoerd, J. Ledvinova, E. Mengel, M. Zschiesche, R. Santer, and K. Harzer, 2005, A new fluorimetric enzyme assay for the diagnosis of Niemann-Pick A/B, with specificity of natural sphingomyelinase substrate: J Inherit Metab Dis, v. 28, p. 733-41.

van Oostrum, J., and R. M. Burnett, 1985, Molecular composition of the adenovirus type 2 virion: J Virol, v. 56, p. 439-48.

Vihinen-Ranta, M., L. Kakkola, A. Kalela, P. Vilja, and M. Vuento, 1997, Characterization of a nuclear localization signal of canine parvovirus capsid proteins: Eur J Biochem, v. 250, p. 389-94.

Vivès, E., J. Schmidt, and A. Pèlegrin, 2008, Cell-penetrating and cell-targeting peptides in drug delivery: Biochim Biophys Acta, v. 1786, p. 126-38.

Voisset, C., M. Lavie, F. Helle, A. Op De Beeck, A. Bilheu, J. Bertrand-Michel, F. Tercé, L. Cocquerel, C. Wychowski, N. Vu-Dac, and J. Dubuisson, 2008, Ceramide enrichment of the plasma membrane induces CD81 internalization and inhibits hepatitis C virus entry: Cell Microbiol, v. 10, p. 606-17.

Walukiewicz, H. E., J. E. Johnson, and A. Schneemann, 2006, Morphological changes in the T=3 capsid of Flock House virus during cell entry: J Virol, v. 80, p. 615-22.

Wang, E., W. P. Norred, C. W. Bacon, R. T. Riley, and A. H. Merrill, 1991, Inhibition of sphingolipid biosynthesis by fumonisins. Implications for diseases associated with Fusarium moniliforme: J Biol Chem, v. 266, p. 14486-90.

Wang, K., T. Guan, D. A. Cheresh, and G. R. Nemerow, 2000, Regulation of adenovirus membrane penetration by the cytoplasmic tail of integrin beta5: J Virol, v. 74, p. 2731-9.

Wang, T. Y., and J. R. Silvius, 2000, Different sphingolipids show differential partitioning into sphingolipid/cholesterol-rich domains in lipid bilayers: Biophys J, v. 79, p. 1478-89.

Webster, A., R. T. Hay, and G. Kemp, 1993, The adenovirus protease is activated by a virus-coded disulphide-linked peptide: Cell, v. 72, p. 97-104.

Westerhoff, H. V., D. Juretić, R. W. Hendler, and M. Zasloff, 1989, Magainins and the disruption of membrane-linked free-energy transduction: Proc Natl Acad Sci U S A, v. 86, p. 6597-601.

Wickham, T. J., E. J. Filardo, D. A. Cheresh, and G. R. Nemerow, 1994, Integrin alpha v beta 5 selectively promotes adenovirus mediated cell membrane permeabilization.: J Cell Biol, v. 127, p. 257-64.

Wickham, T. J., P. Mathias, D. A. Cheresh, and G. R. Nemerow, 1993, Integrins alpha v beta 3 and alpha v beta 5 promote adenovirus internalization but not virus attachment: Cell, v. 73, p. 309-19.

Wiethoff, C. M., H. Wodrich, L. Gerace, and G. R. Nemerow, 2005, Adenovirus protein VI mediates membrane disruption following capsid disassembly: J Virol, v. 79, p. 1992-2000.

Williamson, J. A., J. P. Loria, and A. D. Miranker, 2009, Helix stabilization precedes aqueous and bilayer-catalyzed fiber formation in islet amyloid polypeptide: J Mol Biol, v. 393, p. 383-96.

Wimley, W. C., 2010, Describing the mechanism of antimicrobial peptide action with the interfacial activity model: ACS Chem Biol, v. 5, p. 905-17.

Wodrich, H., A. Cassany, M. A. D'Angelo, T. Guan, G. Nemerow, and L. Gerace, 2006, Adenovirus core protein pVII is translocated into the nucleus by multiple import receptor pathways: J Virol, v. 80, p. 9608-18.

Wodrich, H., T. Guan, G. Cingolani, D. Von Seggern, G. Nemerow, and L. Gerace, 2003, Switch from capsid protein import to adenovirus assembly by cleavage of nuclear transport signals: EMBO J, v. 22, p. 6245-55.

Wold, W. S., and K. Toth, 2013, Adenovirus vectors for gene therapy, vaccination and cancer gene therapy: Curr Gene Ther, v. 13, p. 421-33.

Wolfrum, N., and U. F. Greber, 2013, Adenovirus signalling in entry: Cell Microbiol, v. 15, p. 53-62.

Won, A., A. Ruscito, and A. Ianoul, 2012, Imaging the membrane lytic activity of bioactive peptide latarcin 2a: Biochim Biophys Acta, v. 1818, p. 3072-80.

Wu, P. S., R. W. Ledeen, S. Udem, and Y. A. Isaacson, 1980, Nature of the Sendai virus receptor: glycoprotein versus ganglioside: J Virol, v. 33, p. 304-10.

Wu, W., J. L. Booth, K. M. Coggeshall, and J. P. Metcalf, 2006, Calcium-dependent viral internalization is required for adenovirus type 7 induction of IL-8 protein: Virology, v. 355, p. 18-29.

Yachi, R., Y. Uchida, B. H. Balakrishna, G. Anderluh, T. Kobayashi, T. Taguchi, and H. Arai, 2012, Subcellular localization of sphingomyelin revealed by two toxin-based probes in mammalian cells: Genes Cells, v. 17, p. 720-7.

Yang, L., T. A. Harroun, T. M. Weiss, L. Ding, and H. W. Huang, 2001, Barrel-stave model or toroidal model? A case study on melittin pores: Biophys J, v. 81, p. 1475-85.

Yano, M., E. Kishida, Y. Muneyuki, and Y. Masuzawa, 1998, Quantitative analysis of ceramide molecular species by high performance liquid chromatography: J Lipid Res, v. 39, p. 2091-8.

Yeager, M., K. A. Dryden, N. H. Olson, H. B. Greenberg, and T. S. Baker, 1990, Three-dimensional structure of rhesus rotavirus by cryoelectron microscopy and image reconstruction: J Cell Biol, v. 110, p. 2133-44.

Yonamine, I., T. Bamba, N. K. Nirala, N. Jesmin, T. Kosakowska-Cholody, K. Nagashima, E. Fukusaki, J. K. Acharya, and U. Acharya, 2011, Sphingosine kinases and their metabolites modulate endolysosomal trafficking in photoreceptors: J Cell Biol, v. 192, p. 557-67.

Zha, X., L. M. Pierini, P. L. Leopold, P. J. Skiba, I. Tabas, and F. R. Maxfield, 1998, Sphingomyelinase treatment induces ATP-independent endocytosis: J Cell Biol, v. 140, p. 39-47.

Zhang, L., M. A. Agosto, T. Ivanovic, D. S. King, M. L. Nibert, and S. C. Harrison, 2009, Requirements for the formation of membrane pores by the reovirus myristoylated micro1N peptide: J Virol, v. 83, p. 7004-14.

Zhang, Y., and J. M. Bergelson, 2005, Adenovirus receptors: J Virol, v. 79, p. 12125-31.

Zhou, R., X. Cao, C. Watson, Y. Miao, Z. Guo, J. G. Forte, and X. Yao, 2003, Characterization of protein kinase A-mediated phosphorylation of ezrin in gastric parietal cell activation: J Biol Chem, v. 278, p. 35651-9.

Zhu, H., P. Lin, G. De, K. H. Choi, H. Takeshima, N. Weisleder, and J. Ma, 2011, Polymerase transcriptase release factor (PTRF) anchors MG53 protein to cell injury site for initiation of membrane repair: J Biol Chem, v. 286, p. 12820-4.

Zlotnick, A., V. S. Reddy, R. Dasgupta, A. Schneemann, W. J. Ray, R. R. Rueckert, and J. E. Johnson, 1994, Capsid assembly in a family of animal viruses primes an autoproteolytic maturation that depends on a single aspartic acid residue: J Biol Chem, v. 269, p. 13680-4.

Zádori, Z., J. Szelei, M. C. Lacoste, Y. Li, S. Gariépy, P. Raymond, M. Allaire, I. R. Nabi, and P. Tijssen, 2001, A viral phospholipase A2 is required for parvovirus infectivity: Dev Cell, v. 1, p. 291-302.

ACKNOWLEDGEMENTS

Thank you Urs for being a great supervisor full of enthusiasm! Your natural curiosity to learn more about biological processes is contagious and very motivating for me. With your guidance and critical thinking, I learned how science should be done.

A special thank also to you, Maarit! You were always so kind and patient and shared with me your enormous theoretical and practical knowledge. I like to think of you as a problem-solving fairy.

Thank you Silvio for having introduced me to the fascinating field of adenovirus during my master thesis and for the constructive suggestions during our frequent lab meetings.

Many thanks to the other members of my thesis committee, Ari Helenius and Howard Riezman, for the valuable scientific discussions and helpful advices.

Many thanks to Karin for the crucial support with EM!

Thank you Leta for the nice time spent together, I always appreciated your peaceful and very kind personality.

I enjoyed very much the time in the lab, especially during these last months. The social life in the girl's office kept me in a good mood even when my experiments did not work. So thank you Nicole, Daria, Rebecca, Rodinde (you unofficially belong here) and Bettina! Also thanks to Pascal, Robert, Tobias and Mark for good laughs at the bench. Tobias, I also thank you for your scientific engagement on this project. Jessy and Artur, I appreciated your 'senior' advices during my time here. Thanks to the whole group for the nice atmosphere and helpful hints, it was a pleasure to work with you!

A special thanks to my friends in Zürich, Ticino and Lausanne for the relaxing and funny moments outside of the lab.

Pius, you already know everything :-)

Last but not least, a huge thanks to my family, that has been supportive, helpful and kind to me since ever and especially during my moments of need. I feel very lucky having you!

CURRICULUM VITAE

Stefania Luisoni

Adresse: Binzmühlestrasse 41
8050 Zürich
Tel.: +41 79 576 36 26
E-mail: stefania.luisoni@uzh.ch
Geburtstag: 22. Oktober 1986
Nationalität: Schweizerin
Heimatort: Stabio, TI

Ausbildung

Nov. 2010 - Jan. 2015	PhD in Molecular Life Sciences, *Universität Zürich* Betreuer: Prof. Urs F. Greber Thesis: „Lipid requirements during Adenovirus infection“
Okt. 2008 - Apr. 2010	Master in Biochemie, *ETH Zürich* Betreuer: Prof. Ari Helenius, im Labor von PD Silvio Hemmi Thesis: „Generation of adenoviral vectors retargeted to Her2 expressing cancer cells” Durchschnittnote: 5.45
Okt. 2005 - Aug. 2008	Bachelor in Biochemie, *Universität Fribourg* Durchschnittnote: 5.39
Sept. 2001 - Juni 2005	Wissenschaftliche Matura, *Gymnasium Bellinzona* Durchschnittnote: 5.65

Arbeitserfahrung

Sept. 2009 - Mai 2013	Teilzeiterwerb (20%) im Pflegehaus Integriertes Wohnen für Behinderte in Zürich
2007 - 2010	Lehrerersatz für Biologie und Chemie im Gymnasium in Bellinzona (insgesamt 8 Wochen)
Juni 2008 - Aug. 2008	Neurobiolgie-Laborpraktikum bei Prof. Galizia, Konstanz (DE)
2003 - 2007	Schweizer Post, Bellinzona (Teamarbeit im Distributionszentrum während den Schulferien)
2002	Gesundheits-, Schul- und Sportdepartement, Bellinzona (Büroarbeit während den Schulferien)

Sprachen

Italienisch:	Muttersprache	Französisch:	Fliessend
English:	Fliessend	Deutsch:	Fliessend

Besondere Fähigkeiten

Betreuung von Studenten: direkte Betreuung von einem Masterstudenten für ein Jahr und Betreuung und Organisation von Labor Praktika für Bachelor und Master Studenten zusammen mit anderen Doktoranden.

IT Fähigkeiten

Word, Excel, Power Point, Adobe Illustrator, ImageJ, FlowJo, Matlab, GraphPad Prism, BD FACSDiva, Leica LAS AF, EndNote, DNAStrider, TeamViewer

Publikationen

- Maarit Suomalainen, **Stefania Luisoni**, Karin Boucke, Sarah Bianchi, Daniel A. Engel, and Urs F. Greber, *A direct and versatile assay measuring membrane penetration of adenovirus in single cells,* Journal of Virology, 2013

- Roger Geiger, **Stefania Luisoni**, Kai Johnsson, Urs F. Greber and Ari Helenius, *Investigating Endocytic pathways to the endoplasmic reticulum and to the cytosol using SNAP-trap*, Traffic, 2012

- Roger Geiger, Daniel Andritschke, Sarah Friebe, Fabian Herzog, **Stefania Luisoni**, Thomas Heger, and Ari Helenius, *Bap31 and BiP are essential for dislocation of SV40 from the endoplasmic reticulum to the cytosol*, Nature Cell Biology, 2011

Präsentationen an Konferenzen

- Swiss virology meeting, *September 9-10, 2014, Thun*
- Early events in virus infection, *August 25-28, 2014, Monte Verità, Ascona*
- Protein and lipid function in secretion and endocytosis, *Januar 14-19, 2014, Goldegg am See, Österreich*
- Membrane dynamics in physiology and disease, *Juni 5-8, 2012, Zentrum für Lehre und Forschung, Universität Basel*
- Glycolipid & sphingolipid biology, *April 22-27, 2012, Renaissance Tuscany Il Ciocco Resort, Lucca (Barga), Italien*

Sonstiges

- Mitglied vom Molecular Life Sciences lecture organizing committee, 2012-2013.
- Seit 1995 Mitglied vom Kunstturnverein SFG Lugano.
- Private Lehrstunden für Gymnasiasten im Rahmen des Studentenvereins MISE.
- Hobbies: wandern, kochen, joggen, skifahren, lesen, reisen.